Delft University of Technology, Faculty of Mechanical, Maritime and Materials Engineering
Department of Biomechanical Engineering, Delft Institute of Prosthetics and Orthotics

Design of a Flat Dynamic Hand Orthosis Finger for DMD Patients

Master of Science Thesis

M.D. Baan

TU Delft

Design of a Flat Dynamic Hand Orthosis Finger for DMD Patients

Master of Science Thesis

M.D. Baan

TU Delft

Delft University of Technology, Faculty of Mechanical, Maritime and Materials Engineering
Delft, The Netherlands

The undersigned hereby certify that they have read, and recommend to the Faculty of Mechanical, Maritime and Materials Engineering for acceptance, a thesis entitled **Design of a Flat Dynamic Hand Orthosis Finger for DMD Patients** submitted by **M.D. Baan** in partial fulfillment of the requirements for the award of the degree of **Master of Science**.

Dated: 25 October 2019

Professor: ______________________________
Prof.dr. F.C.T. van der Helm

Supervisor: ______________________________
Dr.ir. D.H. Plettenburg

External examiner: ______________________________
To be defined

Preface

This thesis summarizes the work of the final graduation project for my Master of Science degree in Biomedical Engineering at the Faculty of Mechanical, Maritime and Materials Engineering at Delft University of Technology. I am interested in the combination of health care and engineering. This is also the main interest of my thesis: the design of a flat dynamic hand orthosis for DMD patients. I am proud that I managed to design and develop a working prototype.

I would like to thank my supervisor Dick, for the weekly meetings and for the feedback you gave me during these sessions. You made me enthusiastic to finish my studies. Furthermore, I would like to thank Jan van Frankenhuyzen for the design discussions, the talks about the project and your assistance with 3D printing. Juan Cuellar Lopez, thanks for using your 3D printer. Thank you everyone from the IWM, to help me with my fabrication. Jos van Driel, thanks for writing the LabVIEW scripts and setting up the sensors. Furthermore, I would like to give specials thanks to my parents, my brother, my boyfriend and my friends for their support and interest in my final graduation project.

M.D. Baan
Delft, 25 October 2019

Table of contents

List of figures

List of tables

Nomenclature

List of acronyms

ADL	Activities of daily living
CSA	Cross sectional area
DIP	Distal interphalangeal
DMD	Duchenne muscular dystrophy
DOF	Degree of freedom
EMG	Electromyography
FBD	Free body diagram
FEM	Finite element method
FLS	Fishbone-like structure
MCP	Metacarpophalangeal
PAM	Pneumatic artificial muscle
PIP	Proximal interphalangeal
PLA	Polylactic acid
SMA	Shape memory alloy
SPA	Soft pneumatic actuator
TCP	Twisted polymeric muscle
TPU	Thermoplastic polyurethane

List of symbols

A	Area	m^2
F_{out}	Output force	N
H	Height	m
p	Pressure	Pa
r	Radius	m
r_{in}	Input moment arm	m
r_{out}	Output moment arm	m

1
Introduction

1.1 Background

1.1.1 Duchenne muscular dystrophy

Duchenne muscular dystrophy (DMD) is a recessive X chromosome-linked neuromuscular disease. DMD affects approximately 1:4700 boys (Van den Bergen et al., 2014). A recessive X chromosome-linked disease means that when the mother is carrier of that mutation, there is fifty percent chance that her daughter is carrier and fifty percent chance that her son will get the mutation. This is shown in Figure 1.1. The mutation that causes DMD is a mutation in the dystrophin gene. This results in the absence of the dystrophin protein. Dystrophin is present in skeletal and cardiac muscles. It links the muscle cytoskeleton with the extracellular matrix. Furthermore, dystrophin plays a role in cell signaling. Because of the absence of the protein dystrophin, skeletal and cardiac muscle degeneration takes place. This causes muscle weakness, functional losses and cardiac and respiratory problems. At this moment, there is no treatment available to stop the disease. Therefore, the treatment is focused on the symptoms. One treatment is glucocorticoid therapy to slow down the process (Sawnani et al., 2019). This increases the life expectancy of DMD patients with a median age above thirty years (Passamano et al., 2012). A biophysical model of the working mechanism and treatments of the upper limb is made by Janssen (2017) and shown in Figure 1.2. This model shows that the possibility to move the arm actively is dependent on both the passive range of motion of the joint and the available joint torque. The joint torque depends on the muscle capacity and moment arm. The muscle capacity is influenced by the muscle activation and muscle force. The maximum muscle force that can be reached depends on the maximum muscle strength and the cross sectional area (CSA) of the muscle. The pharmacotherapy treatment is still in development. However, physical exercises, stretching and the use of splints and arm support have been shown to be functional. The first symptoms will become visible before the age of five. Around the age of ten they will end up in a wheelchair (Seferian et al., 2015). The phase when they are in need of a wheelchair is also called the early non-ambulatory phase. The different stages of upper extremity functioning could be measured with the Brooke scale, as summarized in Table 1.1 (Lu and Lue, 2012). Around the age of ten/eleven years old, the Brooke scale grade 2 will be reached. At this stage, problems begin proximal of the arm and move to the distal parts of the arms and hands. Problems with the fingers will start at Brooke scale grades 4, 5, and 6. This will be in the early and late non-ambulatory phase (Janssen et al., 2014). This means that they become dependent of others. This has influence on the performance of activities of daily living (ADL) and their quality of life (Klingels et al., 2017). In the mild weakness phase, splints give enough support for DMD patients. However, as soon as severe weakness happens, active support is needed. Following Jones and Lederman (2006), tactile sensing, proprioceptive sensing, prehension, and non-prehensile skilled movements are the main categories for hand functioning. People with DMD experience problems with their prehension and non-prehensile skilled movements but their tactile and propioceptive senses are working fine.

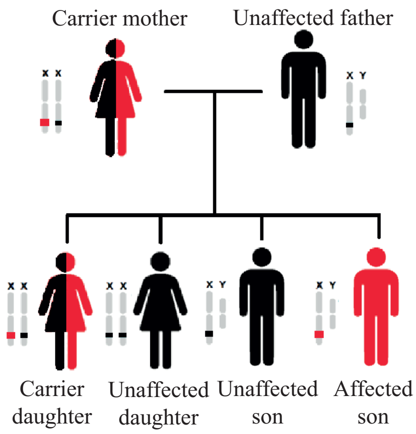

Figure 1.1 Inheritance dystrophin gen mutation with a carrier mother. Black indicates a healthy gen, red represents the mutation.

Table 1.1 Different levels of the Brooke scale grades for upper extremities (Lu and Lue, 2012).

Grade	Description
1	Starting with arms at the sides, the patient can abduct the arms in a full circle until they touch above the head.
2	Can raise arms above head only by flexing the elbow (shortening the circumference of the movement) or using accessory muscles.
3	Cannot raise hands above head, but can raise an 8-oz glass of water to the mouth.
4	Can raise hands to the mouth, but cannot raise an 8-oz glass of water to the mouth.
5	Cannot raise hands to the mouth, but can use hands to hold a pen or pick up pennies from the table.
6	Cannot raise hands to the mouth and has no useful function of hands.

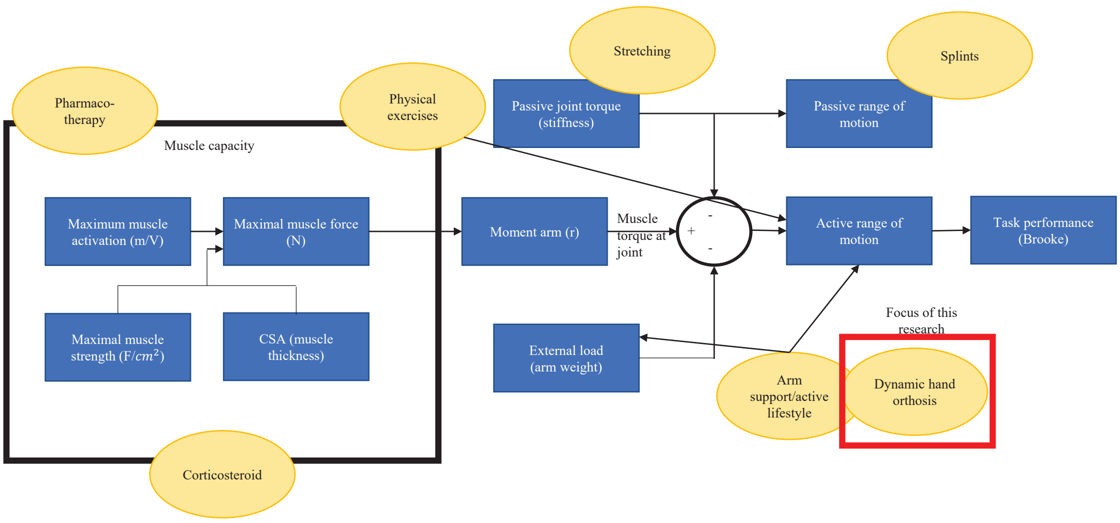

Figure 1.2 Biophysical model working mechanism of the upper extremity in DMD, including different treatment options and focus of this research (adapated from Janssen (2017)).

1.1.2 Hand orthoses

To support DMD patients during ADL, a dynamic hand orthosis could be a solution. Dynamic hand orthoses comprise hand exoskeletons, rehabilitation robots and assistive devices (Bos et al., 2016). A dynamic hand orthosis is designed and placed around the human hand. To make a dynamic hand orthosis as comfortable as possible, it is important that it fits to the hand anatomy and its range of motion. Therefore, a lot of different hand orthoses are designed. Hand orthoses can be wearable or non wearable. This research focuses on the wearable designs. There are static orthoses, also called splints, which mainly serve to stabilize and support a joint in a certain position. On the contrary, there are dynamic orthoses, which make it possible to generate movements of weak muscles (Glasgow et al., 2008). Recent years have seen an increasing development in dynamic hand orthoses. This does not only apply for rehabilitation, but also for use during ADL. The small space on the hand makes it hard to design a flat and lightweight dynamic hand orthosis (Bos et al., 2018). A literature study was carried out as a start of this research. This literature study analyzed forty-eight different flat dynamic designs. A maximum finger orthosis height of 20 mm on top of the own finger was seen as flat. Yet, only one of these designs is made available on the market. This is the Seabo flex described by Hoffman and Blakey (2011). The rest of the designs is still in development or did not work that well. There were some designs which showed promising solutions for DMD patients, but there were still some adaptations needed. Although, hand splints are available for DMD patients at this moment, they are not possible to use during tasks of ADL. This is because the splints are static. However, they have been proven to be functional (Weichbrodt et al., 2018). The dynamic hand orthosis should be small, light-weight, generate enough pinch force to use for ADL and should be comfortable. Comfort is really important because the device should be worn the whole day. Next to comfort, the cosmetics is an important factor to keep in mind (Plettenburg, 1998). It is important to note that DMD patients have a really sensitive skin and their own tactile senses are still functioning (Jones and Lederman, 2006). Therefore, for a proper design, these senses should still be used and on the other hand the forces should be adaptable to prevent damage on the skin.

1.2 Problem statement

DMD is a chronic disease. As shown in Figure 1.2 different treatments are possible to slow down the process. However, this is only to decrease the symptoms and not to cure the disease. As soon as DMD patients reach Brooke scale grade 4, they will suffer from a limited hand function. This makes them dependent of others to help them with their ADL tasks. A dynamic hand orthosis could be a solution. However, none of the existing devices fits the special needs of these patients. They are too bulky, the forces are not high enough, they cannot use their own tactile senses anymore or they need their other hand to activate the device. To help DMD patients and to make them more independent, a new flat dynamic hand orthosis should be developed. The size is seen as the most important criteria as this has influence on the cosmetics and the ease of use (Plettenburg, 1998).

1.3 Research objective

The research objective can be formulated as follows.

> **To design and to prototype a wearable flat dynamic hand orthosis finger for DMD patients with Brooke scale grade 4, 5, or 6 and to test its functioning by measuring the output force and flexion angle.**

A maximum finger orthosis height of 20 mm was seen as flat. The focus of this research is on one finger. The control mechanism and attachment system are beyond the scope of this research. Figure 1.3 shows an overview of the steps taken during the process. This goal is reached by first accomplishing a literature study to get an overview of all available flat dynamic hand orthoses. With the help of this information, design criteria were made. Then different concepts were designed and a final concept was selected. This prototype was manufactured and tested. As a result of the tests, the prototype was optimized and tested again.

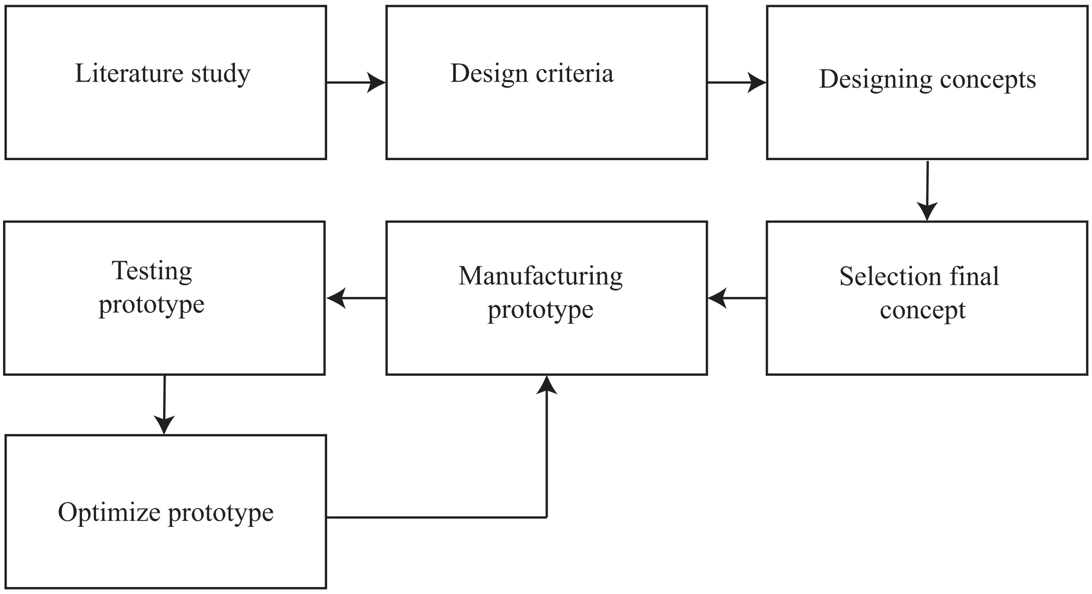

Figure 1.3 Schematic overview of the steps taken during the research process.

1.4 Report's structure

This thesis report is divided into three different parts. Part I contains the scientific paper with the most relevant information and results on the conducted research. Part II consists of chapters related to the literature study. It lists the different flat hand orthoses found in literature. Part III consists of different appendices with supplemental information about the design process and the experiments.

- Part I shows the research paper that describes the final design. It shows the methods used during the research, explains the results and gives a discussion with recommendations. Additional information is put in the appendix of the paper. This part can be read independent from the rest.
- Part II is the literature study that was performed at the beginning of this thesis. It answers the research question: 'Which available actuation system is most suitable to design a wearable flat dynamic hand orthosis for DMD patients?' In order to answer the main research question of this report, Chapter 2 describes the method that is used for the literature review. Here, the aspects of signal domain, energy domain and mechanical domain will be explained. Chapter 3 shows the results of the search strategy. The tables in this chapter show each actuation system separately. Subquestions are answered by means of these tables. Besides that, it is shown which actuators are used in the categories. This is followed by the discussion in Chapter 4, where the results will be explained based on the framework of signal domain, energy domain and mechanical domain. Finally, conclusions are drawn in Chapter 5 to sum up the whole report and to answer the main research question.
- Part III describes the design process which was not shown in Part I. It consists of different appendices. Appendix B describes the human hand anatomy. Appendix C shows the conceptual design with the steps taken to come up with the final design. Appendix D describes the prototypes which are manufactured. Finally, Appendix E shows additional information for the paper.

I

Paper

Design of a Flat Dynamic Hand Orthosis Finger for DMD Patients

M. D. Baan, D. H. Plettenburg, and F. C. T. van der Helm

***Abstract*—People with Duchenne muscular dystrophy (DMD) will suffer from a limited hand function. Therefore, a dynamic hand orthosis could be one of the solutions to improve their hand function and quality of life. However, at this moment, none of the obtainable hand orthoses fits their special needs. The goal of this research is to design a flat dynamic hand orthosis finger for DMD patients with Brooke scale grades 4, 5, or 6 and to test its functioning. The design consists of a silicone outer part, and an inner part from polylactic acid. The presented prototype is small, can generate a flexion movement and has a finger mass of 20 g. Output forces were tested in horizontal and vertical direction and different designs were compared in relation to the bending angle. The reached output forces in horizontal and vertical direction with a certain pressure were 3.4 N (10.5 N target) at 1.75 bar and 0.6 N at 2 bar, respectively. The bending angles were 35° for the MCP joint, 78° for the PIP joint, and 58° for the DIP joint. To conclude, this paper presented a new design of a finger for a hand orthosis. The prototype is flat, can generate flexion movements and has a finger mass of 20 g. Except for the MCP joint, the bending angles meet the requirements. Only the output forces were too low. An outer structure of another material might solve this.**

***Index Terms*—DMD, soft pneumatic actuator, dynamic hand orthosis.**

Nomenclature

μ	Friction coefficient.
A	Area, m^2.
F	Output force, N.
F_{Pinch}	Pinch force, N.
g	Gravity, m/s^2.
m	Mass, kg.
p	Pressure, Pa.

I. Introduction

DUCHENNE muscular dystrophy (DMD) is a recessive X chromosome linked neuromuscular disease. Therefore, most of the time it only affects boys and the affecting rate is 1:4700 boys [1]. The absence of the protein dystrophin causes muscle weakness, functional losses and cardiac and respiratory problems. The disease is chronic and no treatment is available to stop the disease. However, some medication is available to slow down the process and to increase patient life expectancy to above the age of thirty years [2]. The arm function of boys with DMD deteriorates in the early non-ambulatory phase and they lose the ability to walk around the age of ten [3]. The Brooke scale is used to measure the stages of upper extremity activity level. The focus of this research is on patients with Brooke scale grades 4, 5 and 6, since these are the stages at which the fingers start to dysfunction [4]. Limitations in the hand function have an impact on the autonomy of the patients, especially on the performance of activities of daily living (ADL) and their quality of life [5]. To give these patients more autonomy, a portable dynamic hand orthosis could be a solution [6]. Dynamic hand orthoses are able to generate movements of the hand and fingers [7]. In the last decades, more studies have been focusing on the development of hand orthoses. However, the limited space on the hand makes it hard to develop a flat and lightweight hand orthosis [8]. Preliminary research found that there are dynamic hand orthoses available which were actuated with either the help of the other hand, an electromagnetic actuation system, a pneumatic actuator, or a thermal system [9], [10]. Both the electromagnetic and pneumatic actuation systems might be suitable for DMD patients. However, electromagnetic devices have disadvantages, such as large weight, aligning difficulties and less comfort. The soft pneumatic actuator might be more suitable than the electromagnetic actuator because of its inherent compliance, flexibility, weight, safety, and interaction with the fingers [11]. However, the output forces are a weak point of the pneumatic actuators. Two designs of soft pneumatic actuators were able to generate output forces of 10.25 N and 11.38 N, respectively [12], [13]. However, these devices cannot be used by DMD patients, as the pneumatic actuator is integrated into the glove which will cover the own tactile senses [12]. For the design presented in [13], the bending can only be controlled with the other hand and DMD patients can use neither of their hands. This means that none of the devices currently on the market do completely fit the special needs of DMD patients. These needs include the usability of their own tactile senses [14], the ability to adapt the forces to prevent damage on their skin, and the weight and size of the hand orthosis. Since no dynamic hand orthoses are available for DMD patients, splints are used as an alternative. It was shown that only 9% of the DMD patients used a splint, though the percentage of patients that mentioned having difficulties with their upper extremities was much higher [3]. A reason for this could be that the splint does not give natural support or it is too prominently visible. For hand orthoses which are used for ADL, both cosmetics and comfort are really important as they are worn the whole day [15].

The authors are with the Delft Institute of Prosthetics and Orthotics, Department of Biomechanical Engineering, Faculty of Mechanical, Maritime and Materials Engineering, Delft University of Technology, 2628 CD Delft, The Netherlands.

This study aims to design a flat dynamic hand orthosis for DMD patients with Brooke scale grades 4, 5, or 6. A maximum finger orthosis height of 20 mm was seen as flat. This research focuses on a one-finger orthosis and not on a complete hand orthosis. Furthermore, the main goal is that the finger is able to generate a flexion movement and generates enough force to use the device during ADL. It is beyond the scope of this study to design the control mechanism and attachment system of the hand orthosis.

The structure of the paper is as follows. Section II describes the design criteria, the design and manufacturing of the prototype, and the experimental tests. The results from the design criteria, the final prototype, and the experimental tests will be shown in Section III. The results will be discussed in Section IV. Recommendations to improve the prototype will be described in Section V. Conclusions are drawn in Section VI. Appendix A gives an overview of the shape analysis that is carried out. The raw data is shown in Appendix B.

II. Materials and Methods

The following three phases were identified in order to develop a new finger for a hand orthosis.

A. Design Criteria. The different design criteria will be explained in this section, and an overview is given in the results.
B. Design and Manufacturing of Prototype. The design of the prototype will be explained in this phase. Furthermore, a description of the manufacturing process will be given.
C. Experimental Tests. Two different tests were carried out to analyze the prototype. These tests will be explained in this phase. The data analysis from the test results will be shown as well.

A. Design Criteria

This phase explains the design criteria used to evaluate the design of this research. As the focus of this paper is only on a one-finger orthosis, the design criteria are also focusing on the finger itself. The control mechanism and the attachment system are beyond the scope of this research.

1) Size: To make the device as comfortable as possible, the device should not be bigger than a cross-sectional area of 20 mm $\times$ 18 mm. This is the mean size of the finger of an adult man found on the DINED anthropometric database [16]. It is important to make the device as flat as possible to increase cosmetics and cause less harm to the user [15].

2) Weight: A maximum weight of 500 g for a complete hand orthosis was suggested by Aubin et al. [17]. As the device will be worn the whole day, weight is really important to increase the comfort [15]. When it is too heavy it is not comfortable to wear the device. Therefore, the finger part of the device should weigh no more than 50 g [18]. When a total weight of 300 g is seen as maximum weight, there is a weight of 50 g left for the hand part.

3) Forces: It is shown that all tasks for ADL, except for closing a horizontal zipper and inserting and removing a plug, require a maximum pinch force of 10.4 N [19]. Next to that, (1) can be used.

$$F_{\text{Pinch}} = \frac{mg}{4\mu} \tag{1}$$

Here, m is the mass to lift up, g the gravity and μ the friction coefficient. The number 4 represents four fingers [20]. Assuming $\mu = 0.25$, 10 N is necessary to lift up an object of 1 kg with four fingers [21]. Therefore, the goal is to reach a maximum output force of 10.5 N. Except for the output forces, shear force on the skin between the orthosis and the finger is important as well. Ideally, there should be no shear force on the skin between the finger and the orthosis, because the skin of DMD patients is very sensitive [8]. As the orthosis is placed on top of the finger, shear force is inevitable. The amount of shear force depends on how the orthosis is attached to the finger and is therefore out of scope of this research.

4) Degrees of freedom: The human finger has four degrees of freedom (DOF). Three DOF for flexion and extension in the metacarpophalangeal (MCP), proximal interphalangeal (PIP) and distal interphalangeal (DIP) joint and one for abduction and adduction in the MCP joint [22]. The human finger has mechanical coupling and synergies between tendons. This means that the control of the joints is coupled. This is called functional degrees of freedom (fDOF). For this study, the aim is to generate one fDOF, only for the flexion and extension. It is not necessary to generate support for abduction and adduction of the finger. However, flexion and extension are needed to grip something [23].

5) Range of motion: To make a flexion movement possible, flexion angles have to be defined. The range of motion (ROM) of the fingers is 20°–80° [24]. The MCP, PIP and DIP joints have functional angles of 61°, 60°, and 39°, respectively [18]. These values represents the movements of the human hand. With these movements, the device should be able to make palmar grasps and pinch grasps [25]. The human finger has a coupled motion between the MCP and PIP joint. Therefore, this design should also have a coupled motion [26].

6) Material of the device: The material of the device should not irritate the skin as the device should be worn the whole day. If the device causes skin irritation, this would decrease the comfort.

7) Use of the device: The hand orthosis should be used during ADL. It should be portable, light weight, and be able to generate the right movements for both palmar and pinch grasp [25].

B. Design and Manufacturing Prototype

The design is based on a soft pneumatic actuator. This actuator will be placed on top of the own finger to keep the own tactile senses intact. Note, the attachment system is beyond the scope of this research. A schematic overview is shown in Fig. 1. This prototype consists of an outer structure from silicone and an inner structure from polylactic acid (PLA). The inner structure is placed to give the air chamber a certain shape to control the inflation movement of the silicone.

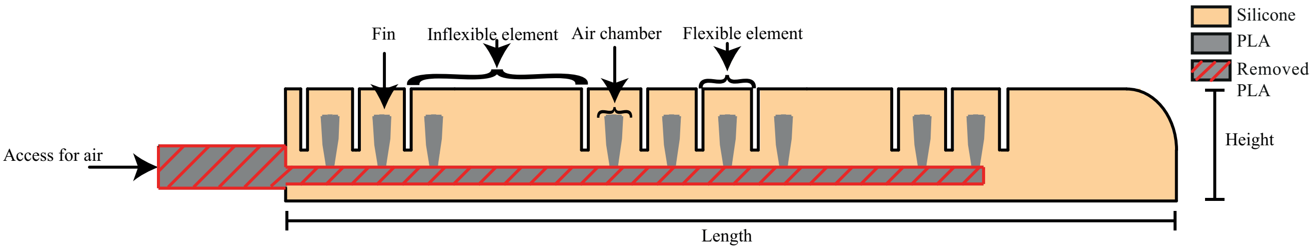

Fig. 1. Schematic drawing of the design of the finger from the side. The red marked area is the PLA rod that will be removed. This will become the access for air when the rod is removed. The gray PLA fins will stay inside the silicone. The air chamber is the space between the fins and the silicone.

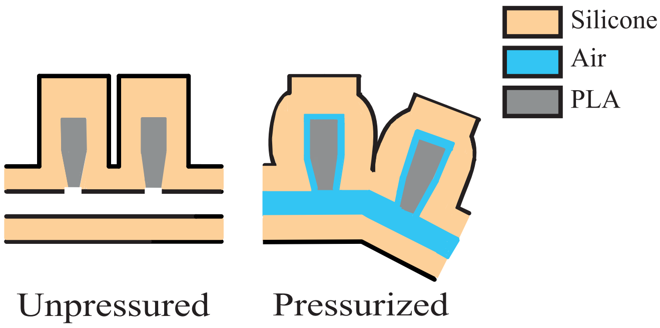

Fig. 2. Schematic drawing of two air chambers of the finger during unpressured state and pressurized state. The camel color part is the silicone, the blue part is the air and the grey part is the PLA. The white part is the open space in the silicone for the air.

This final shape has been reached with the help of finite element method (FEM) analysis. The outer shape and the inner structure, so called fins, were analyzed. For these fins, different tests were carried out as well. The results from the FEM analysis and tests are shown in Appendix A. The finger consists of air chambers, with fins inside. The PLA fins and the PLA rod are printed at once and then placed in the silicone. The fins were separated from the rod and the rod was removed to create an air tube. This is the red market part in Fig. 1. This resulted in an open space between the fins and the air tube. The air chambers are located at the positions of the MCP, PIP, and DIP joints. These are flexible elements. Between these joints there is only silicone which are inflexible elements. This change of flexible and inflexible elements resembles the human finger and results in a more optimal interaction with the fingers. As the human finger consists of inflexible phalanges and flexible joints as well. As pressure builds up in the air tube, the air will force its way past the fin, as the silicone does not bind here to the PLA. The difference in silicone thickness next to the fin and on top of the fin will result in an optimal inflation of the silicone next to the fin. Next to that, it will prevent radial expansion. The balloons will make contact with each other when they are sufficiently inflated. Therefore, the air chambers will set off against each other. This causes a moment on the air chamber, resulting in a bending motion of the finger. A schematic drawing of the bending motion is shown in Fig. 2. The air is shown in blue in this figure. As the material should be flexible, be able to extend, and be stiff enough to generate movements, the outer structure is made of Dragon Skin silicone with shore hardness A30. The inner structure is made of 3D printed PLA. This was fast to manufacture and made it possible to separate the fins from the rod. The air tube is connected to the finger with sil-poxy silicone adhesive. The manufacturing process consisted of the following steps:

1) The mold was designed with CAD software (Dassault Systèmes SolidWorks Corp., USA) and 3D printed (Ultimaker 3, The Netherlands) in TPU.
2) The Dragon skin silicone A30 (Smooth-On, Inc., PA, USA) was mixed within the ratio of 1:1.
3) The mixed silicone was placed in a vacuum chamber (Eurovacuum d513) for 5 minutes.
4) The silicone was casted into the mold, together with the 3D printed fins and rod from PLA (Ultimaker 3, The Netherlands).
5) The mold with the silicone was placed in a pressure chamber with a pressure of 4 bar for sixteen hours.
6) After removing the mold, the fins were separated from the PLA rod and the rod was removed.
7) A polyamide tube was added at the entrance as an air tube and connected to the finger with sil-poxy glue (Smooth-On, Inc., PA, USA).

C. *Experimental Tests*

1) Test setup: The finger was tested in both horizontal and vertical direction. Within these tests, the two extreme states of the actuator could be measured. The same test setup was used as described by [11] to make it possible to compare the results. In horizontal direction the finger was imbedded and the tip ended on a junior load cell (LSB200 1 Ib Futek JR S-Beam Load Cell 4.5 Newton, FUTEK Advanced Sensor Technology, USA). A detailed overview is shown in Fig. 3. The finger holder kept the finger in its position, and made it possible that only the tip was moving. To measure the output force from the tip, the tip should land perpendicular to the force sensor. Therefore, the force sensor was placed in an angle. Within this setup the output force of one flexible element could be measured. CO_2 gas was added to the finger with

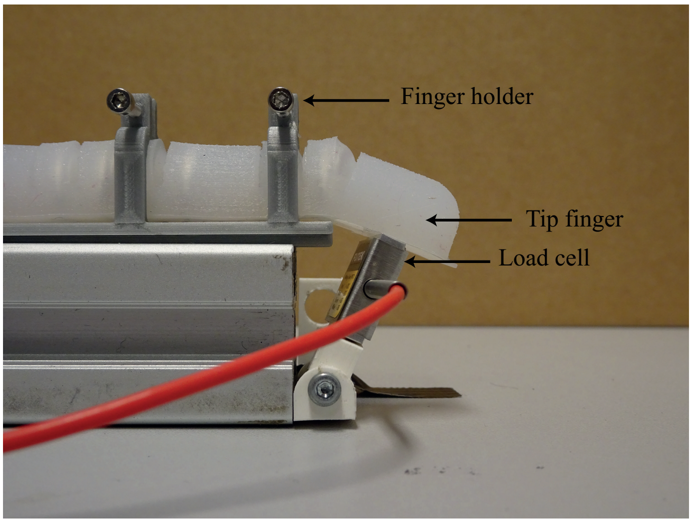

Fig. 3. Overview of the test setup in horizontal direction with the holder, the finger orthosis, and the load cell. The output force of the tip of the finger is measured in this position. This test is carried out with Version 1, consisting of three fins at the MCP joint, four fins at the PIP joint, and two fins at the DIP joint.

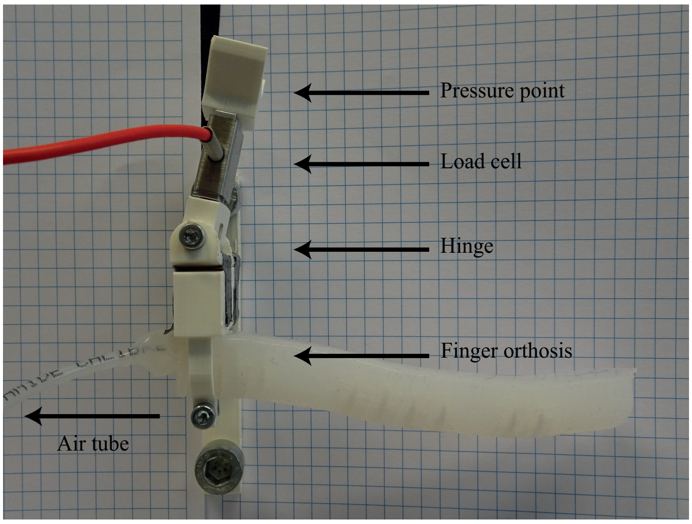

Fig. 4. Start position of the vertical test setup. This is the situation without air in the system. The pressure point leads the tip of the finger to the load cell, the load cell is placed in the correct angle with the hinge and is then blocked in this position.

a gas tank in small amounts. To measure the force in relation to the pressure, a pressure sensor (Gems sensors, 0-2.5 bar) was added to the system. The load cell was connected to the Multifunction I/O Device (National Instruments, 8 AI (12-Bit, 10 kS/s), 2 AO (150 Hz), 12 DIO USB), which was connected to the power and the analog signal conditioner (Feteris Scaime, Analog signal conditioner CPJ, board version) and connected to the computer. The data was observed with LabVIEW 2018 (National Instruments, USA). The finger was placed in the holder and tested ten times.

To analyze the bending angle and to measure the maximum output force during bending, a vertical test setup was made. This is shown in Fig. 4. The pressure point was used to lead the finger to the force sensor. In this situation, the output force was measured on its maximal bending position. The finger started in the position shown in Fig. 4, by adding CO_2 to the finger, the finger started to bend and moved upwards. The force sensor was positioned in such a way that the tip of the finger would land on the force sensor. A picture was taken in this position to measure the bending angle of each joint. Two different prototype versions were tested:

- Version 1: Three fins at the MCP joint, four fins at the PIP joint, and two fins at the DIP joint.
- Version 2: Three fins at the MCP joint, three fins at the PIP joint, and one fin at the DIP joint.

This was done to compare the differences between the bending angles and the number of fins. Less fins would reduce the chance for leakage but results in a sharper bending angle. Each test was carried out for at least five times to eliminate random error.

2) Data analysis: The data generated with LabVIEW was analysed with MATLAB 2018 (The MathWorks, The Netherlands). The raw data plots can be found in Appendix Figs. B.7–B.10. The results from the horizontal tests did not need any adaptations. On the contrary, a 1D digital filter was used for the results of the vertical tests. This filter slides along the data with a certain window of length N. The average value of the data within this window is calculated and plotted. Equation (2) shows the difference equation that defines the moving-average filter of a vector x. For N, a value of 6 was used.

$$y(n) = \frac{1}{N}(x(n) + x(n-1) + \cdots + x(n-(N-1))) \quad (2)$$

III. Results

A. Results Design Criteria

The results of the design criteria are shown in Table I. The table indicates if the design criteria is achieved or not. Except for the output force and the bending angle of the MCP joint all the criteria were achieved.

TABLE I
Overview design criteria and the results.

Design criteria	Requirement	Prototype results	Achieved
Size	$\leq$ 20 mm $\times$ 18 mm	13.5 mm $\times$ 13.2 mm	Yes
Weight	$\leq$ 50 g	20 g per finger	Yes
Output force	10.5 N	3.4 N horizontal	No
		0.6 N vertical	No
DOF	1 fDOF	1 fDOF	Yes
ROM	MCP 61°	MCP 35°	No
	PIP 60°	PIP 78°	Yes
	DIP 39°	DIP 58°	Yes
Joint motion	Should be coupled	Coupled	Yes
Material	No skin irritation	Silicone	Yes

B. Prototype

A schematic overview of the final design is shown in Fig. 1. The total length of the finger is 105 mm, the height is 13.2 mm, and the width is 13.5 mm. The total weight of the finger is 20 g. The finger consists of nine different air chambers, seven flexible elements and three inflexible elements. The combination of the mold with the fins and rod is shown in Fig. 5. The final size was based on the size used in [11], to make it possible to compare the results.

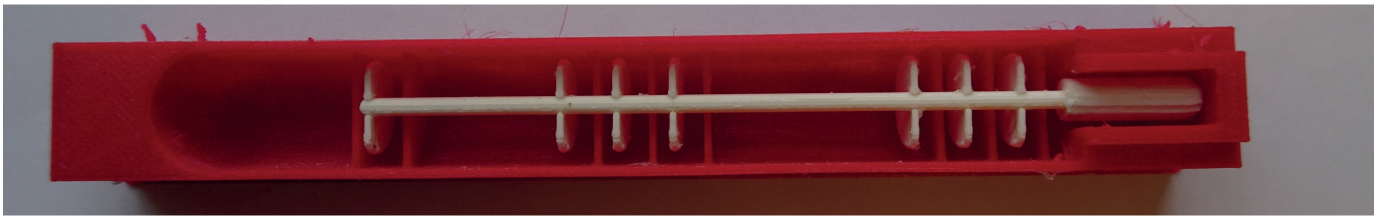

Fig. 5. Overview of the used mold in red, made from TPU, and the PLA fins inside in white.

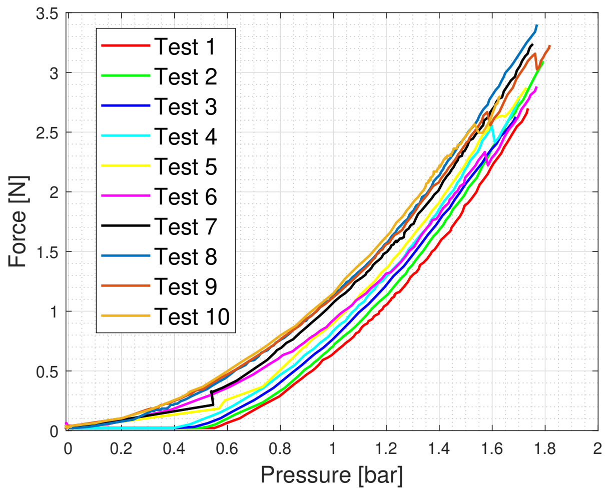

Fig. 6. The relation between the measured output force and the pressure in horizontal position. The tests were carried out with Version 1 consisting of three fins at the MCP joint, four fins at the PIP joint, and two fins at the DIP joint. Ten tests were carried out. Note the shift in the needed pressure to generate a movement from test 5 till 10.

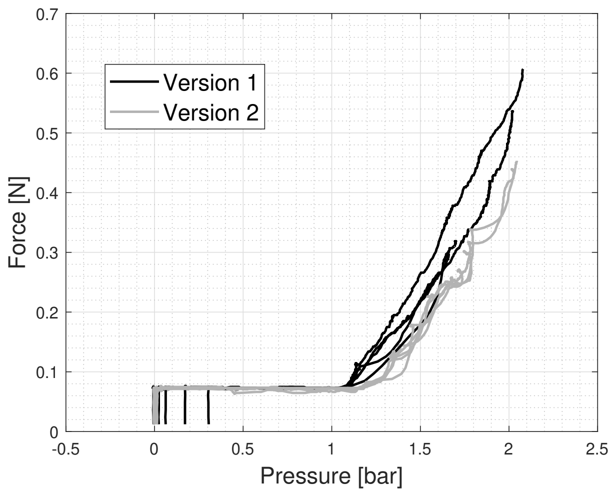

Fig. 7. The output force in relation to the pressure in maximal bending position. Finger Version 1 with three fins at the MCP, four fins at the PIP and two fins at the DIP joint and finger Version 2 with three fins at the MCP joint, three fins at the PIP joint, and one fin at the DIP joint were tested. For each finger five tests are shown. Note the difference in maximum output force between Version 1 and Version 2.

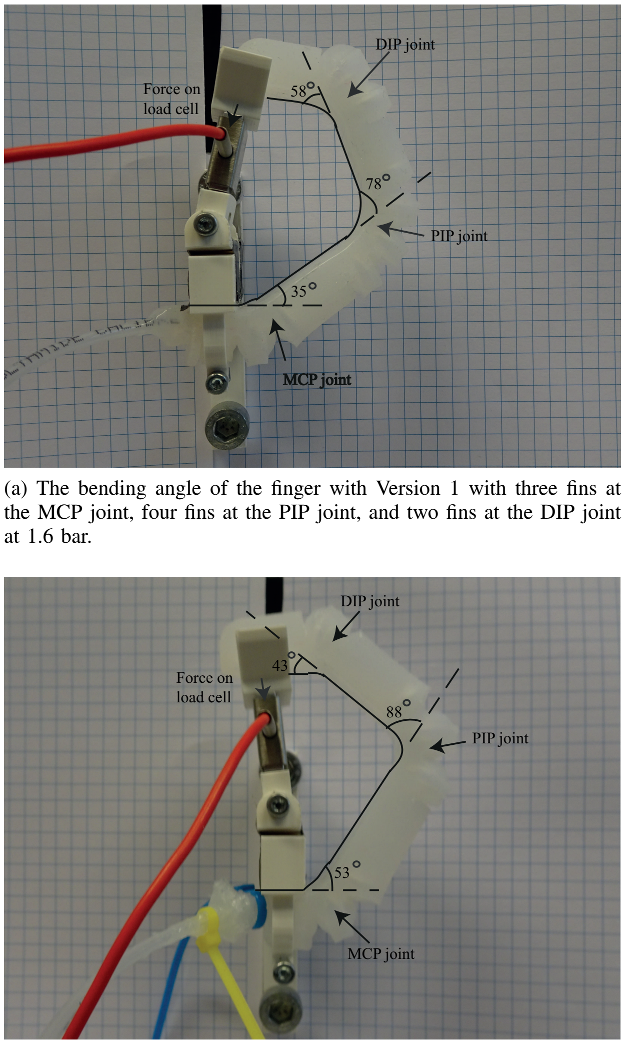

(a) The bending angle of the finger with Version 1 with three fins at the MCP joint, four fins at the PIP joint, and two fins at the DIP joint at 1.6 bar.

(b) The bending angles of the finger with Version 2 with three fins at the MCP joint, three fins at the PIP joint, and one fin at the DIP joint at 1.6 bar.

Fig. 8. The finger orthosis position at a pressure of 1.6 bar. The force on the load cell is measured in this position. The bending angles of the joints are mentioned. (a) shows Version 1 (b) shows Version 2.

C. *Results Experimental Tests*

1) Horizontal test: The results of the ten horizontal tests of the finger Version 1 are shown in Fig. 6. The maximum output force was 3.4 N at a pressure of 1.75 bar. Note that a shift takes place for tests five till ten for the needed pressure before the finger starts to move.

2) Vertical test: Fig. 7 shows the results of five vertical tests with both versions of the finger to compare the difference in output force in relation to the bending angle. The output forces for Version 1 were higher than for Version 2 with maximum output forces of 0.6 N and 0.44 N, respectively. The bending angles are presented in Fig. 8 and Table II to compare the influence of the number of fins. In Fig. B.11 in Appendix B, a detailed picture is presented to show the weak point of the finger in the maximal bending angle position at 2 bar.

TABLE II
BENDING ANGLE PER JOINT FOR DIFFERENT AMOUNT OF FINS.

Joint	Version 1	Version 2
MCP	35°	53°
PIP	78°	88°
DIP	58°	43°

IV. DISCUSSION

A. Design Interpretation

This paper presented the design of a finger for a new soft pneumatic actuator for DMD patients. This design is smaller than the mentioned criteria and is lightweight. Each finger weighs 20 g, whereas a weight lower than 50 g was set in the design criteria. This means that there is enough space left to make a frame to attach the fingers and to place it on the hand. It should be possible to make this with a maximum weight of 200 g. The finger is able to generate a flexion movement. In this design, the finger extends as soon as the air tube was disconnected from the gas tank. Therefore, the extension movement is not controlled. This means that there is 1 fDOF. However, it is not optimal as it is not comfortable to disconnect the device every time and to extend the finger in an uncontrolled movement. In this design, the motion of all joints is coupled. When willing by the user, it is possible to change the design in such a way that a decoupled motion is possible. This can be done by connecting the fins of each joint to its own air tube. This results in three air tubes to control. Furthermore, the device is made of silicone. Most users do not suffer from skin irritation after wearing a silicone device [27]. In case that the user experiences any irritation, it is possible to place another material between the finger and the device. The results from the output forces and the bending angles will be discussed based on the results from the tests.

B. Interpretation Tests

The horizontal tests were carried out for finger Version 1 and were shown in Fig. 6. Version 2 was not tested, as in this setup only the last air chamber was measured. The fingers were of the same length and material and therefore no differences were expected between Version 1 and Version 2. Ten tests were carried out to measure the maximum output force and to eliminate random error. This resulted in a maximum output force of 3.4 N at a pressure of 1.75 bar. It is striking that every test gave a higher output force with the same pressure. Furthermore, there is noted that for tests one till four, an output force will be measured from 0.4 bar, while from tests five till ten, an output force is already measured from the beginning. An equilibrium stage has been reached from test numbers 8, 9 and 10. This can be explained by elastic hysteresis of the silicone [28]. The shift is due to the strain of the polymer chains of the silicone [29]. On one hand, it is beneficial that the force becomes higher every time you use it. On the other hand, it will become hard to control the device if the output force is different every time you want to use it. As an equilibrium stage has been reached, this was not seen as a problem.

The vertical tests were done with the finger within Version 1 and Version 2. Five tests of each finger were carried out. A lower maximum output was expected compared to the horizontal position, as in horizontal position the force distribution is optimal. All the air chambers inflate, but because no bending takes place the contact surface between the inflated parts keeps optimal. That will cause that all the force within the system will reach the DIP joint. In vertical position, some losses take place, as all the air chambers inflate and the finger starts to bend. The maximum output force with Version 1 was 0.6 N at 2.1 bar. Note that this was really the maximum output force as the finger exploded at this moment. This happened at the last air chamber of the DIP joint. This is the weakest point of the finger as shown in Fig. B.11. The extreme inflation happened at this joint because the silicone had the space to do this. As the tip of the finger will be pushed away, the silicone get its space to inflate in the wrong direction. This causes an extreme inflation with a weak point as result. This shows that the silicone is not the optimal material for this geometry. As it was possible to carry out all the tests, and finding the most optimal material was out of scope of this research, no other material was used. The maximum output force with Version 2 was 0.44 N at 2 bar. This means that the number of fins and air chambers does not only effect the bending angles but also the maximum output forces. This is because Version 1 generated a bending angle of 58° for the DIP joint, while Version 2 had a bending angle of 43°. As the DIP joint in Version 1 consisted of two fins, each air chamber consisted of a bending angle of 29°. No bending means no force loss, as this is the optimal position. The bigger the angle, the more the air chamber will lose its strength. The contact area of the inflated part will become smaller, when the bending angle is bigger. Therefore, the output forces of Version 2 were smaller. Another point of interest is that the elastic hysteresis was not noticed here in vertical direction. Low output forces, might be the cause that this effect is not noticed. Furthermore, there were differences noticed between the bending angles of Version 1 and Version 2. The bending angles for the MCP joints were expected to be the same, as the same number of fins were used. Additionally, higher bending angles were expected, as the same number of fins were used as for the PIP joint of Version 2. However, that was not the case with a bending angle of 35° for the MCP joint of Version 1, 53° for MCP joint of Version 2, and 88° for the PIP joint of Version 2. This can be explained by the way the finger was attached to the holder. As can be seen in Fig. 8, Version 2 is placed more proximal compared to Version 1. In addition, the flexible element starts to bend as soon as it passed the block where it is connected. This means that for the final design, it is important to be aware how to connect the MCP joint to the hand part, as this has influence on the bending angle. The PIP and DIP joints were able to generate a bigger bending angle than necessary for both versions. Version 1 was chosen to be the preferred one, because the bending angle of the PIP joint is the closest to the bending of the own finger. Furthermore, the movement is smoother which will increase the comfort of the user. Also, the output forces were shown to be higher.

The differences in output forces for the horizontal and vertical position of the finger during measurements are large. Whereas in horizontal position the maximum output force can reach 3.4 N with a pressure of 1.75 bar, in vertical position the output force does not exceed the 0.6 N with 2.1 bar. This might be because in horizontal position the force distribution is optimal, all the pressure in the system goes to the DIP joint to exert a force. In vertical position some losses take place, as the finger starts to bend and inflates all the air chambers. Every bending means a loss of some percent of the output force. By comparing these results with literature, the maximum output force in horizontal position is higher than the design presented in [11]. This design reached a value of 3 N at 2 bar for the version with an outer structure and reached a value of 0.6 N at 1.2 bar for the version without an outer structure. Another design which also consists of flexible and inflexible elements results in output forces of 0.8 N at a pressure of 0.8 bar [30]. These results are comparable with the results presented in current research. The design placed an inflatable inner structure within the air chambers, instead of PLA fins. This means that the PLA fins do not have benefits to stay inside, but they do not have any drawbacks either. Better results with output forces around 10 N during bending were shown in [12], [13]. These devices used the same material as in current research, except that their finger was covered with an elastic material and hard material, respectively. This means that an outer structure would increase the output forces as well.

To sum up, the output forces in horizontal and vertical direction did not match the design criteria because of the limitations of the silicone. Furthermore, the other design criteria were met.

V. Recommendations

As the output force was not reached, some improvements are needed. One way to improve the output force is to find another material to fabricate the device. This material should be stronger than the silicone used in this design. The chance on leakages should be reduced, and the extreme inflation in the wrong direction of the DIP air chamber should be prevented. Therefore, another material would have multiple benefits. Another way to improve the output force could be to extend the air tube more distal on the inside and add an extra fin. This extra air chamber will inflate as well. This results in an extra contact area between the DIP joint and the finger tip. The bigger the contact area, the more forces will be passed. This might result in a higher output force. The last way to improve the output forces is to add an outer structure as done in [12], [13]. Nylon could be a solution. This will make the device not too stiff but it makes it possible to control the inflation of the silicone which will positively influence the output force. Dependent of the design this could prevent the extreme expansion in the DIP joint as well.

To let the device extend without first decoupling the device, a valve could be added to the entrance of the finger. One air tube is used to flex the finger as it does now. By changing the direction, an open connection is the result which will extend the finger again. Dependent on how the valve is controlled, a controlled extension movement could be the result. Furthermore, springs or elastics could be added on top of the finger to make an extension movement possible. However, more research would be needed to add this in an optimal way to prevent that the device will become too large.

To switch from a coupled motion to a decoupled motion, three separated inner structures should be made. First the inner structure for the MCP joint, these fins should be connected by an air tube on the left side. In the middle and on the right, the fins should have an opening for the air tubes for the PIP and DIP joints. The fins representing the PIP joint should be connected to the air tube in the middle and should have an opening on the right. The fins for the DIP joint should be connected to the air tube on the right. Important is that the openings should be big enough to prevent that the air tubes of the other fins touch the fins of the other joints. In this way, it should be possible to control each joint independently.

In this design, a solution was found for the connection between the finger and the air tube with the sil-poxy glue. However, this solution is not optimal for the long term as cable ties were needed for extra support. Therefore, a more reliable solution should be found.

VI. Conclusion

This paper presented a new design of a finger for a hand orthosis, consisting of a soft pneumatic actuator which can be used for DMD patients. This design consists of a silicone outer part and a 3D printed PLA inner part. The final design is flat, lightweight and able to generate a controlled flexion movement and an uncontrolled extension movement. The motion is coupled and the material does not irritate the skin. The required output forces were not reached due to limitations of the material and a lack of optimal inflation of the air chamber at the DIP joint. The bending angles were bigger than needed, except for the MCP joint, but this was due to the way it was attached to the holder during the experiments. Adding a cover on the outside of the silicone part of the hand orthosis might be a way to increase the output forces of the design. When it is possible to increase the output force and to design a controlled extension movement, this design could be further developed to make it possible to use it for DMD patients with Brooke scale grades 4, 5 or 6.

References

[1] J. C. Van den Bergen, H. B. Ginjaar, A. J. van Essen, R. Pangalila, I. J. M. de Groot, P. J. Wijkstra, M. P. Zijnen, N. A. M. Cobben, M. J. Kampelmacher, B. H. A. Wokke, I. de Coo, J. Fock, A. Horemans, M. van Tol, E. Vroom, M. Rijlaarsdam, C. Straathof, E. Niks, and J. Verschuuren, "Forty-Five Years of Duchenne Muscular Dystrophy in The Netherlands," *Journal of Neuromuscular Diseases*, vol. 1, no. 1, pp. 99–109, 2014.

[2] H. Sawnani, P. S. Horn, B. Wong, A. Darmahkasih, I. Rybalsky, K. C. Shellenbarger, C. Tian, M. M. Rutter, N. Simakajornboon, R. Amin, N. Gurbani, J. Pascoe, C. Burrows, S. Khirani, A. Amaddeo, and B. Fauroux, "Comparison of Pulmonary Function Decline in Steroid-Treated and Steroid-Naïve Patients with Duchenne Muscular Dystrophy," *The Journal of Pediatrics*, vol. 210, pp. 194 –200.e2, 2019.

[3] M. M. Janssen, A. Bergsma, A. C. Geurts, and I. J. De Groot, "Patterns of decline in upper limb function of boys and men with DMD: an international survey," *Journal of Neurology*, vol. 261, no. 7, pp. 1269–1288, 2014.

[4] Y.-M. Lu and Y.-J. Lue, "Strength and Functional Measurement for Patients with Muscular Dystrophy," in *Muscular Dystrophy*, M. Hegde and A. Ankala, Eds. IntechOpen, 2012, ch. 17, pp. 321–330.

[5] K. Klingels, A. G. Mayhew, E. S. Mazzone, T. Duong, V. Decostre, U. Werlauff, E. Vroom, E. Mercuri, N. M. Goemans, and U. L. C. O. Group, "Development of a patient-reported outcome measure for upper limb function in Duchenne muscular dystrophy: DMD Upper Limb PROM," *Developmental Medicine & Child Neurology*, vol. 59, no. 2, pp. 224–231, 2017.

[6] J. Weichbrodt, B.-M. Eriksson, and A.-K. Kroksmark, "Evaluation of hand orthoses in Duchenne muscular dystrophy," *Disability and Rehabilitation*, vol. 40, no. 23, pp. 2824–2832, 2018.

[7] C. Glasgow, L. Tooth, and J. Fleming, "Which splint? Dynamic versus static progressive splinting to mobilise stiff joints in the hand," *The British Journal of Hand Therapy*, vol. 13, no. 4, pp. 104–110, 2008.

[8] R. A. Bos, K. Nizamis, D. H. Plettenburg, and J. L. Herder, "Design of an Electrohydraulic Hand Orthosis for People with Duchenne Muscular Dystrophy Using Commercially Available Components," in *7th IEEE International Conference on Biomedical Robotics and Biomechatronics*, 2018, pp. 305–311.

[9] M. D. Baan, "Designs of flat dynamic hand orthosis a literature review," 2019, unpublished Literature Study, Delft University of Technology, Faculty of Mechanical, Maritime and Materials Engineering.

[10] R. A. Bos, C. J. W. Haarman, T. Stortelder, K. Nizamis, J. L. Herder, A. H. A. Stienen, and D. H. Plettenburg, "A structured overview of trends and technologies used in dynamic hand orthoses," *Journal of NeuroEngineering and Rehabilitation*, vol. 13, no. 1, p. 62, 2016.

[11] Z. Sun, Z. Guo, and W. Tang, "Design of wearable hand rehabilitation glove with soft hoop-reinforced pneumatic actuator," *Journal of Central South University*, vol. 26, no. 1, pp. 106–119, 2019.

[12] H. K. Yap, N. Kamaldin, J. H. Lim, F. A. Nasrallah, J. C. H. Goh, and C.-H. Yeow, "A Magnetic Resonance Compatible Soft Wearable Robotic Glove for Hand Rehabilitation and Brain Imaging," *IEEE Transactions on Neural Systems and Rehabilitation Engineering*, vol. 25, no. 6, pp. 782–793, 2016.

[13] Y. Jiang, D. Chen, P. Liu, X. Jiao, Z. Ping, Z. Xu, J. Li, and Y. Xu, "Fishbone-inspired soft robotic glove for hand rehabilitation with multi-degrees-of-freedom," in *IEEE International Conference on Soft Robotics*, 2018, pp. 394–399.

[14] L. A. Jones and S. J. Lederman, *Human Hand Function*. New York, NY: Oxford University Press, 2006.

[15] D. H. Plettenburg, "Basic requirements for upper extremity prostheses: the WILMER approach," in *Proceedings of the 20th Annual International Conference of the IEEE Engineering in Medicine and Biology Society*, vol. 5, 1998, pp. 2276–2281.

[16] J. Molenbroek, *DINED antropometric database*, Delft University of Technology, 2004. [Online]. Available: https://dined.io.tudelft.nl/en/database/tool

[17] P. M. Aubin, H. Sallum, C. Walsh, L. Stirling, and A. Correia, "A pediatric robotic thumb exoskeleton for at-home rehabilitation: the Isolated Orthosis for Thumb Actuation (IOTA)," in *IEEE 13th International Conference on Rehabilitation Robotics*, 2013, pp. 1–6.

[18] Q. A. Boser, M. R. Dawson, J. S. Schofield, G. Dziwenko, and J. S. Hebert, "Defining the design requirements for an assistive powered hand exoskeleton," *bioRxiv*, 2018, advance online publication.

[19] N. Smaby, M. E. Johanson, B. Baker, D. E. Kenney, W. M. Murray, and V. R. Hentz, "Identification of key pinch forces required to complete functional tasks." *Journal of Rehabilitation Research & Development*, vol. 41, no. 2, 2004.

[20] P. Polygerinos, K. C. Galloway, E. Savage, M. Herman, K. O'Donnell, and C. J. Walsh, "Soft robotic glove for hand rehabilitation and task specific training," in *IEEE International Conference on Robotics and Automation*, 2015, pp. 2913–2919.

[21] S. Derler and L. Gerhardt, "Tribology of skin: review and analysis of experimental results for the friction coefficient of human skin," *Tribology Letters*, vol. 45, no. 1, pp. 1–27, 2012.

[22] R. A. Bos, D. H. Plettenburg, and J. L. Herder, "Exploratory design of a compliant mechanism for a dynamic hand orthosis: Lessons learned," in *International Conference on Rehabilitation Robotics*. IEEE, 2017, pp. 603–608.

[23] C. J. Nycz, T. Bützer, O. Lambercy, J. Arata, G. S. Fischer, and R. Gassert, "Design and characterization of a lightweight and fully portable remote actuation system for use with a hand exoskeleton," *IEEE Robotics and Automation Letters*, vol. 1, no. 2, pp. 976–983, 2016.

[24] G. Bain, N. Polites, B. Higgs, R. Heptinstall, and A. McGrath, "The functional range of motion of the finger joints," *Journal of Hand Surgery*, vol. 40, no. 4, pp. 406–411, 2015.

[25] T. Feix, J. Romero, H.-B. Schmiedmayer, A. M. Dollar, and D. Kragic, "The GRASP Taxonomy of Human Grasp Types," *IEEE Transactions on Human-Machine Systems*, vol. 46, no. 1, pp. 66–77, 2015.

[26] A. D. Nimbarte, R. Kaz, and Z.-M. Li, "Finger joint motion generated by individual extrinsic muscles: a cadaveric study," *Journal of Orthopaedic Surgery and Research*, vol. 3, no. 1, p. 27, 2008.

[27] S. Jung, J. Schleusener, F. Knorr, M. Kraft, G. Thiede, H. Richter, M. E. Darvin, S. Schanzer, S. Gallinger, U. Wegener, and J. Lademan, "Influence of polyester spacer fabric, cotton, chloroprene rubber, and silicone on microclimatic and morphologic physiologic skin parameters in vivo," *Skin Research and Technology*, vol. 25, no. 3, pp. 389–398, 2019.

[28] H. K. Yap, J. H. Lim, F. Nasrallah, J. C. H. Goh, and R. C. H. Yeow, "A soft exoskeleton for hand assistive and rehabilitation application using pneumatic actuators with variable stiffness," in *IEEE International Conference on Robotics and Automation*, 2015, pp. 4967–4972.

[29] S. Wang, P. Wang, and T. Ding, "Resistive viscoelasticity of silicone rubber/carbon black composite," *Polymer Composites*, vol. 32, no. 1, pp. 29–35, 2011.

[30] J. Wang, Y. Fei, and W. Pang, "Design, Modelling and Testing of a Soft Pneumatic Glove with Segmented PneuNets Bending Actuators," *IEEE/ASME Transactions on Mechatronics*, 2019.

[31] H. Zhang, Y. Wang, M. Y. Wang, J. Y. H. Fuh, and A. S. Kumar, "Design and analysis of soft grippers for hand rehabilitation," in *12th International Manufacturing Science and Engineering Conference*. ASME, 2017.

[32] Y. Shapiro, A. Wolf, and K. Gabor, "Bi-bellows: Pneumatic bending actuator," *Sensors and Actuators A: Physical*, vol. 167, no. 2, pp. 484–494, 2011.

[33] P. Polygerinos, Z. Wang, J. T. Overvelde, K. C. Galloway, R. J. Wood, K. Bertoldi, and C. J. Walsh, "Modeling of Soft Fiber-Reinforced Bending Actuators," *IEEE Transactions on Robotics*, vol. 31, no. 3, pp. 778–789, 2015.

Appendix A
Shape analysis

A. Methods

1) FEM analysis: First a FEM analysis was carried out to analyze the shape of the flexible elements. Three different shapes of the silicone part were previously described in literature, namely a rectangular [31], a circular [32], and a semicircular shape [33]. All shapes were equal in width and thickness. The height was dependent on the geometry, and therefore it was different. The shape distribution and the output forces were analyzed. This was done in SolidWorks with the simulation section. A static analysis was chosen. The material selected for analysis was silicone as it was available in SolidWorks. As the goal of the FEM analysis was to compare the shape distributions relative to each other it was not a problem that the properties of the material were not exactly the same as the used silicone for the prototype. Assuming that a pressure of 2 bar was added to the finger, the resulted force on the finger was calculated. Equation (3) was used.

$$p = \frac{F}{A} \tag{3}$$

With p pressure, F the output force and A the area on which the force is working. An overview of the shape and the displacement is shown in Table A.ii.

Furthermore, a FEM analysis was used to compare three newly designed shapes of the fins. Three different shapes were compared. The first design was half as height as the original one, the second design was a curved design which was wider on top than at the bottom and the third design was a shape that was twice as thick as the original one. The thickness of the original fin was 0.6 mm as this was the minimal thickness that could be 3D printed without breaking. By reducing its height with a factor 2, the expanded area will become smaller and located lower. This might work for a more optimal connection area. By making a more curved shape of the fin, the silicone around the thicker part will be thinner. A thinner silicone means less resistance which influences the expansion of the silicone. The expansion area and connection area will become bigger, compared to the original one which will increase the output force. A thickened fin will also result in less silicone resistance and therefore a bigger expansion area. Air chambers were made in SolidWorks with an open inner structure with different fin shapes. A pressure of 2 bar was added during the FEM analysis on the inside of the air chambers. This pressure resulted in a deformation of the fin. The location and the size of this deformation were compared with the measured output forces of the different shapes.

The different fin shapes were analyzed with the horizontal tests. First the tests were done with the original fins inside with the A20 silicone. After that, one finger with three fins of each shape was manufactured and tested. By pushing the finger forward in the horizontal holder, each fin could be placed on top of the force sensor. In these positions, the output forces were measured. This was done with both the A20 and A30 silicone.

2) Data analysis: The data generated with LabVIEW was analyzed with MATLAB 2018 (Mathworks, The Netherlands). The raw data plots can be found in Figs. B.1 – B.6 in Appendix B. To compare the results from the shape analysis, the mean was taken for each shape. This was done for both the A20 and A30 silicone. The matrices of each test were not of the same length, and the increase of the pressure was also in different steps. Therefore, the values of each test with the same shape were placed below each other to make a new matrix. These values were sorted from low to high for the output forces. These values were all plotted. A 1D digital filter was used to plot one line. The values used for the windowSize (N) are shown in Table A.i. The fins with a half height made from the A30 silicone were more or less of the same length. By extending the shortest matrix with NaN, the mean between these two could be calculated. For these results was no filter necessary.

TABLE A.i
WindowSize settings for different shapes of the fins.

Shape	A20 silicone	A30 silicone
Half height	6	n/a
Curved	5	20
Twice as thick	8	5

B. Results

Table A.ii shows the different shapes of the flexible elements and the FEM analysis. The force that is stated in the table is the force that is needed with a pressure of 2 bar. The FEM analysis represents the displacement distribution. The maximum displacement values for the rectangular shape, round shape and semicircular shape were, 2.738×10^{-1} mm, 2.5555×10^{-1} mm, and 1.636×10^{-1} mm, respectively. As the differences were small, the semicircular shape was chosen since this shape will have a better fit on the users finger. The input force in relation to the displacement is smaller compared to the rectangular shape, and the bending resistance is lower compared to the other shapes [33].

In Table A.iii the results of the FEM analysis for the different shapes of the fins are shown. The measured output forces are the output forces measured during testing at a pressure of 0.6 bar. The first values are the results with the A20 silicone and the

TABLE A.ii
RESULTS DIFFERENT SHAPES FLEXIBLE ELEMENTS WITH THE FEM ANALYSIS.

Shape	Drawing of the shape	FEM result
Rectangular 114 N	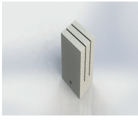	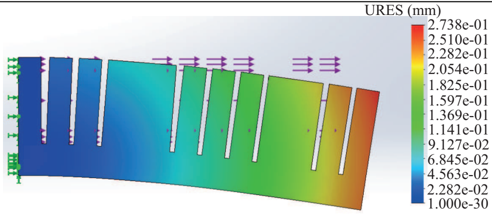
Circular 70 N	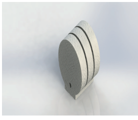	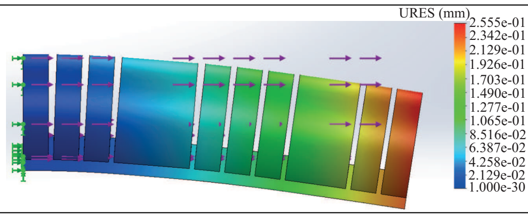
Semicircular 73 N	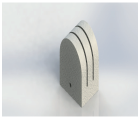	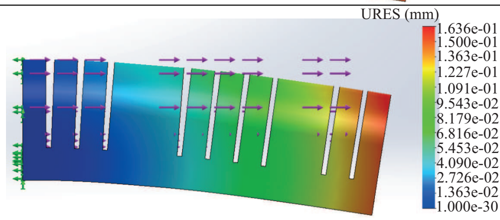

second with the A30. The maximum displacement values of the fin with half height, curved fin and thick fin were 3.993×10^{-5} mm, 2.240×10^{-4} mm, and 2.981×10^{-4} mm, respectively. The differences were really small, however the deformation location is different for each design as expected.

TABLE A.iii
RESULTS DIFFERENT FIN SHAPES WITH THE FEM ANALYSIS.

Shape	Result	Measured output force A20 and A30
 Fin with half height	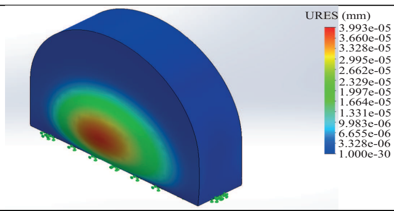	0.3 N and 0.4 N
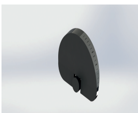 Curved fin	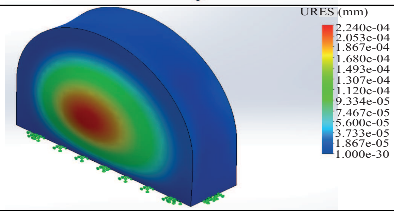	0.9 N and 0.5 N
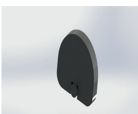 Thick fin	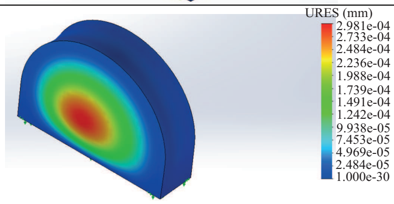	0.6 N and 0.3 N

Fig. A.1 shows the output forces with a certain pressure for the A20 and A30 silicone with different fin shapes. Here the original shape of the fin with A20 is also added. Because this value was lower than the value with the curved fin with the A20, this design was not tested with the A30 silicone. From these results the curved fin was chosen as final shape. For both the A20 and A30 silicone, this output force was the highest at 0.6 bar.

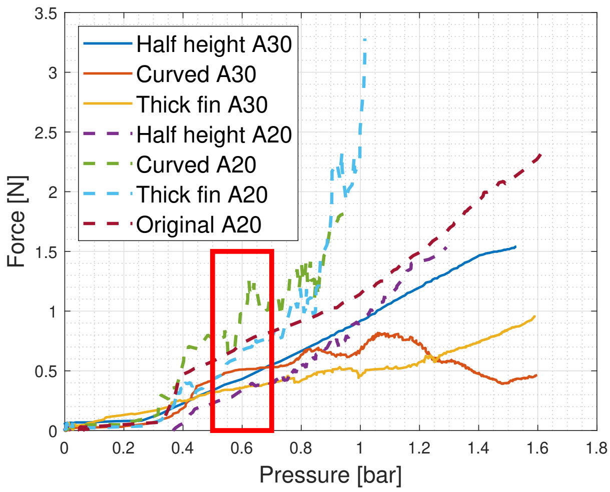

Fig. A.1. Plot with the results of the different shapes of the fins. The mean output for force in relation to the pressure for each fin shape is shown. The red square shows the area in which the shapes were compared. This is at 0.6 bar.

C. Discussion

The differences between the results from the FEM analysis for the flexible elements were small. As bigger differences were expected, this means that the FEM analysis was not optimal compared to the results found in [11], [33]. Therefore, the choice was not only based on the simulation but also on the results found in [11], [33]. The goal was to make a device as flat as possible to increase the comfort for the user [15]. Therefore, the semicircular shape was chosen. The results from the FEM analysis for the fins matched the expectations made beforehand. From the FEM analysis, the thick fin gave the most deformation as the resistance of the silicone was the lowest. However, the maximum expansion location of the curved fin was located lower than from the thickest fin, which resulted in a bigger contact area between the air chambers. This is in accordance with the results from the experimental tests. Note that the deformation scale is really low in the FEM. This has most probably to do with the fact that the properties of the simulated silicone were not exactly the same as the properties of the silicone used in the prototype. As not all the properties were known from the used silicone, it was decided to use the silicone properties which were available in SolidWorks. From the information that was known, it could be found that the simulated silicone was stiffer than the used silicone for the prototypes. This reduces the deformation of the silicone.

The shape analysis plot in Fig. A.1 was made to find the most optimal shape for the inner structure of the finger. It was expected that the A20 silicone would result in higher forces than the A30 silicone and that the different shapes would score in the same order. The curved fin shape gave the best results for both the A20 and A30 silicone. However, the half height and thickened fin showed different results between both types of silicone. This is because the means of multiple tests were plotted. The original data showed that the differences between the half height fins with A30 silicone were big, this resulted in a higher mean output force compared to the thick fin. This was not the case in the A20 silicone. Furthermore, the different lines fluctuate a lot. The key problem was what happened during the activation of the finger. Note that the fins were all placed in one finger. As soon as one of these fins was placed on top of the force sensor, the rest part of the finger was able to bend. At this moment the finger started to set off from the force sensor. This resulted in fluctuations in the output force. As for values higher than 0.6 bar this became more, there was decided to compared the results at 0.6 bar.

APPENDIX B
RAW DATA

The final design is made in the small size. To check what the optimal shape of the fin should be, different shapes were analyzed. As for each shape, at least two tests were carried out, the mean was taken to compare the results. This data was filtered to get the mean. The original data with the mean is shown in Figs. B.1 – B.6. To compare the influence of the amount of fins on the bending angle, two designs were made. Figs. B.7 – B.10 show a plot of the unfiltered data and filtered data for different number of fins in vertical position. As the A20 silicone was less reliable than the A30, there has been chosen to use the A30 silicone for the other tests. Fig. B.11 shows the details of the weak point of the finger.

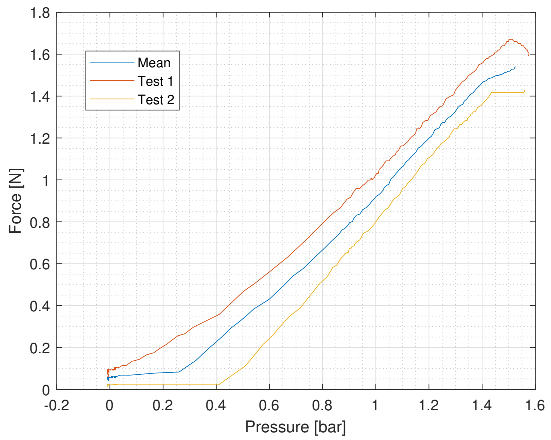

Fig. B.1. The output force in relation to the pressure is presented. The original data and the mean between the two tests is shown. This is for the half height of the fin shape with A30 silicone.

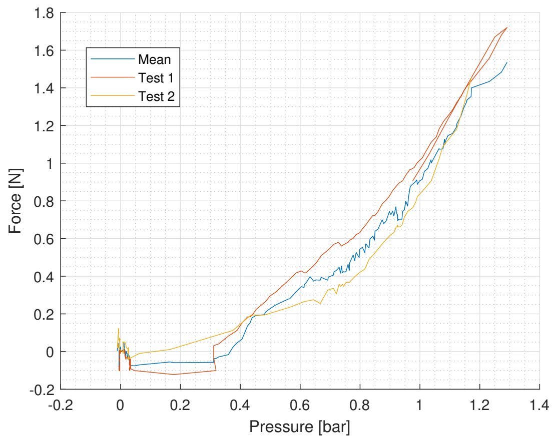

Fig. B.2. The output force in relation to the pressure is presented. The original data and the mean between the two tests is shown. This is for the half height of the fin shape with A20 silicone.

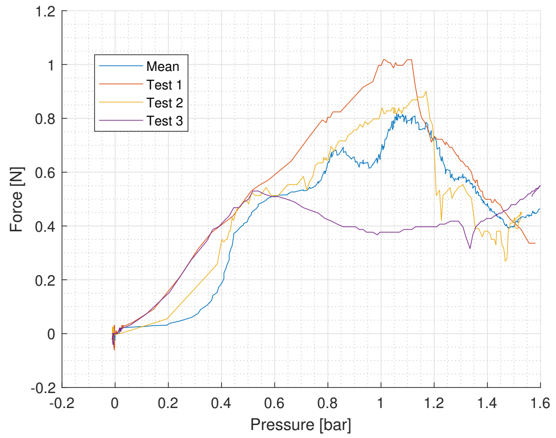

Fig. B.3. The output force in relation to the pressure is shown in the graph. The original data and the mean between the three tests is shown. This is for the curved fin shape with A30 silicone.

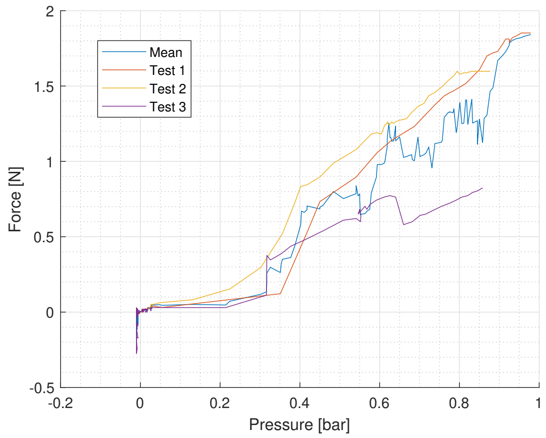

Fig. B.4. The output force in relation to the pressure is shown in the graph. The original data and the mean between the three tests is shown. This is for the curved fin shape with A20 silicone.

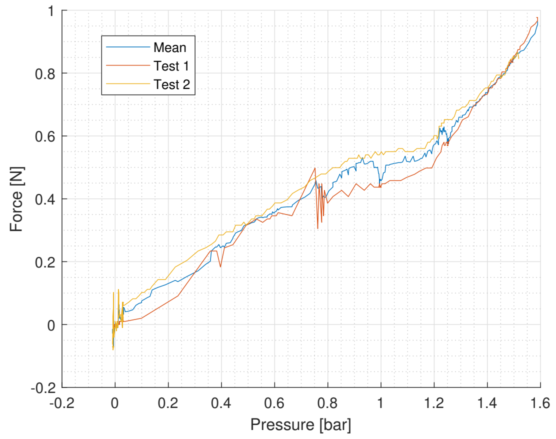

Fig. B.5. The output force in relation to the pressure is shown in the graph. The original data and the mean between the two tests is shown. This is for the thickened fin shape with A30 silicone.

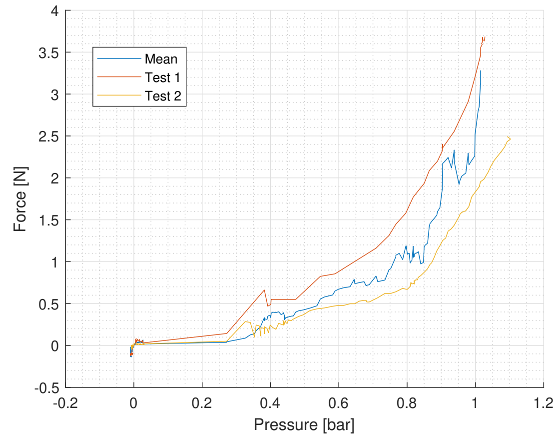

Fig. B.6. The output force in relation to the pressure is shown in the graph. The original data and the mean between the two tests is shown. This is for the thickened fin shape with A20 silicone.

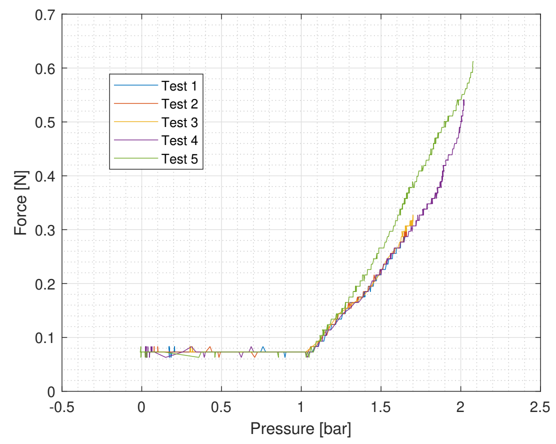

Fig. B.7. The output force in relation to the pressure is shown in the graph. This is the original unfiltered data of the finger Version 1with two fins at the DIP joint, four fins at the PIP joint and three fins at MCP joint.

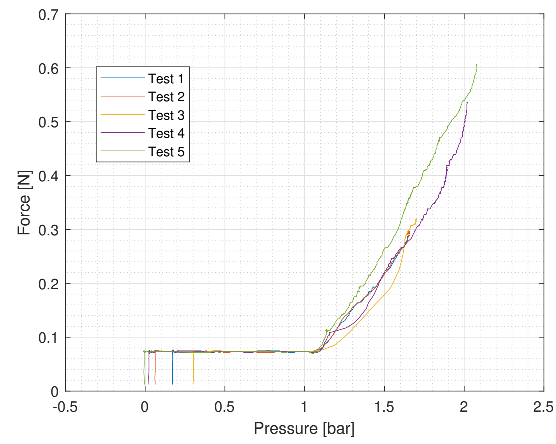

Fig. B.8. The output force in relation to the pressure is shown in the graph. This is the filtered data of the finger Version 1 with two fins at the DIP joint, four fins at the PIP joint and three fins at MCP joint.

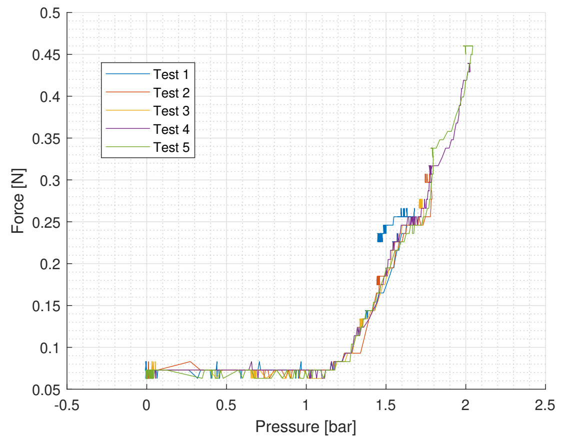

Fig. B.9. The output force in relation to the pressure is shown in the graph. This is the original unfiltered data of the finger Version 2with one fin at the DIP joint, three fins at the PIP joint and three fins at MCP joint.

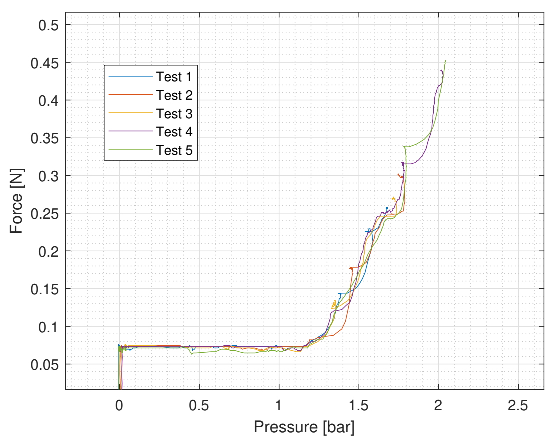

Fig. B.10. The output force in relation to the pressure is shown in the graph. This is the filtered data of the finger Version 2 with one fin at the DIP joint, three fins at the PIP joint and three fins at MCP joint.

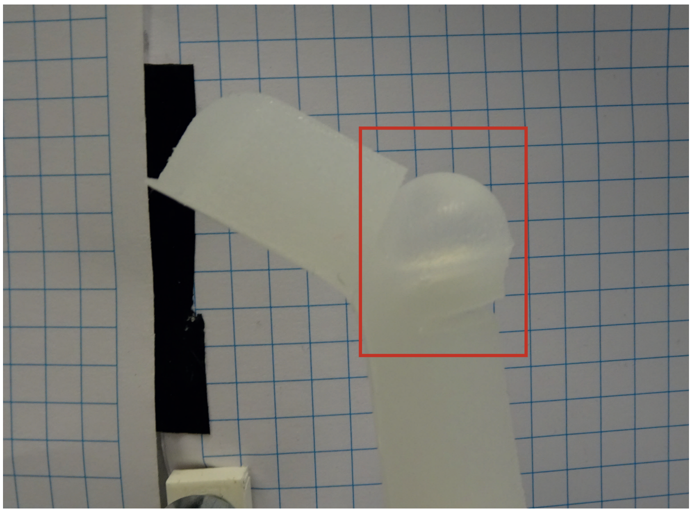

Fig. B.11. Overview of the weak air chamber at the DIP joint at 2 bar of finger Version 2, marked with the red square.

II

Literature study

2

Methods

In this chapter the search strategy will be shortly explained. This includes the inclusion and exclusion criteria used to select the right literature.

The structured overview from Bos et al. (2016) was used as a basis for this literature study. The current study will update the search done in Bos et al. (2016). Firstly, the "flat" wearable orthoses were selected from Bos et al. (2016). Assumed was that flat means a maximum thickness of 20 mm of the device on top of the own finger. This selection was made based on the images shown in the papers. The haptic devices which were used as a training device and not as an assistive device were excluded. These devices were excluded because, DMD patients need an assistive device to support with the daily tasks. Scopus database was used where the literature was selected from January 2016 until January 2019. The keywords used as search entries were[1]:

> **"(hand OR finger OR grasp*) AND (rehab* W/10 robot* OR glove OR exoskelet* OR orthosis OR "orthotic")".**

Table 2.1 shows the inclusion and exclusion criteria to select the right literature.

Table 2.1 Inclusion and exclusion criteria to select the right literature.

Inclusion criteria	Exclusion criteria
• Publication year was between 2016 and 2019 • The study presented at least a design of a dynamic hand orthosis • The image of the design shows a maximum height of 20 mm on the device • The dynamic hand orthosis supports at least one finger joint	• Non English literature • Incomplete articles • The device was not wearable • The device could not be used for ADL

After applying the inclusion and exclusion criteria, a first selection of the papers based on the title was made. The same inclusion and exclusion criteria were used to make a selection based on the abstract. From these results the images were checked, and only the flat dynamic hand orthoses were selected. Besides that, additional sources were added based on references or publications from the same author. These results were combined with the final selection from the structured overview from Bos et al. (2016). A schematic overview is shown in Figure 2.1.

[1] W/10 means that the terms rehab and robot must be mentioned within 10 terms, the order does not matter.

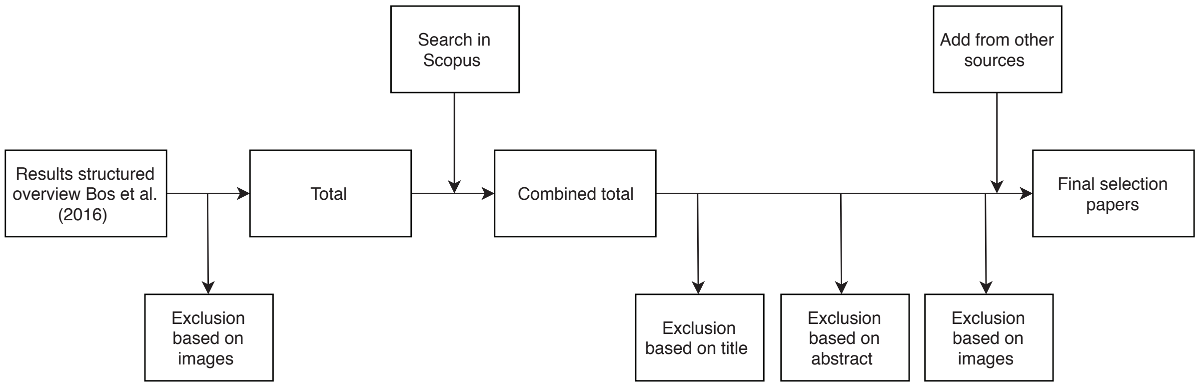

Figure 2.1 Visual representation of the search method.

3

Results

This chapter shows the different designs found during the literature study. Section 3.1 shows the search results. After that, in Section 3.2 the results structure which consists of the framework will be explained. Section 3.3 shows tables with the answers on the four sub-questions. These tables are categorised based on their actuation system. Finally, the most useful working principles will be explained in the Section 3.4.

3.1 Search results

The search entries in Scopus database resulted in a total of n=534 papers. Based on the title a first selection was made. After applying the inclusion and exclusion criteria, a total of 176 papers were left for analysis. This means that 358 papers were excluded. By applying the inclusion and exclusion criteria on the abstracts, 46 papers were excluded which resulted in a total of 130 papers. From these results the images of the orthoses were checked, and only the flat dynamic hand orthoses were selected. Besides that, additional sources were added based on references or publications from the same author. These results were combined with the final selection from the structured overview from Bos et al. (2016). This resulted in a total of 71 papers with 48 designs. An overview of the selection procedure including the numbers is shown in Figure 3.1.

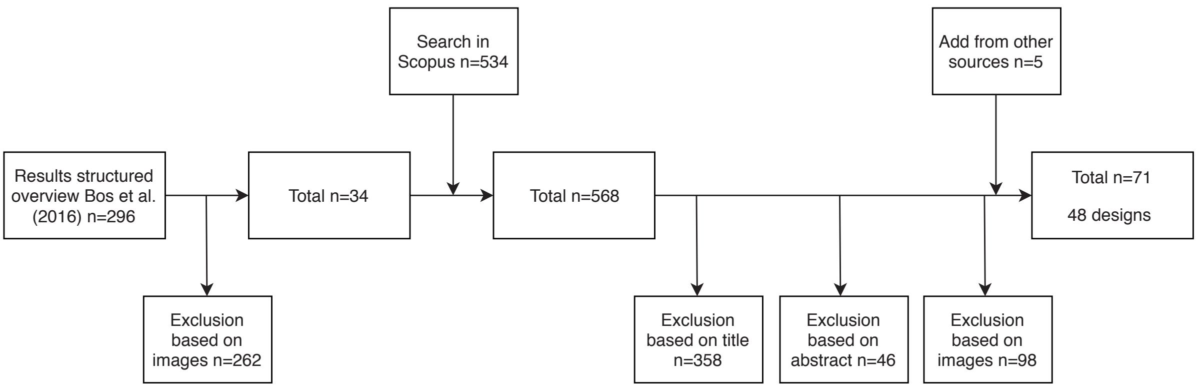

Figure 3.1 Visual representation of the search method and results.

3.2 Results structure

To organize the papers, the same framework as used in Bos et al. (2016) was implemented in current report. The framework is shown with the help of tree diagrams shown in Figures 3.2 - 3.4. The tree diagrams are extended with the newly found designs. The red numbers were the papers of Bos et al. (2016) and the black numbers indicate the new search. Not all subcategories will have a number because this literature research is only focused on devices which could be used for ADL. The tree diagrams are subdivided into three different areas:

- Signal domain, which consists of the controller, command signal and user feedback.
- Energy domain, that shows the energy storage and actuation of the dynamic hand orthosis.
- The mechanical domain, which distinguish the transmission and mechanism.

Furthermore, the complete framework is summarised in a table. This table can be found in Table A.1 in Appendix A.

3.2.1 Signal domain

Figure 3.2 shows how the different parts of the signal domain are related to each other and how often each result occurs. The signal shows how the device can be controlled by the user and how the device's status is shown to the user. This means that the controller can be assistive, active, passive, passive-mirrored, active-assistive, corrective, path guidance and resistive. These interim stages are the same as used in Basteris et al. (2014). An assistive controller means that the subject is the one who controls the orthosis. However, the system could support the user with some weights or forces. An active controller is used as a measurement device without forces on the limbs of the subject. The orthosis performs the movement in the case of the passive controller. The passive-mirrored controller means that the affected side is controlled by the unimpaired limb. Besides, there is a possibility for active-assistive control. That means that there is only assistance when needed. Using corrective control, the user can stop the orthosis when errors take place. Next to that, the orthosis is working on its own. Path guidance control means that that subject is guided through preprogramed path. This is merely used for training than for daily tasks. Finally, resistive control means that the orthosis provides force against the movement. The command signal of the orthosis could be in series, parallel and external. Brain, nerve or muscle activity are parts of the series signals, together with muscle contraction, plant movement and plant forces. Where plant is a mechanical structure of a skeleton and passive tissues. The parallel command signals could be generated with the eyes, head, mouth or other limbs. The external command signals could be generated by another person. Finally, the feedback part is subdivided into augmented feedback and attenuated feedback.

3.2.2 Energy domain

The relation between the energy storage and actuation system is shown in Figure 3.3. The energy domain establishes the source of energy and shows how the energy is converted into mechanical work. The energy storage could be chemical, electric/magnetic or mechanical. From this subdivision it is separated into liquid fuel and metabolic for the chemical part. Battery, capacitor or magnetic field are parts of the electric/magnetic part. The mechanical part consists of elastic energy, hydraulic pressure, pneumatic pressure and kinetic energy. The actuation systems are subdivided into, chemical, electric/magnetic, mechanical or thermal category. Chemical system could be a human muscle or a combustion engine. Electromagnetic, ceramic piezoelectric polymeric piezoelectric and smart fluid are part of the electrical/magnetic actuation system. Hydraulic and pneumatic are mechanical actuation systems. Bimetallic, shape memory alloy (SMA) and twisted polymeric muscle (TCP) are placed into thermal.

3.2.3 Mechanical domain

To establish the transportation of the mechanical work and the assistance of the joints, the next division was made as shown in Figure 3.4. The components consist of cable-conducts, fluidic transmission, direct transmission and a pulley system. There are three types of cables used: Bowden cables, push-pull cables and cables with a flexible shaft. Bowden cables are flexible cables that transmit forces by using an inner cable (Hofmann et al., 2018). The push pull cables are able to transmit forces between two fixed points. Flexible shaft cables transmit rotary motion between two objects which are not fixed relative to each other. The fluid transmission could be hydraulic or pneumatic. Hydraulic transmission uses hydraulic fluids which is pressurized to power hydraulic systems. Because of the pressure differences there is a transfer of energy. The difference with a pneumatic system is that gases are used instead of liquid. Direct, bar linkage, compliant mechanism, gears and cam-followers are all part of the direct transmission component. The pulley system could be a cable, chain or belt. The last part is the mechanical mechanism which could be divided into device structure, joint articulation, underactuation and constraints. The structure could be portable or fixed.

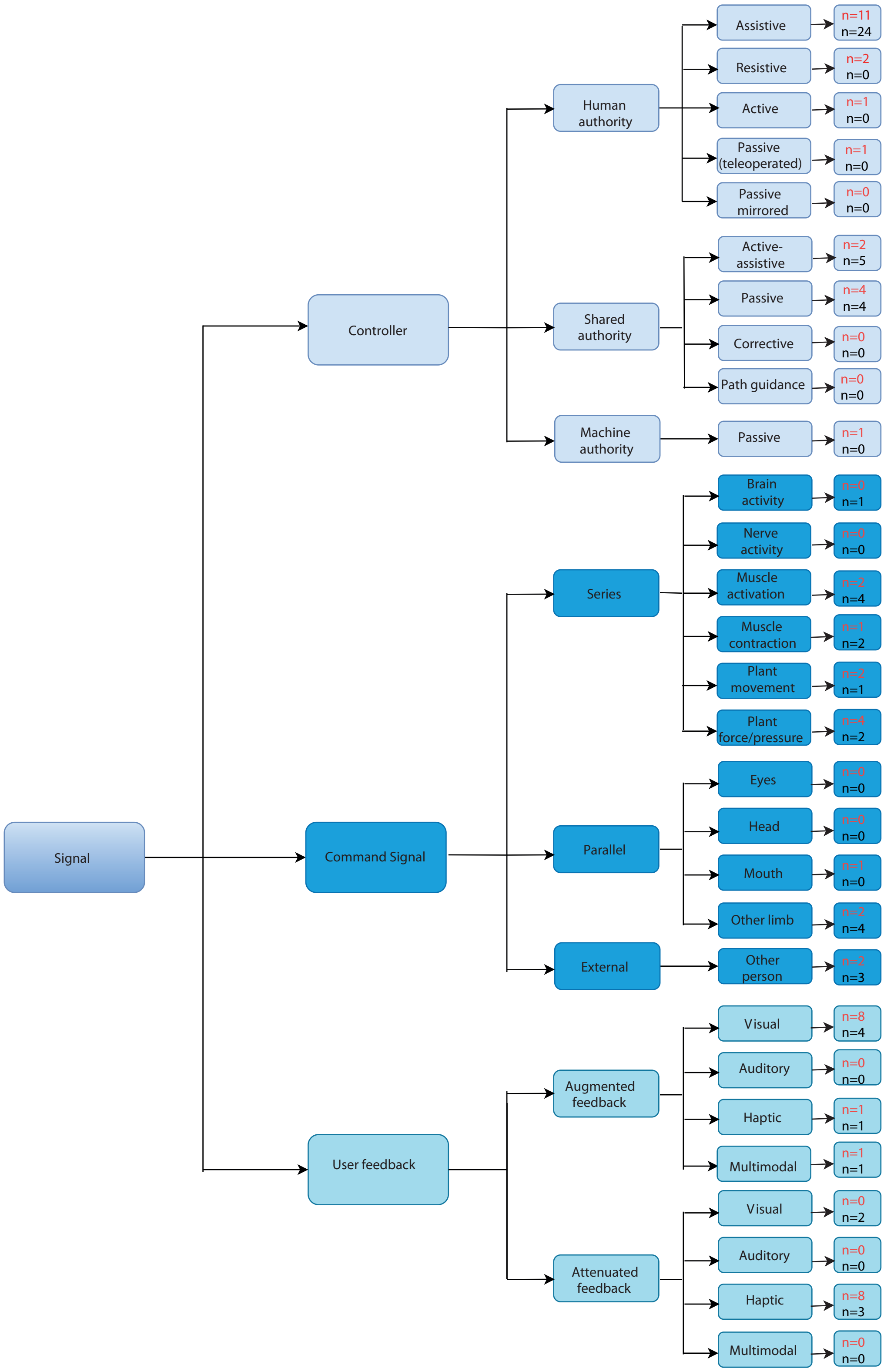

Figure 3.2 Tree diagram signal domain, showing the correlation between control and feedback (numbers in red from Bos et al. (2016), numbers in black for current study).

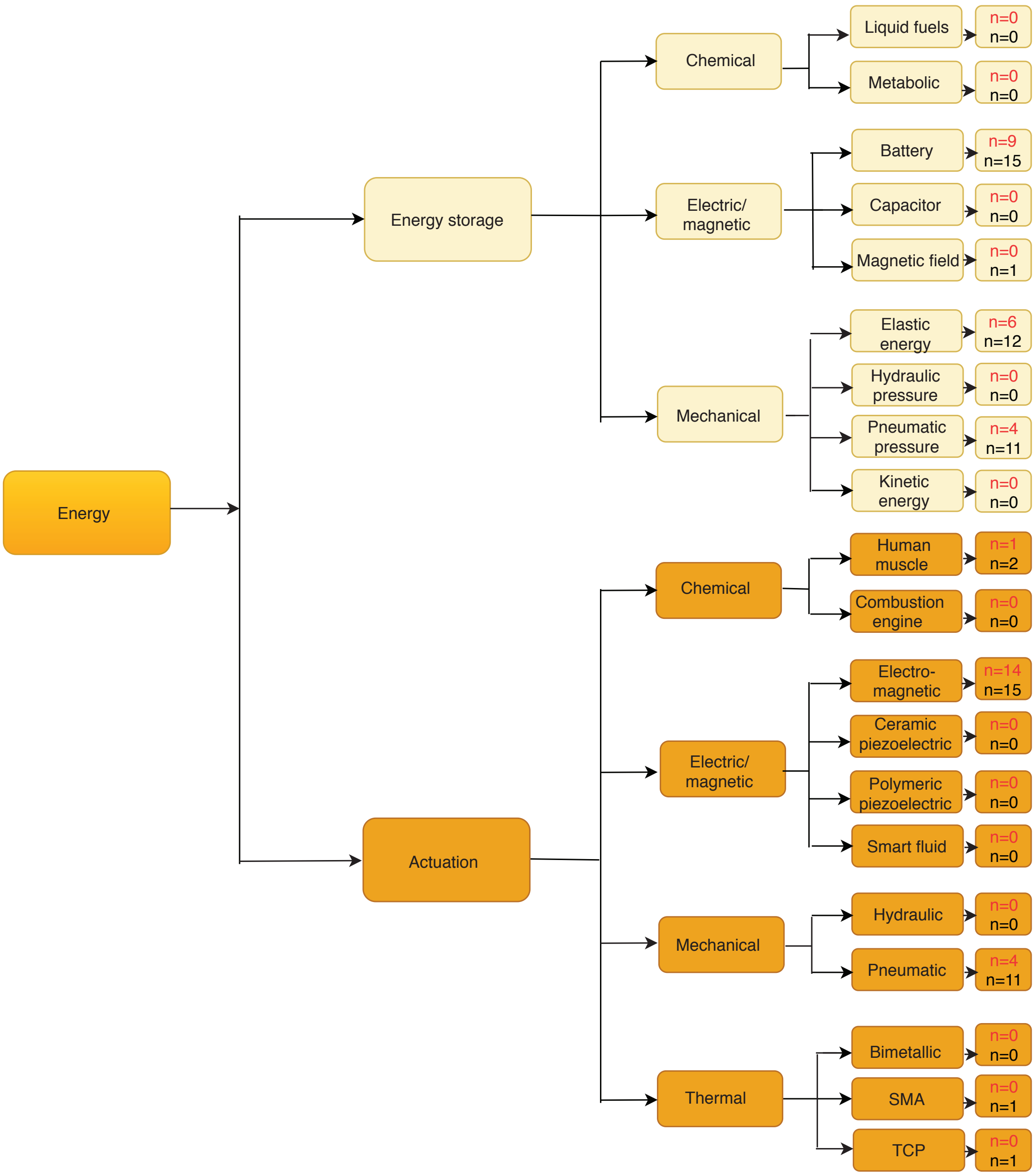

Figure 3.3 Tree diagram energy domain,showing the correlation between energy storage and actuation (numbers in red from Bos et al. (2016), numbers in black for current study).

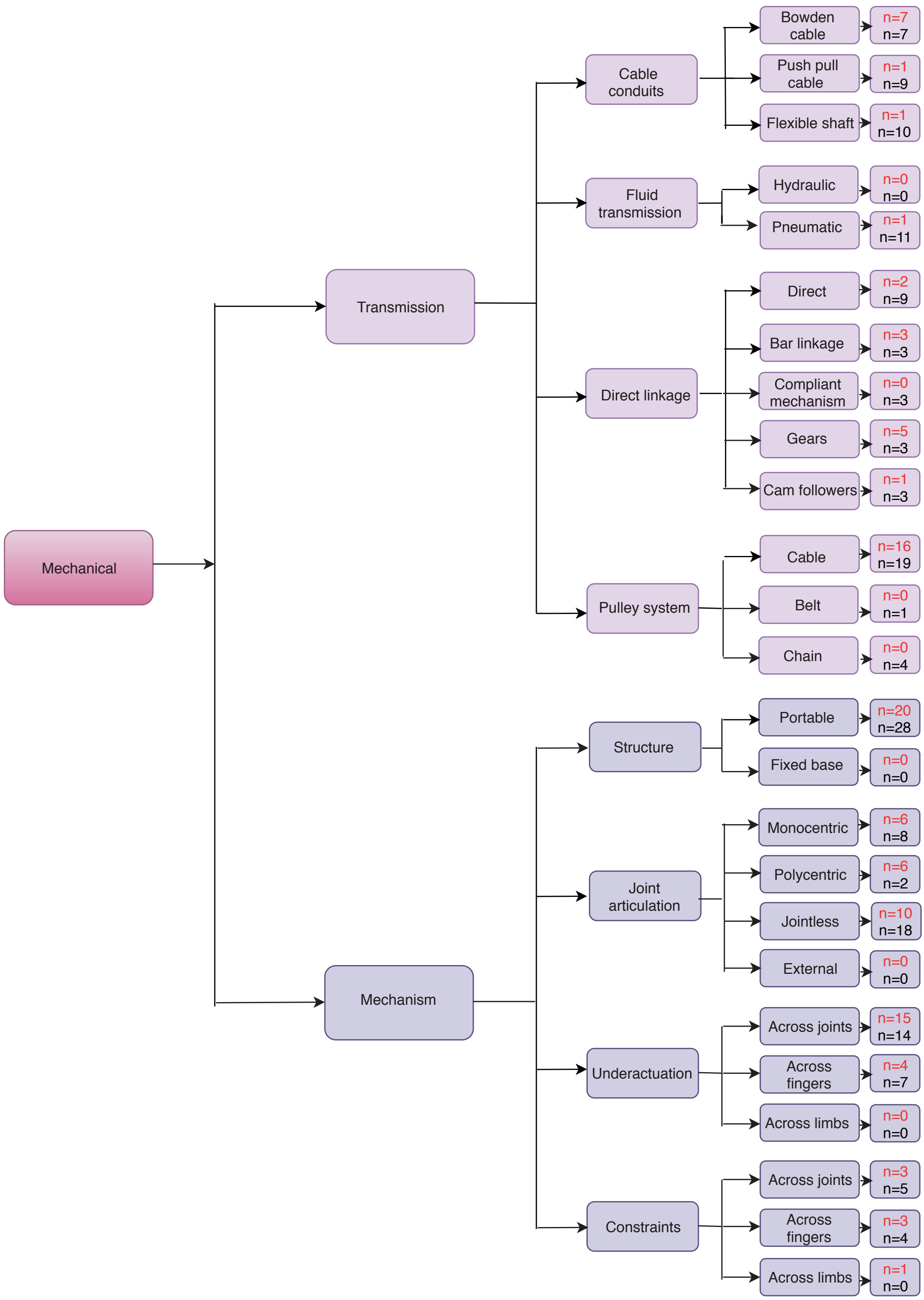

Figure 3.4 Tree diagram mechanical domain, showing the correlation between transmission and mechanism (numbers in red from Bos et al. (2016), numbers in black for current study).

The joint articulation is divided into monocentric, polycentric, jointless or external. Monocentric is when the joint can only move in one direction. Polycentric is when the joint can move in multiple directions. Jointless are the gloves which do not have any joints. External joint articulation are end effector devices. The underactuation is across joints, fingers or limbs. Underactuation means that there are more degrees of freedom than actuators. The constraints are also across joints, fingers or limbs.

3.3 Results sub-questions

The results of the different orthoses designs will be shown in different tables categorised into the following groups.

- Chemical: human muscle
- Electric/magnetic: electromagnetic
- Mechanical: pneumatic
- Thermal: SMA and TCP
- Miscellaneous

The human muscle actuation system comprises the systems which only use the human muscle to control the orthosis. These are listed in Table 3.1. The actuator systems with electro motors are set out in Table 3.2. It is important, that only the designs which really mention that they use a motor are placed in this category. In the mechanical category are all the pneumatic orthoses placed. This is illustrated in Table 3.3. The designs which use both an electro motor and a pneumatic actuation system, are placed in both tables. The SMA is the thermal actuation system shown in Table 3.4 together with the TCP. The miscellaneous table provides the designs which did not clearly mention the actuator system. This is in Table 3.5.
The results of the four sub-questions as mentioned in Chapter 1 will be shown in the tables. The maximum forces are given in Newton units. A maximum force of at least 18 N is seen as the minimum force that is needed to use the orthosis for ADL. These values are shown in bold in the tables. For the verification and validation is shown if there were simulations, dummy hand tests, healthy person tests or patient tests. In case of patient tests, the number of patients is mentioned. Note that the Sub-question 1: ‘To what extent is the design reproducible?’ and Sub-question 2 ‘Which design of the hand orthosis can be used for DMD patients?’ are shown in this chapter, however, they will be explained in Chapter 4, the discussion.

Table 3.1 Results chemical actuation system.

Name	**Design reproducible**	**Promising for DMD**	**Maximum forces**	**Verification and validation**	**Reference**
GRIPIT glove	no	no	unknown	4 patients	Kim et al. (2017)
SaeboFlex	maybe	no	unknown	on the market	Hoffman and Blakey (2011)
HandSome	maybe	no	unknown	7 patients	Chen et al. (2017a)

Table 3.2 Results electric/magnetic actuation system.

Name	Design reproducible	Promising for DMD	Maximum forces	Verification and validation	Reference
PMHand	maybe	maybe	unknown	1 healthy subject	McConnell et al. (2014)
HX HANDEXOS	yes	yes	unknown	4 healthy subjects	Cempini et al. (2015) Cempini et al. (2013a) Chiri et al. (2012) Chiri et al. (2009)
OHAE	yes	yes	**29.4 N**	4 healthy subjects	Gearhart et al. (2016) Baqapuri et al. (2012) Martinez et al. (2010) Rotella et al. (2009)
Toochinda	maybe	maybe	4.9 N	1 healthy subject	Toochinda and Wannasuphoprasit (2018)
HIT-glove	no	maybe	unknown	1 healthy subject	Zhang et al. (2014) Fu et al. (2011)
PU	yes	yes	5 N	dynamic model tests	Pu et al. (2015) Pu et al. (2014)
Cui	maybe	maybe	unknown	unknown	Cui et al. (2015)
Vanderbilt	yes	yes	**50 N**	1 patient	Gasser et al. (2017) Gasser and Goldfarb (2015)
BiomHed	yes	no	unknown	4 patients, 10 healthy subjects	Lee et al. (2014) Kim et al. (2014)
X-glove J-glove	yes	maybe	unknown	13 patients	Ghassemi et al. (2018) Yuan et al. (2017) Ochoa et al. (2011) Ochoa et al. (2009)
Flexo-glove	yes	maybe	**48 N**	different grips	Mohammadi et al. (2018)
Exotendon glove	yes	no	**20 N**	1 healthy subject	Kudo et al. (2014)
EXO-Glove	maybe	maybe	**40 N**	1 patient, 1 healthy subject	In et al. (2015) Jeong et al. (2015)
Delph II	maybe	no	unknown	unknown	Nycz et al. (2015)
M.ReS	maybe	yes	unknown	unknown	Weiss et al. (2013)
FEX	yes	yes	unknown	4 patients, 4 healthy subjects	Sale et al. (2017)
Yang	maybe	no	unknown	dummy hand	Yang et al. (2016)
Soft robotic exo-sheath	maybe	yes	**35 N**	dummy hand	Guo et al. (2018) Lu et al. (2016)
PU II	yes	yes	unknown	simulation	Pu et al. (2016)
Hasegawa	no	maybe	2.5 N	none	Hasegawa and Suzuki (2015) Hasegawa et al. (2008)
Refour	yes	yes	10 N	dummy hand	Refour et al. (2018)
MR glove	maybe	no	**41 N**	1 healthy subject	Yap et al. (2017) Yap et al. (2016)
Biggar	no	no	unknown	dummy	Biggar and Yao (2016)
AirExglove	maybe	no	5 N	1 patient	Stilli et al. (2018)
Lin	maybe	no	**55 N**	simulation	Lin et al. (2018)
RELab tenoexo	yes	yes	**40 N**	1 healthy subject	Nycz et al. (2016)
Niestanak	no	no	unknown	no complete test	Niestanak et al. (2017)
Liang	no	no	unknown	variable stiffness	Liang et al. (2018)
Cheng	yes	yes	**95 N**	1 healthy subject	Cheng et al. (2018)

Table 3.3 Results mechanical actuation system.

Name	Design reproducible	Promising for DMD	Maximum forces	Verification and validation	Reference
MRC- glove	maybe	maybe	9.25 N	1 healthy subject	Yap et al. (2015b) Yap et al. (2015a)
Jiralerspong	maybe	maybe	1 N	1 bending test	Jiralerspong et al. (2018)
PneuGlove	maybe	no	unknown	14 test subjects	Connelly et al. (2010)
UoA hand exoskeleton	maybe	maybe	**30 N**	simulation	Tjahyono et al. (2013) Surendra et al. (2012)
Cappello	maybe	maybe	unknown	9 patients	Cappello et al. (2018) Polygerinos et al. (2015)
Shiota	maybe	maybe	unknown	Kapanji test	Shiota et al. (2019) Shiota et al. (2016)
Refour	yes	yes	10 N	dummy hand	Refour et al. (2018)
Al-Fahaam	maybe	maybe	**40 N**	1 healthy subject	Al-Fahaam et al. (2018)
MR glove	maybe	no	**41 N**	1 healthy subject	Yap et al. (2017) Yap et al. (2016)
Rehab glove	maybe	maybe	**20 N**	dummy hand	Wang et al. (2017)
Jiang	maybe	maybe	11.38 N	1 healthy subject	Jiang et al. (2018) Jiang et al. (2017)
AirExglove	maybe	no	5 N	1 patient	Stilli et al. (2018)
Lin	maybe	no	**55 N**	simulation	Lin et al. (2018)
Gobee	no	maybe	**50 N**	6healthy subjects	Gobee et al. (2017)
Lobster inspired	maybe	maybe	2.5 N	dummy hand	Chen et al. (2017b)

Table 3.4 Results thermal actuation system.

Name	Design reproducible	Promising for DMD	Maximum forces	Verification and validation	Reference
ASR glove	maybe	no	**40 N**	dummy hand	Hadi et al. (2018)
iGrab	maybe	no	2.84 N	dummy hand	Saharan et al. (2017a) Saharan et al. (2017b)

Table 3.5 Results of the miscellaneous actuation systems.

Name	Design reproducible	Promising for DMD	Maximum forces	Verification and validation	Reference
PRoGS	no	no	unknown	none	Wee et al. (2011)
Ong	no	maybe	unknown	dummy hand	Ong and Bugtai (2018)
Tape spring orthosis	maybe	yes	unknown	unknown	Haarman et al. (2018)

3.4 Explanation designs

To make it more clear which devices are found in literature, this section describes the mechanisms that are used the most. The subsections represent the different actuation systems as mentioned before.

3.4.1 Chemical actuation system

The chemical actuation system that works on the human muscle consists of three different mechanisms presented in Figure 3.5. First, the GRIPIT (Kim et al., 2017) shown in Figure 3.5(a) will be explained. In this design a wire is used. With the other hand the wire is pulled tight which makes it possible to grip something. Second, the Saeboflex (Hoffman and Blakey, 2011) is found in Figure 3.5(b). The user grasps an object by flexing her or his fingers by themselves. At a certain point the fingers will relax, then the extension spring system helps to extend the fingers and release the object. One spring is connected to all the fingers and let the fingers extend when the spring contracts. Third, the Handsome (Chen et al., 2017a), this is a four bar linkage mechanism as seen in Figure 3.5(c). The mechanism helps to coordinate the movement of the fingers and the thumb. When the subject grips an object, the spring assistance decreases and assist weak extensor muscles. By adjusting or removing the number of cords the assistance level can be changed.

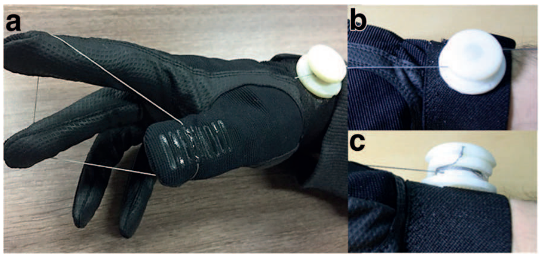

(a) Overview working mechanism GRIPIT (Kim et al., 2017). The wire is the part that makes it able to grip something.

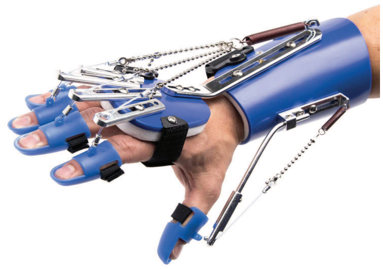

(b) The design of the Saeboflex (Hoffman and Blakey, 2011). The springs shown in the figure let the fingers extend.

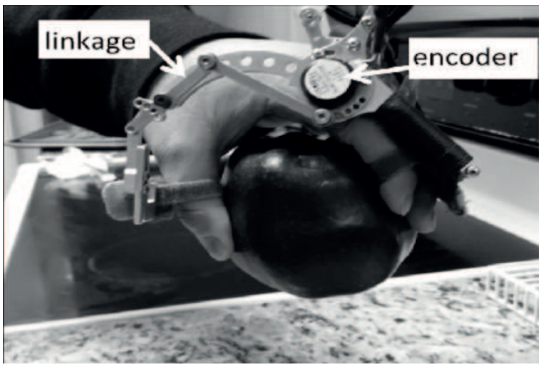

(c) The mechanism of the Handsome (Chen et al., 2017a). The four bar linkage mechanism helps during extension.

Figure 3.5 Overview human muscle hand orthoses.

3.4.2 Electromagnetic actuation system

The electromagnetic actuation system consists of 29 devices. Not all of them will be discussed, because a lot of systems are based on the same principle. Therefore, the most used working mechanisms will be explained and illustrated in Figure 3.6. To start with the X-glove (Ghassemi et al., 2018) shown in Figure 3.6(a). The X-glove is attached to the forearm. The motors are located here as well. One end of the cables is connected to the motor while the rest of the cables is connected to a glove. Three parallel cables are placed on top of one finger. The applied forces can assist extension or resist flexion of a digit. Next, Guo et al. (2018) describes the soft robotic exo-sheath, presented in Figures 3.6(c) and 3.6(d). This design is a combination of Bowden cables, pulleys and grippers. With the help of the Bowden cable will the output power of the motor be transferred to the pulley. From here the power is transferred to two fin-ray grippers. These grippers help the user to flex or extend their fingers. Another possibility is to add springs to the fingers of the hand orthosis. For example, the Relabtenoexo, a design of Nycz et al. (2016) illustrated in Figures 3.6(e) and 3.6(f). Here a centre spring is pushed which results in a bending motion in the direction of finger flexion. This happens because the fingers are sliding springs. A Bowden cable is used to push the spring. Sale et al. (2017) shows another way to use springs in combination with DC motors in Figures 3.6(g) and 3.6(h). In this design, cuboid blocks with finger spine structure are placed dorsal of the fingers. All the blocks can separate and rotate in respect to each other by a specific distance and angle. Finger extension is possible when a cable is being pulled from the proximal side of the device by a DC motor. The cable is passed through all the blocks except for the last one. A pulley drives the main actuation tendon. Springs are attached to this tendon. For each finger is a different spring with its own spring constant. Furthermore, there is a cable-driven power transmission system as described in Cheng et al. (2018). By fixing one end of the cable at the transmission wheel and the other end connecting to the hand orthosis, fingers can flex and extend. The same mechanism is used by the EXO-Glove, shown in Figures 3.6(i) and 3.6(j) (In et al., 2015). However, here a soft wearable robot is made. Besides that, Gasser et al. (2017) combine the different mechanisms. The name of the design is Vanderbilt and presented in Figure 3.6(b). There are cables with pulleys to flex the fingers and at the end of the fingers there are extensor springs to extend the fingers. To reduce the number of motors, two spools on a single motor shaft were designed by Mohammadi et al. (2018), shown in Figure 3.6(k) and is called the Flexo-glove. With this system two cables can move in opposite direction and upon the spool. This mechanism makes it possible to flex the fingers with one cable and use the other cable to extend the fingers.

3.4.3 Mechanical actuation system

The pneumatic actuation system consists of 15 devices. The different working principles will be discussed and presented in Figure 3.7. To start with the soft pneumatic actuators shown in Figure 3.7(a). These actuators consist of three fabric layers and two air-tight bladders located on top of the fingers. The bladders are selectively pressurised with an air pump, finger flexion and extension is possible (Cappello et al., 2018). Some variations on this mechanism are possible. Gobee et al. (2017) show a combination of flexible and non-flexible tubes together with elastic bands in Figures 3.7(b) and 3.7(c). By independently opening and closing the valves in the non-flexible tubes, the finger can bend. The fiber-reinforced actuators consist of two actuators which can be seen in Figure 3.7(e). Jiralerspong et al. (2018) describes a bending and a rotating actuator. The bending actuator consists of a single air chamber with an air inlet at the proximal end. The outside of the actuator is made of inelastic fibres with a double helix pattern. This is attached with the strain limiting layer at the bottom. This is done to promote the bending motion. Two different movements happen, the areas attached to the limiting layers bend, while the non-attached areas extend along its axial direction. The rotary actuator is in principle the same as the bending actuator. It is again a single air chamber with an air inlet. However, this actuator has a V-shaped design which limits the movement to rotation about the z-axis. The bending actuators are place on a glove on top of the subject's own fingers and the rotary actuator is placed between the index finger and the thumb. Chen et al. (2017b) made a lobster inspired pneumatic actuator illustrated in Figure 3.7(d). This consists of a soft chamber located inside rigid shells. When air enters the chamber, the chamber pushes against the inner wall of the rigid shell. This will produce a bending motion though the next shell segment. Furthermore, there is a fishbone inspired pneumatic actuator shown in Figures 3.7(f) and 3.7(g) (Jiang et al., 2018). In this design a soft pneumatic actuator (SPA), a fishbone-like structure (FLS) and two nylon strings form the single actuator. The nylon strings make different motion patterns possible. This can be done by tightening the strings selectively. As soon as air enters the SPA the fingers are able to bend, dependent on which strings are tightened. The pneumatic artificial muscle (PAM) is used in different ways. A PAM consists of an internal elastomeric bladder covered by a shell which is braided. One method is to place the PAM at the forearm as shown in Figure 3.7(h) (Tjahyono et al., 2013). The PAM is coupled in series with a linear spring. By generating pushing and pulling forces, the finger joint can flex and extend. Another way to use the PAM is to place it on top of the glove. This is described in Al-Fahaam et al. (2018) and presented by Figure 3.7(i). In this design the PAM are strengthened along one side. Therefore, one side of the actuator could keep at a fixed length. This results in a bending movement of the PAM when air enters the PAM.

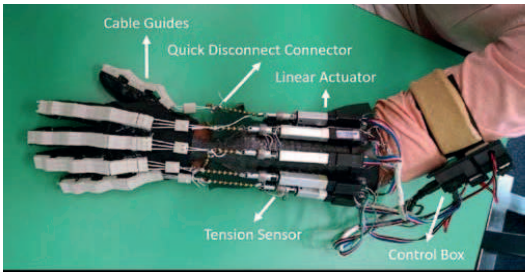

(a) Overview of the X-glove with linear servomotor (Ghassemi et al., 2018). The actuators pull on the cables during extension.

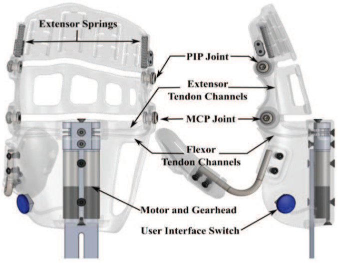

(b) Overview design Vanderbilt (Gasser et al., 2017). Cables with pulleys flex the fingers and the extensor springs extend the fingers.

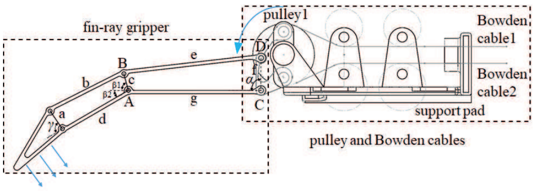

(c) Mechanism soft robotic exo-sheath (Guo et al., 2018). Bowden cable 1 will extend the finger, Bowden cable 2 will flex the finger.

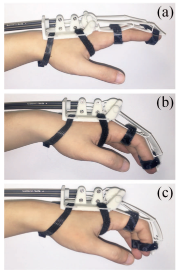

(d) Overview soft robotic exo-sheath on the users finger (Guo et al., 2018).

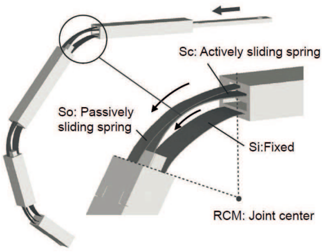

(e) Overview sliding springs fingers Relabtenoexo (Nycz et al., 2016). Sliding of the springs results in flexion movement.

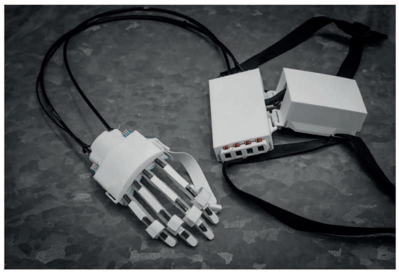

(f) Overview design Relabtenoexo completely assembled (Nycz et al., 2016).

Figure 3.6 Overview of the different designs with electromagnetic actuation system.

3.4.4 Thermal actuation system

The thermal actuation system consists of a device which uses SMA and a device that uses TCP. These are shown in Figure 3.8. The SMA, as designed by Hadi et al. (2018), is a SMA tendon based actuation system shown in Figures 3.8(a) and 3.8(b). There are two tendons in this mechanism. One tendon is connected to the proximal phalanx and the other one is fastened to the end of the distal phalanx. An SMA actuator is connected to the tendons and somewhere on the platform that is located on the forearm. After activation of the SMA, with the help of an air fan, a difference in tension force and length arises. This results in a movement of the finger. Different motions can be generated by activating the distal or proximal phalanx tendon. The iGrab makes use of TCP muscles illustrated in Figure 3.8(c) (Saharan et al., 2017a). The working principle is the same as described earlier. One end of the TCP muscles is connected to a stitched part and the other end to the tendons for the fingers. By heating the TCP muscles the tendons will be activated which result in flexion and extension of the fingers.

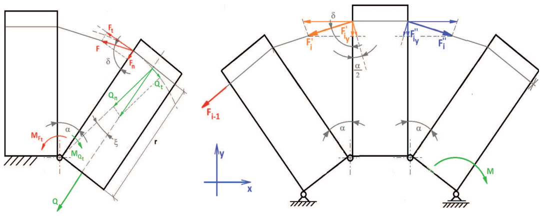

(g) Movement of the blocks of the FEX (Sale et al., 2017). By pulling on the cable that connects the block, a movement takes place.

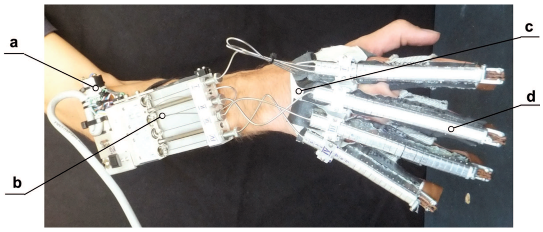

(h) Overview of the FEX hand orthosis on someones hand (Sale et al., 2017).

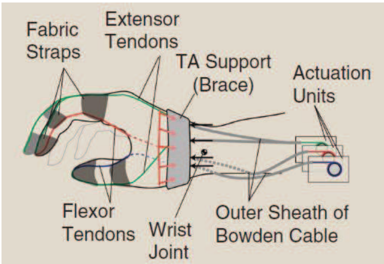

(i) Working mechanism EXO-Glove (In et al., 2015). The extensor tendons generate an extension movement. The flexor tendons generate a flexion movement.

(j) Overview EXO-Glove soft wearable hand orthosis with the integrated working mechanism (Jeong et al., 2015).

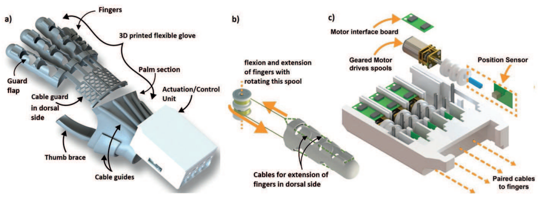

(k) Double spool mechanism Flexo-glove (Mohammadi et al., 2018). The flexion and extension cables are placed on one spool.

Figure 3.6 (continued)

3.4.5 Miscellaneous system

In the miscellaneous group is the Tape spring device placed, designed by Haarman et al. (2018) and can be seen in Figures 3.9(a) and 3.9(b). The fingers consist of a tape spring mechanism. With the help of Bowden cables a pulling force will let the tape springs sliding outwards which results in finger flexion. To make finger extension possible, a constant force spring is placed in the hand slider and pulls the tape spring back. The principle of the ProGs works the same as the EXO-glove. The other device that belongs to this miscellaneous group is the Ong. This mechanism works the same as the X-glove.

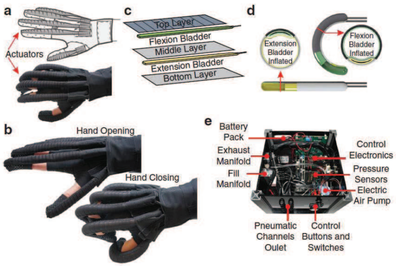

(a) Working principle Cappello (Cappello et al., 2018). The flexion bladder on top generates a flexion movement. The extenten bladder on the bottom layer results in extension movements.

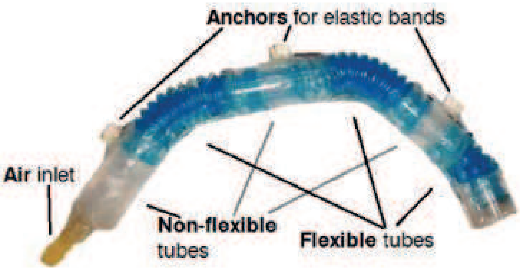

(b) Design of the soft pneumatic actuator of Gobee (Gobee et al., 2017). The flexible tubes generate flexion movements. The elastic bands result in an extension movement.

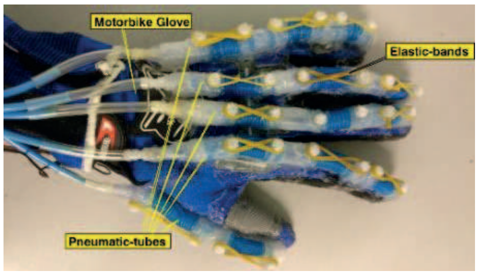

(c) Overview of the soft hand orthosis Gobee on a motorbike glove (Gobee et al., 2017).

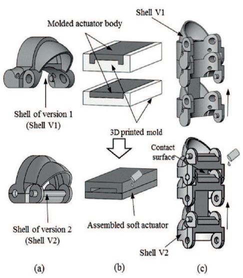

(d) Overview rigid shell of the lobster inspired hand orthosis (Chen et al., 2017b). Inside the shells is a silicone layer to generate the movements.

(e) The pneumatic actuators of Jiralerspong for the fingers and the thumb (Jiralerspong et al., 2018).

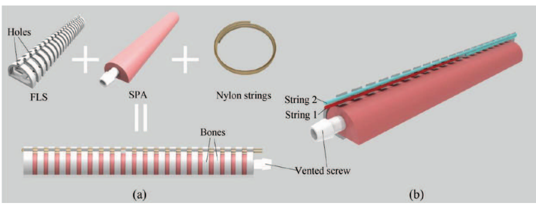

(f) The different parts of the Fishbone inspired pneumatic actuator (Jiang et al., 2018). The FLS covers the SPA. The nylon strings make a bending movement possible.

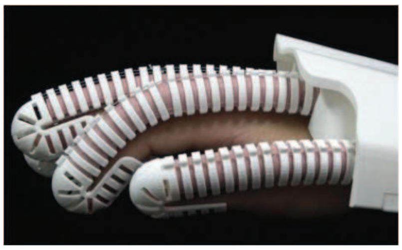

(g) Overview of the fishbone inspired hand orthosis Jiang on the users hand (Jiang et al., 2018).

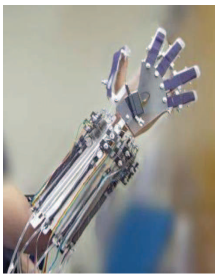

(h) Overview of PAM in Uoa hand orthosis (Tjahyono et al., 2013). The PAMs are located at the forearm. These contractions let connected fingers flex and extend.

(i) Design of Al Fahaam hand orthosis(Al-Fahaam et al., 2018). In this situation is the PAM placed on top of the fingers.

Figure 3.7 Overview designs pneumatic actuators.

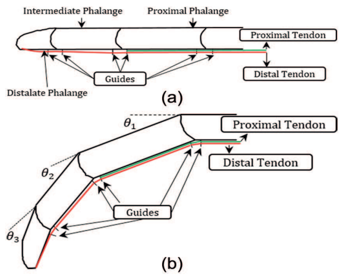

(a) Working principle of the tendons of the ASR glove (Hadi et al., 2018). One tendon is connected to the proximal phalange, the other one to the distal phalange. Activation of the tendons results in a movement of the finger.

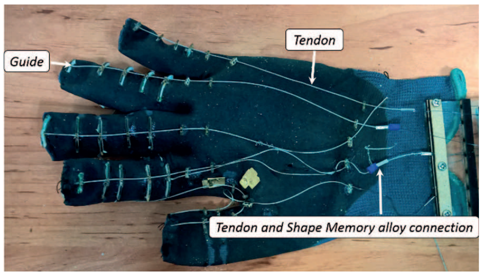

(b) Overview of the ASR glove with the tendonds (Hadi et al., 2018).

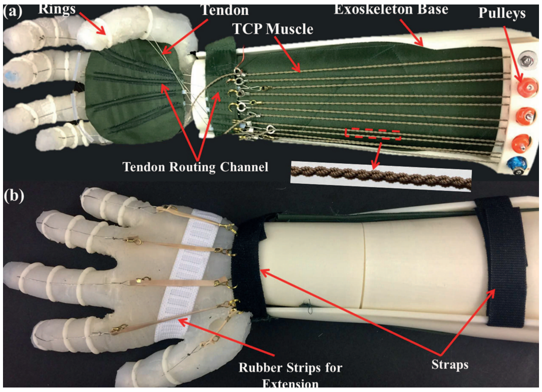

(c) Overview of the iGrab (Saharan et al., 2017a). Heating up the TCP muscle results in a difference in the tendon length. This generates a flexion or extension movement of the fingers.

Figure 3.8 Designs of the thermal actuator systems.

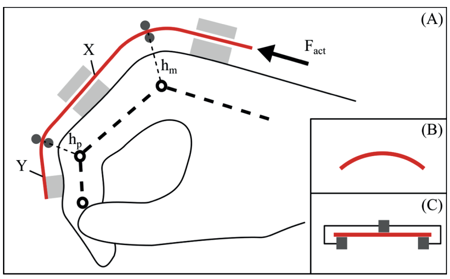

(a) Working principle of the Tape spring (Haarman et al., 2018). A pulling force results in a transformation of the tape spring. This results in a flexion movement.

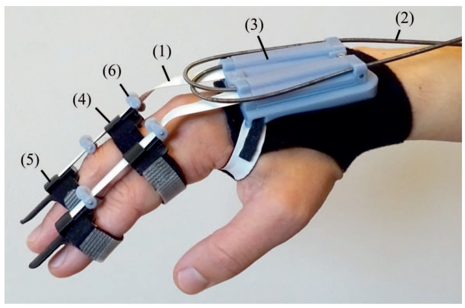

(b) Overview of the design of the Tape spring (Haarman et al., 2018). A constant force spring is placed at number 3 to make extension possible.

Figure 3.9 Design of the Tape spring.

4 Discussion

In this part the results will be discussed. Forty-eight designs of dynamic hand orthoses were analysed and categorised into a framework. This framework consists of the signal domain, the energy domain and the mechanical domain. The results from the framework will be discussed in the matching sections (signal domain, energy domain and mechanical domain). Furthermore, the devices were mentioned in tables based on their actuation system. Namely, the chemical actuation system, electrocmagnetic actuation system, mechanical actuation system and there is a miscellaneous group. For each device were the four sub-questions answered. These answers were analysed in the synthesis section. Finally, the research question was answered.

4.1 Signal domain

Most of the designs are assistive devices. This is because most of the selected devices focused on ADL. Some of the devices have shared authority (13 out of 48). In this case the control is active or passive. This is seen in one SMA and six pneumatic systems, from the eight devices with an electromagnetic actuation system were two devices a combination of both electric and pneumatic actuation system.

More series (18 compared to 7) commands are used than parallel. In series commands, muscle cocontraction and activation are used the most. Series control is the most intuitive because it is similar to natural control. Series control has more useful functionalities (Pedrocchi et al., 2013). However, for muscle cocontraction and activation it is important that the right electromyograph (EMG) signals are used. As described by Lobo-Prat et al. (2017), sEMG could be used by DMD patients to control the orthosis. It is found that for the parallel command signal the other limb is used the most. This is often combined with the option: 'together with another person'. Which means that the other limb could also be someone else who controls the orthosis. Pneumatic systems use this method the most. However, this command signal is not optimal because it makes it harder to carry out a bimanual task.

It is found that more designs are based on augmented feedback than attenuated feedback (16 compared to 13). Augmented feedback is only seen in devices with electromagnetic actuation. Attenuated feedback is seen both in human muscle and pneumatic systems. In general, the low rate of feedback is most probably because there is no virtual reality in these devices as they are used for ADL tasks and not only for rehabilitation. Besides that, not all the papers mention something about feedback. Therefore, it could be the case that more devices make use of it.

4.2 Energy domain

The chemical actuation system with the human muscle uses elastic energy in two cases. As already explained in the results, the flexion of the fingers is performed with the own muscles. The springs then start working and make extension of the fingers possible. Therefore, these designs are not possible for DMD patients. For the electromagnetic actuators, which is the biggest group consisting of 29 designs, batteries and elastic energy are used as storage. DC motors are used the most within this group. Some of these electromagnetic designs use also a pneumatic system. All the pneumatic actuators use pneumatic pressure as storage energy. Sometimes in combination with springs (five times). In this case, elastic energy is used. It can be seen that soft pneumatic actuators are used the most, followed by the pneumatic artificial muscles. The SMA and TCP actuation both need a battery. With the help of heat from some air fans the orthosis can be controlled. How to control the motion speed and the force needs some more research as described in Hadi et al. (2018). The designs which did not mention the actuation system are placed in the miscellaneous group. However, the energy storage was mentioned. In one case a battery is used. For two cases, was elastic energy based on springs used.

4.3 Mechanical domain

The Bowden cable is used 14 times, while the push-pull cable is used 10 times. This is because these systems resemble the human hand the most (Bos et al., 2016). Most of the designs using these cables are using electro motors as actuation system. The flexible shafts are used in combination with soft pneumatic gloves and soft wearable gloves. Furthermore, direct linkage is used in 11 designs. This is more often applied than bar linkage, which is used six times. Direct linkage is used the most in pneumatic systems, and bar linkage in electromagnetic. This is because with an electromagnetic actuation system torque control or position control are both possible. Therefore, in eight times are gears used for electromagnetic actuation, three times a compliant mechanism and three times cam followers. 35 out of 48 are using a cable.

Most of the designs are jointless (28 out of 48). Mainly the pneumatic actuation systems are jointless, this is because with a soft pneumatic system you do not need a hard exoskeleton. A glove is a good solution and often used as a frame. This glove results in a jointless articulation system. Monocentric is used in all the actuation systems and is seen 14 times. This means that there is a chance of misalignment in most cases. Polycentric joints prevent this problem with implemented self-aligning mechanisms. Cempini et al. (2013b) describe that there are methods for self-aligning. Surprisingly, the smallest group is the polycentric joint articulation with eight times. This means that there is a chance of misalignment in most cases. From the polycentric joint articulation mechanisms, are seven devices using an electromagnetic actuation system and one device a pneumatic actuation system. The underactuation mechanism is to make the device less complex, that is also visible when you compare it with the design which does not make use of an underactuation system. There is more underactuation across joints than across fingers (29 against 11). By looking at the different grips mostly used during ADL tasks, underactuation across fingers is not needed (Feix et al., 2015).

4.4 Synthesis

In this section will the answers on the sub-questions be discussed. This is done in the order of the different actuation systems and the miscellaneous group. This section will end with the answer on the main research question. By means of Tables 3.1 till 3.5 the sub-questions as stated in Chapter 1 can be answered. These sub-questions were:

1. **To what extent is the design reproducible?**
2. **Which design of the hand orthosis can be used for DMD patients?**
3. **What are the maximum output forces of the fingers of the hand orthosis?**
4. **Which verification and validation procedures are employed to analyse the design of the dynamic hand orthosis?**

The interpretations on Sub-question 1 were done in the following way.

- Yes: there is a working prototype presented in the paper and promising results are shown.
- Maybe: there is potential but some more information or changes are needed.
- No: there is no working design presented in the paper or the design is too complex.

The answer on Sub-question 2 consists also of a Yes, Maybe and No with the following interpretations.

- Yes: when it was an assistive device, which made it possible to still use the tactile and proprioceptive senses of the hand and when tests were done on human hands.
- Maybe: when it is with some adaptation possible to use for DMD patients or when some more information is needed.
- No: when the design cannot be used for DMD patients, even after some adaptations.

It is important to note that these findings may be somewhat limited by the fact that the answers on these sub-questions, and the interpretation of the images to select the "flat" designs is limited by the authors perspective. By looking at the actuation systems, it can be concluded that the human muscle is not used that often. Besides that, in the case of DMD patients this method cannot be used. Muscle force is necessary for these designs and that is the problem of DMD disease. Therefore, the human muscle is not a design with potency for DMD patients. The maximum forces of these designs are unknown, so this actuation system has less potential for DMD patients. However, because only the human muscle is used, it is easier to test on subjects not suffering from DMD or to bring it on the market.

The electric/magnetic actuation system is the system that is used the most. This is often done in combination with Bowden cables or push pull cables. One reason for this could be that there are a lot of possibilities for position and torque control (Bos et al., 2016). It has been suggested by In et al. (2011) that 18 N is enough force for using a dynamic hand orthosis for ADL. However, Arata et al. (2013) describe that 35 N is necessary. Therefore, for now, the minimum force of 18 N is chosen. This means that 10 out of 29 designs generate the right amount of force. During the follow up study to develop a hand orthosis, force tests will be carried out to discover which force is really needed. Only seven of the designs did some patient tests. This means that these seven designs have a higher technology readiness than the ones which did no patient tests. This makes these designs a more promising solution.

Until now, there are less pneumatic than electromagnetic hand orthoses. This does not mean that electromagnetic is better. A reason could be that less is known about pneumatics. This results in the less available products as well. Pneumatic systems could have potential for a flat hand orthosis for people with DMD. However, most of them are using a soft exoskeleton in the shape of a glove. This is not an optimal solution for DMD patients as, they still want to use their own tactile sensing and propioceptive sensing. By using gloves this is not possible anymore. The designs which received a maybe for the possibility for DMD are using a glove. However, it is not leading for the design, because they do not need the hand palm. This means that an alternative solution for the glove should work as well. There are six designs with a force of at least 18 N. As already mentioned, this is the minimum of the found values. Furthermore, there are not that many tests carried out on patients. This makes the designs for now less reproducible.

By looking at the thermal actuation, there is one design that makes use of SMA actuation system and one design that uses TCP. SMA could not have potential to work for DMD patients. There are some points that still have to be tested like the durability of the mechanism and the prototype need some more improvements. Furthermore, the speed is a problem. When the orthosis is used during ADL it does not work when it takes a while before you can pick up something. Besides that, the hand palm is covered which makes it not usable for DMD patients. At least the force which can be generated is with 40 N high enough. The same problems are seen for TCP. The difference is that an output force of 2.8 N would never be high enough.

There are three devices placed in the miscellaneous group. The reason for this was that their actuation system was not clear or not mentioned. With unknown maximum forces, and hardly no tests it is not possible to say if one of these methods would be a good design for a new hand orthosis for DMD patients.

To sum up, four different actuation systems and a miscellaneous group are compared in this study. Human muscle and a thermal actuation do not have potential for DMD patients like the miscellaneous group. However, the electromagnetic and the pneumatic actuation system both have potential. That brings us to the answer of the research question:

> **Which available actuation system is most suitable to design a wearable flat dynamic hand orthosis for DMD patients?**

It turns out that there are two suitable actuation systems. Namely, electromagnetic and pneumatic. This means that both actuation systems will be considered. The final choice will depend on the design criteria. Then a decision can be made on which actuator system has the most potential to fit the special needs for a flat dynamic hand orthosis for DMD patients.

5 Conclusions

People with Duchenne muscular dystrophy (DMD) suffer from hand impairments and are in need of a dynamic hand orthosis. However, at this moment there are no dynamic hand orthoses on the market that fit their special needs. Therefore, a literature review was carried out focusing on different flat dynamic hand orthoses. They were collected and organised within a framework. This resulted in 48 different designs which were analysed based on their signal domain, energy domain and mechanical domain. The literature review describes not only the framework, also one main research question and four sub-questions were answered. Next to that, the working mechanism of different devices were explained. Most designs are assistive with human authority, the command signal is more in series than in parallel and the user feedback is not mentioned that often. Most actuation systems are electro/magnetic with a battery as energy storage. A lot of these devices are using Bowden cables or push-pull cables. This study has found that, most devices are jointless and there is underactuation across joints. Furthermore, most of the devices are not reproducible and 13 devices are suitable for DMD patients. A total of 15 devices have output forces above 18 N. In 9 cases there were some tests with patients. Altogether, by looking at the actuation systems is the electromagnetic used the most. It looks like that both electromagnetic and pneumatic actuation are suitable to design a wearable flat dynamic hand orthosis for DMD patients. Therefore, a choice will be made after making the design criteria in the follow up study.

References

Al-Fahaam, H., Davis, S., and Nefti-Meziani, S. (2018). The design and mathematical modelling of novel extensor bending pneumatic artificial muscles (EBPAMs) for soft exoskeletons. Robotics and Autonomous Systems, 99:63–74.

Arata, J., Ohmoto, K., Gassert, R., Lambercy, O., Fujimoto, H., and Wada, I. (2013). A new hand exoskeleton device for rehabilitation using a three-layered sliding spring mechanism. In IEEE International Conference on Robotics and Automation, pages 3902–3907.

Bain, G., Polites, N., Higgs, B., Heptinstall, R., and McGrath, A. (2015). The functional range of motion of the finger joints. Journal of Hand Surgery, 40(4):406–411.

Baqapuri, H. I., Nizami, H. A., Siddiqui, S., Iqbal, J., and Shahbaz, U. (2012). Prefabrication design of an actuated exoskeleton for traumatized and paralytic hands. In International Conference on Robotics and Artificial Intelligence, pages 108–111. IEEE.

Basteris, A., Nijenhuis, S. M., Stienen, A. H. A., Buurke, J. H., Prange, G. B., and Amirabdollahian, F. (2014). Training modalities in robot-mediated upper limb rehabilitation in stroke: a framework for classification based on a systematic review. Journal of Neuroengineering and Rehabilitation, 11(1):111.

Biggar, S. and Yao, W. (2016). Design and evaluation of a soft and wearable robotic glove for hand rehabilitation. IEEE Transactions on Neural Systems and Rehabilitation Engineering, 24(10):1071–1080.

Bos, R. A., Haarman, C. J. W., Stortelder, T., Nizamis, K., Herder, J. L., Stienen, A. H. A., and Plettenburg, D. H. (2016). A structured overview of trends and technologies used in dynamic hand orthoses. Journal of Neuroengineering and Rehabilitation, 13(1):62.

Bos, R. A., Nizamis, K., Plettenburg, D. H., and Herder, J. L. (2018). Design of an electrohydraulic hand orthosis for people with Duchenne muscular dystrophy using commercially available components. In IEEE International Conference on Biomedical Robotics and Biomechatronics, pages 305–311.

Bos, R. A., Plettenburg, D. H., and Herder, J. L. (2017). Exploratory design of a compliant mechanism for a dynamic hand orthosis: Lessons learned. In 2017 International Conference on Rehabilitation Robotics (ICORR), pages 603–608. IEEE.

Boser, Q. A., Dawson, M. R., Schofield, J. S., Dziwenko, G., and Hebert, J. S. (2018). Defining the design requirements for an assistive powered hand exoskeleton. bioRxiv, page 492124.

Cappello, L., Meyer, J. T., Galloway, K. C., Peisner, J. D., Granberry, R., Wagner, D. A., Engelhardt, S., Paganoni, S., and Walsh, C. J. (2018). Assisting hand function after spinal cord injury with a fabric-based soft robotic glove. Journal of Neuroengineering and Rehabilitation, 15(1):59.

Case, L. E., Apkon, S. D., Eagle, M., Gulyas, A., Juel, L., Matthews, D., Newton, R. A., and Posselt, H. F. (2018). Rehabilitation management of the patient with Duchenne muscular dystrophy. Pediatrics, 142(Supplement 2):S17–S33.

Cempini, M., Cortese, M., and Vitiello, N. (2015). A powered finger–thumb wearable hand exoskeleton with self-aligning joint axes. IEEE/ASME Transactions on mechatronics, 20(2):705–716.

Cempini, M., De Rossi, S. M. M., Lenzi, T., Cortese, M., Giovacchini, F., Vitiello, N., and Carrozza, M. C. (2013a). Kinematics and design of a portable and wearable exoskeleton for hand rehabilitation. In IEEE international conference on Rehabilitation robotics, pages 1–6.

Cempini, M., De Rossi, S. M. M., Lenzi, T., Vitiello, N., and Carrozza, M. C. (2013b). Self-alignment mechanisms for assistive wearable robots: A kinetostatic compatibility method. IEEE Trans. Robotics, 29(1):236–250.

Chen, J., Nichols, D., Brokaw, E. B., and Lum, P. S. (2017a). Home-based therapy after stroke using the hand spring operated movement enhancer (HandSOME). IEEE Transactions on Neural Systems and Rehabilitation Engineering, 25(12):2305–2312.

Chen, Y., Le, S., Tan, Q. C., Lau, O., Wan, F., and Song, C. (2017b). A lobster-inspired robotic glove for hand rehabilitation. In IEEE International Conference on Robotics and Automation, pages 4782–4787.

Cheng, L., Chen, M., and Li, Z. (2018). Design and control of a wearable hand rehabilitation robot. IEEE Access, 6:74039–74050.

Chiri, A., Giovacchini, F., Vitiello, N., Cattin, E., Roccella, S., Vecchi, F., and Carrozza, M. C. (2009). HANDEXOS: Towards an exoskeleton device for the rehabilitation of the hand. In IEEE/RSJ International Conference on Intelligent Robots and Systems, 2009., pages 1106–1111.

Chiri, A., Vitiello, N., Giovacchini, F., Roccella, S., Vecchi, F., and Carrozza, M. C. (2012). Mechatronic design and characterization of the index finger module of a hand exoskeleton for post-stroke rehabilitation. IEEE/ASmE Transactions on mechatronics, 17(5):884–894.

Connelly, L., Jia, Y., Toro, M. L., Stoykov, M. E., Kenyon, R. V., and Kamper, D. G. (2010). A pneumatic glove and immersive virtual reality environment for hand rehabilitative training after stroke. IEEE Transactions on Neural Systems and Rehabilitation Engineering, 18(5):551–559.

Cool, J. C. and Van Hooreweder, G. J. O. (1971). Hand prosthesis with adaptive internally powered fingers. Medical & biological engineering, 9(1):33–36.

Cui, L., Phan, A., and Allison, G. (2015). Design and fabrication of a three dimensional printable non-assembly articulated hand exoskeleton for rehabilitation. In 37th Annual International Conference of the IEEE Engineering in Medicine and Biology Society., pages 4627–4630.

Edemekong, P. F. and Levy, S. B. (2019). Activities of daily living (adls). In StatPearls [Internet]. StatPearls Publishing.

Feix, T., Romero, J., Schmiedmayer, H.-B., Dollar, A. M., and Kragic, D. (2015). The grasp taxonomy of human grasp types. IEEE Transactions on Human-Machine Systems, 46(1):66–77.

Fink, D. (2019). 85 db is not a safe noise level to prevent hearing loss. The Hearing Journal, 72(1):26–27.

Fu, Y., Zhang, Q., Zhang, F., and Gan, Z. (2011). Design and development of a hand rehabilitation robot for patient-cooperative therapy following stroke. In International Conference on Mechatronics and Automation (ICMA), pages 112–117. IEEE.

Gasser, B. W., Bennett, D. A., Durrough, C. M., and Goldfarb, M. (2017). Design and preliminary assessment of Vanderbilt hand exoskeleton. In International Conference on Rehabilitation Robotics, pages 1537–1542. IEEE.

Gasser, B. W. and Goldfarb, M. (2015). Design and performance characterization of a hand orthosis prototype to aid activities of daily living in a post-stroke population. In 37th Annual International Conference of the IEEE Engineering in Medicine and Biology Society (EMBC), pages 3877–3880.

Gearhart, C. J., Varone, B., Stella, M. H., and BuSha, B. F. (2016). An effective 3-fingered augmenting exoskeleton for the human hand. In 38th Annual International Conference of the IEEE Engineering in Medicine and Biology Society, pages 590–593.

Ghassemi, M., Ochoa, J. M., Yuan, N., Tsoupikova, D., and Kamper, D. (2018). Development of an integrated actuated hand orthosis and virtual reality system for home-based rehabilitation. In 40th Annual International Conference of the IEEE Engineering in Medicine and Biology Society, pages 1689–1692.

Glasgow, C., Tooth, L., and Fleming, J. (2008). Which splint? Dynamic versus static progressive splinting to mobilise stiff joints in the hand. The British Journal of Hand Therapy, 13(4):104–110.

Gobee, S., Durairajah, V., and Mohammadullah, N. (2017). Portable soft-exoskeleton for finger rehabilitation. In Proceedings of the 2017 International Conference on Biomedical Engineering and Bioinformatics, pages 65–70. ACM.

Guo, J., Yu, S., Li, Y., Huang, T.-H., Wang, J., Lynn, B., Fidock, J., Shen, C.-L., Edwards, D., and Su, H. (2018). A soft robotic exo-sheath using fabric EMG sensing for hand rehabilitation and assistance. In IEEE International Conference on Soft Robotics, pages 497–503.

Haarman, C. J. W., Hekman, E. E. G., Rietman, H. S., and van der Kooij, H. (2018). Pushing the limits: A novel tape spring pushing mechanism to be used in a hand orthosis. In International Symposium on Wearable Robotics, pages 475–479. Springer.

Hadi, A., Alipour, K., Kazeminasab, S., and Elahinia, M. (2018). ASR glove: A wearable glove for hand assistance and rehabilitation using shape memory alloys. Journal of Intelligent Material Systems and Structures, 29(8):1575–1585.

Hasegawa, Y., Mikami, Y., Watanabe, K., and Sankai, Y. (2008). Five-fingered assistive hand with mechanical compliance of human finger. In IEEE International Conference on Robotics and Automation, pages 718–724.

Hasegawa, Y. and Suzuki, T. (2015). Thin and active fixture to hold finger for easy attachment and comfort of grasping support exoskeleton. In IEEE International Conference on Robotics and Automation, pages 4973–4978.

Herath, H., Gopura, R., and Lalitharatne, T. D. (2018). An underactuated linkage finger mechanism for hand prostheses. Modern Mechanical Engineering, 8(02):121–139.

Hoffman, H. B. and Blakey, G. L. (2011). New design of dynamic orthoses for neurological conditions. NeuroRehabilitation, 28(1):55–61.

Hofmann, U. A., Bützer, T., Lambercy, O., and Gassert, R. (2018). Design and evaluation of a Bowden-cable-based remote actuation system for wearable robotics. IEEE Robotics and Automation Letters, 3(3):2101–2108.

In, H., Cho, K.-J., Kim, K., and Lee, B. (2011). Jointless structure and under-actuation mechanism for compact hand exoskeleton. In IEEE International Conference on Rehabilitation Robotics, pages 1–6.

In, H., Kang, B. B., Sin, M., and Cho, K.-J. (2015). Exo-glove: a wearable robot for the hand with a soft tendon routing system. IEEE Robotics & Automation Magazine, 22(1):97–105.

InformedHealth (2018). How do hands work? Institute for Quality and Efficiency in Health Care, Germany.

Janssen, M. (2017). Upper extremity function in Duchenne Muscular Dystrophy Mechanisms of declined task performance. PhD thesis, Radboud Universiteit Nijmegen.

Janssen, M. M., Bergsma, A., Geurts, A. C., and De Groot, I. J. (2014). Patterns of decline in upper limb function of boys and men with DMD: an international survey. Journal of neurology, 261(7):1269–1288.

Jeong, U., In, H., Lee, H., Kang, B. B., and Cho, K.-J. (2015). Investigation on the control strategy of soft wearable robotic hand with slack enabling tendon actuator. In IEEE International Conference on Robotics and Automation, pages 5004–5009.

Jiang, Y., Chen, D., Liu, P., Jiao, X., Ping, Z., Xu, Z., Li, J., and Xu, Y. (2018). Fishbone-inspired soft robotic glove for hand rehabilitation with multi-degrees-of-freedom. In IEEE International Conference on Soft Robotics, pages 394–399.

Jiang, Y., Chen, D., Que, J., Liu, Z., Wang, Z., and Xu, Y. (2017). Soft robotic glove for hand rehabilitation based on a novel fabrication method. In IEEE International Conference on Robotics and Biomimetics, pages 817–822.

Jiralerspong, T., Heung, K. H. L., Tong, R. K. Y., and Li, Z. (2018). A novel soft robotic glove for daily life assistance. In 7th IEEE International Conference on Biomedical Robotics and Biomechatronics, pages 671–676.

Jones, L. A. and Lederman, S. J. (2006). Human Hand Function. Oxford University Press, New York, NY.

Kim, B., In, H., Lee, D.-Y., and Cho, K.-J. (2017). Development and assessment of a hand assist device: GRIPIT. Journal of NeuroEngineering and Rehabilitation, 14(1).

Kim, D. H., Lee, S. W., and Park, H.-S. (2014). Feedback control of biomimetic exotendon device for hand rehabilitation in stroke. In 36th Annual International Conference of the IEEE Engineering in Medicine and Biology Society, pages 3618–3621.

Klingels, K., Mayhew, A. G., Mazzone, E. S., Duong, T., Decostre, V., Werlauff, U., Vroom, E., Mercuri, E., Goemans, N. M., and Group, U. L. C. O. (2017). Development of a patient-reported outcome measure for upper limb function in Duchenne muscular dystrophy: DMD Upper Limb PROM. Developmental Medicine & Child Neurology, 59(2):224–231.

Kudo, S., Oshima, K., Arizono, M., Hayashi, Y., and Moromugi, S. (2014). Electric-powered glove for CCI patients to extend their upper-extremity function. In IEEE/SICE International Symposium on System Integration, pages 638–643.

Lee, S. W., Landers, K. A., and Park, H.-S. (2014). Development of a biomimetic hand exotendon device (BiomHED) for restoration of functional hand movement post-stroke. IEEE Transactions on Neural Systems and Rehabilitation Engineering, 22(4):886–898.

Liang, R., Zhang, S., Luo, A., and Tao, T. (2018). A Novel Variable Stiffness Compliant Finger Exoskeleton for Rehabilitation Based on Electromagnet Control. In 40th Annual International Conference of the IEEE Engineering in Medicine and Biology Society, pages 3926–3929.

Lin, M. X., Ma, G. Y., Liu, F. Q., Sun, Q. S., and Song, A. Q. (2018). Design and dynamic modeling of flexible rehabilitation mechanical glove. In IOP Conference Series: Materials Science and Engineering, volume 320. IOP Publishing.

Lobo-Prat, J., Nizamis, K., Janssen, M. M. H. P., Keemink, A. Q. L., Veltink, P. H., Koopman, B. F. J. M., and Stienen, A. H. A. (2017). Comparison between sEMG and force as control interfaces to support planar arm movements in adults with Duchenne: a feasibility study. Journal of neuroengineering and rehabilitation, 14(1):73.

Lu, X., Yang, Z., Chen, Y., and Wang, J. (2016). Structure design of a wearable device for hand rehabilitation. In 2016 9th International Symposium on Computational Intelligence and Design (ISCID), volume 1, pages 93–96. IEEE.

Lu, Y.-M. and Lue, Y.-J. (2012). Strength and functional measurement for patients with muscular dystrophy. Muscular dystrophy, 32(3):671–688.

Machekposhti, D. F., Tolou, N., and Herder, J. (2015). A review on compliant joints and rigid-body constant velocity universal joints toward the design of compliant homokinetic couplings. Journal of Mechanical Design, 137(3):032301.

Martinez, L. A., Olaloye, O. O., Talarico, M. V., Shah, S. M., Arends, R. J., and BuSha, B. F. (2010). A power-assisted exoskeleton optimized for pinching and grasping motions. In Proceedings of the 2010 IEEE 36th Annual Northeast Bioengineering Conference, pages 1–2.

McConnell, A., Kong, X., and Vargas, P. A. (2014). A novel robotic assistive device for stroke-rehabilitation. In The 23rd IEEE International Symposium on Robot and Human Interactive Communication, pages 917–923.

Mohammadi, A., Lavranos, J., Choong, P., and Oetomo, D. (2018). Flexo-glove: A 3D printed soft exoskeleton robotic glove for impaired hand rehabilitation and assistance. 40th Annual International Conference of the IEEE Engineering in Medicine and Biology Society, 2018:2120–2123.

Molenbroek, J. (2004). DINED antropometric data base. Delft University of Technology.

Niestanak, V. D., Moshaii, A. A., and Moghaddam, M. M. (2017). A new underactuated mechanism of hand tendon injury rehabilitation. In 5th RSI International Conference on Robotics and Mechatronics, pages 400–405.

Nimbarte, A. D., Kaz, R., and Li, Z.-M. (2008). Finger joint motion generated by individual extrinsic muscles: a cadaveric study. Journal of Orthopaedic Surgery and Research, 3(1):27.

Nizamis, K., Schutte, W., Goseling, J., and Koopman, B. F. (2017). Quantification of information transfer rate of the human hand during a mouse clicking task with healthy adults and one adult with Duchenne muscular dystrophy. In International Conference on Rehabilitation Robotics, pages 1227–1232. IEEE.

Nycz, C. J., Bützer, T., Lambercy, O., Arata, J., Fischer, G. S., and Gassert, R. (2016). Design and characterization of a lightweight and fully portable remote actuation system for use with a hand exoskeleton. IEEE Robotics and Automation Letters, 1(2):976–983.

Nycz, C. J., Delph, M. A., and Fischer, G. S. (2015). Modeling and design of a tendon actuated soft robotic exoskeleton for hemiparetic upper limb rehabilitation. In 37th Annual International Conference of the IEEE Engineering in Medicine and Biology Society, pages 3889–3892.

Ochoa, J. M., Kamper, D. G., Listenberger, M., and Lee, S. W. (2011). Use of an electromyographically driven hand orthosis for training after stroke. In IEEE International Conference on Rehabilitation Robotics, pages 1–5.

Ochoa, J. M., Narasimhan, Y. J. D., and Kamper, D. G. (2009). Development of a portable actuated orthotic glove to facilitate gross extension of the digits for therapeutic training after stroke. In Annual International Conference of the IEEE Engineering in Medicine and Biology Society, pages 6918–6921.

Ong, A. P. R. and Bugtai, N. T. (2018). A bio-inspired design of a hand robotic exoskeleton for rehabilitation. In AIP Conference Proceedings, volume 1933, pages 040008–1–040008–8. AIP Publishing.

Passamano, L., Taglia, A., Palladino, A., Viggiano, E., D'AMBROSIO, P., Scutifero, M., Cecio, M. R., Torre, V., De Luca, F., Picillo, E., et al. (2012). Improvement of survival in Duchenne muscular dystrophy: retrospective analysis of 835 patients. Acta Myologica, 31(2):121.

Pedrocchi, A., Ferrante, S., Ambrosini, E., Gandolla, M., Casellato, C., Schauer, T., Klauer, C., Pascual, J., Vidaurre, C., Gföhler, M., et al. (2013). MUNDUS project: Multimodal neuroprosthesis for daily upper limb support. Journal of Neuroengineering and Rehabilitation, 10(1):66.

Plettenburg, D. H. (1998). Basic requirements for upper extremity prostheses: the WILMER approach. In Proceedings of the 20th Annual International Conference of the IEEE Engineering in Medicine and Biology Society, volume 5, pages 2276–2281.

Polygerinos, P., Galloway, K. C., Savage, E., Herman, M., O'Donnell, K., and Walsh, C. J. (2015). Soft robotic glove for hand rehabilitation and task specific training. In IEEE International Conference on Robotics and Automation, pages 2913–2919.

Pu, S.-W., Chang, H.-T., and Chang, J.-Y. (2015). Modeling and development of tension force measurement system for cable-driven hand exoskeleton robot. In IEEE International Conference on Advanced Intelligent Mechatronics, pages 635–640.

Pu, S.-W., Chang, J.-Y., Pei, Y.-C., Kuo, C.-C., and Wang, M.-J. (2016). Anthropometry-based structural design of a hand exoskeleton for rehabilitation. In 23rd International Conference on Mechatronics and Machine Vision in Practice, pages 1–6. IEEE.

Pu, S.-W., Tsai, S.-Y., and Chang, J.-Y. (2014). Design and development of the wearable hand exoskeleton system for rehabilitation of hand impaired patients. In IEEE International Conference on Automation Science and Engineering, pages 996–1001.

Refour, E., Sebastian, B., and Ben-Tzvi, P. (2018). Two-digit robotic exoskeleton glove mechanism: Design and integration. Journal of Mechanisms and Robotics, 10(2).

Ribot-Ciscar, E., Tréfouret, S., Aimonetti, J.-M., Attarian, S., Pouget, J., and Roll, J.-P. (2004). Is muscle spindle proprioceptive function spared in muscular dystrophies? A muscle tendon vibration study. Muscle & Nerve: Official Journal of the American Association of Electrodiagnostic Medicine, 29(6):861–866.

Rotella, M. F., Reuther, K. E., Hofmann, C. L., Hage, E. B., and BuSha, B. F. (2009). An orthotic hand-assistive exoskeleton for actuated pinch and grasp. In IEEE 35th Annual Northeast Bioengineering Conference, pages 1–2.

Saharan, L., de Andrade, M. J., Saleem, W., Baughman, R. H., and Tadesse, Y. (2017a). iGrab: hand orthosis powered by twisted and coiled polymer muscles. Smart materials and structures, 26(10):105048.

Saharan, L., Sharma, A., de Andrade, M. J., Baughman, R. H., and Tadesse, Y. (2017b). Design of a 3D printed lightweight orthotic device based on twisted and coiled polymer muscle: iGrab hand orthosis. In Active and Passive Smart Structures and Integrated Systems 2017, volume 10164, page 1016428. International Society for Optics and Photonics.

Sale, P., Stellin, G., Masiero, S., Becchi, F., and Sieklicki, W. (2017). FEX a fingers extending exoskeleton for rehabilitation and regaining mobility. In International Conference on Robotics in Alpe-Adria Danube Region, pages 813–824. Springer.

Sawnani, H., Horn, P. S., Wong, B., Darmahkasih, A., Rybalsky, I., Shellenbarger, K. C., Tian, C., Rutter, M. M., Simakajornboon, N., Amin, R., Gurbani, N., Pascoe, J., Burrows, C., Khirani, S., Amaddeo, A., and Fauroux, B. (2019). Comparison of Pulmonary Function Decline in Steroid-Treated and Steroid-Naïve Patients with Duchenne Muscular Dystrophy. The Journal of Pediatrics, 210:194 –200.e2.

Schreuders, T. A. R., Brandsma, J. W., and Stam, H. J. (2019). Functional Anatomy and Biomechanics of the Hand, pages 3–21. Springer International Publishing, Cham.

Seferian, A. M., Moraux, A., Annoussamy, M., Canal, A., Decostre, V., Diebate, O., Le Moing, A.-G., Gidaro, T., Deconinck, N., Van Parys, F., Vereecke, W., Wittevrongel, S., Mayer, M., Maincent, K., Desguerre, I., Thémar-Noël, C., Cuisset, J.-M., Tiffreau, V., Denis, S., Jousten, V., Quijano-Roy, S., Voit, T., Hogrel, J.-Y., and Servais, L. (2015). Upper limb strength and function changes during a one-year follow-up in non-ambulant patients with Duchenne muscular dystrophy: an observational multicenter trial. PLoS One, 10(2):e0113999.

Shiota, K., Kokubu, S., Tarvainen, T., Sekine, M., Kita, K., Huang, S., and Yu, W. (2019). Enhanced kapandji test evaluation of a soft robotic thumb rehabilitation device by developing a fiber-reinforced elastomer-actuator based 5-digit assist system. Robotics and Autonomous Systems, 111:20–30. cited By 0.

Shiota, K., Tarvainen, T. V., Sekine, M., Kita, K., and Yu, W. (2016). Development of a robotic thumb rehabilitation system using a soft pneumatic actuator and a pneumatic artificial muscles-based parallel link mechanism. In International Conference on Intelligent Autonomous Systems, pages 525–537. Springer.

Smaby, N., Johanson, M. E., Baker, B., Kenney, D. E., Murray, W. M., and Hentz, V. R. (2004). Identification of key pinch forces required to complete functional tasks. Journal of Rehabilitation Research & Development, 41(2).

Stilli, A., Cremoni, A., Bianchi, M., Ridolfi, A., Gerii, F., Vannetti, F., Wurdemann, H. A., Allotta, B., and Althoefer, K. (2018). AirExGlove—A novel pneumatic exoskeleton glove for adaptive hand rehabilitation in post-stroke patients. In IEEE International Conference on Soft Robotics, pages 579–584.

Surendra, W. A., Tjahyono, A. P., and Aw, K. C. (2012). Portable and wearable five-fingered hand assistive device. In 19th International Conference Mechatronics and Machine Vision in Practice, pages 431–435. IEEE.

Tjahyono, A. P., Aw, K. C., Devaraj, H., Surendra, W., Haemmerle, E., and Travas-Sejdic, J. (2013). A five-fingered hand exoskeleton driven by pneumatic artificial muscles with novel polypyrrole sensors. Industrial Robot: An International Journal, 40(3):251–260.

Toochinda, S. and Wannasuphoprasit, W. (2018). Design and development of an assistive hand device for enhancing compatibility and comfortability. In 2nd International Conference on Engineering Innovation, pages 1–6. IEEE.

Van den Bergen, J. C., Ginjaar, H. B., van Essen, A. J., Pangalila, R., de Groot, I. J. M., Wijkstra, P. J., Zijnen, M. P., Cobben, N. A. M., Kampelmacher, M. J., Wokke, B. H. A., de Coo, I., Fock, J., Horemans, A., van Tol, M., Vroom, E., Rijlaarsdam, M., Straathof, C., Niks, E., and Verschuuren, J. (2014). Forty-Five Years of Duchenne Muscular Dystrophy in The Netherlands. Journal of Neuromuscular Diseases, 1(1):99–109.

Wang, B., McDaid, A., Aw, K. C., and Biglari-Abhari, M. (2017). Design and development of a skinny bidirectional soft glove for post-stroke hand rehabilitation. In Intelligent Systems Conference (IntelliSys), 2017, pages 979–987. IEEE.

Wee, W. T. B., Weilin, M., and Ling, C. S. Y. (2011). Development of a puppetry robotic glove system for the rehabilitation of upper limb functions. In Proceedings of the 5th International Conference on Rehabilitation Engineering & Assistive Technology, page 18. Singapore Therapeutic, Assistive & Rehabilitative Technologies (START) Centre.

Weichbrodt, J., Eriksson, B.-M., and Kroksmark, A.-K. (2018). Evaluation of hand orthoses in Duchenne muscular dystrophy. Disability and rehabilitation, 40(23):2824–2832.

Weiss, P., Heyer, L., Munte, T. F., Heldmann, M., Schweikard, A., and Maehle, E. (2013). Towards a parameterizable exoskeleton for training of hand function after stroke. In IEEE International Conference on Rehabilitation Robotics, pages 1–6.

Yang, J., Xie, H., and Shi, J. (2016). A novel motion-coupling design for a jointless tendon-driven finger exoskeleton for rehabilitation. Mechanism and Machine Theory, 99:83–102.

Yap, H. K., Kamaldin, N., Lim, J. H., Nasrallah, F. A., Goh, J. C. H., and Yeow, C.-H. (2017). A magnetic resonance compatible soft wearable robotic glove for hand rehabilitation and brain imaging. IEEE transactions on Neural Systems and Rehabilitation Engineering, 25(6):782–793.

Yap, H. K., Lim, J. H., Goh, J. C. H., and Yeow, C.-H. (2016). Design of a soft robotic glove for hand rehabilitation of stroke patients with clenched fist deformity using inflatable plastic actuators. Journal of Medical Devices, 10(4):044504.

Yap, H. K., Lim, J. H., Nasrallah, F., Goh, J. C. H., and Yeow, R. C. H. (2015a). A soft exoskeleton for hand assistive and rehabilitation application using pneumatic actuators with variable stiffness. In IEEE International Conference on Robotics and Automation, pages 4967–4972.

Yap, H. K., Lim, J. H., Nasrallah, F., Low, F.-Z., Goh, J. C., and Yeow, R. C. (2015b). MRC-glove: A fMRI compatible soft robotic glove for hand rehabilitation application. In IEEE International Conference on Rehabilitation Robotics, pages 735–740.

Yuan, N., Thielbar, K., Zhang, L.-Q., and Kamper, D. G. (2017). Use of an actuated glove to facilitate hand rehabilitation after stroke. In Converging Clinical and Engineering Research on Neurorehabilitation II, pages 551–555. Springer.

Zhang, F., Hua, L., Fu, Y., Chen, H., and Wang, S. (2014). Design and development of a hand exoskeleton for rehabilitation of hand injuries. Mechanism and Machine Theory, 73:103–116.

A

Framework overview

Table A.1 shows the framework which is used for the found literature. A ‘y’ stands for Yes, ‘n’ means No and ‘?’ means unknown. Each page shows 12 columns out of a total of 48.

Table A.1 Schematic overview different designs and domains (columns 1–12).

number				1	2	3	4	5	6	7	8	9	10	11	12
Name				PMHand	HX Handexos	OHAE	Toochinda	HIT-glove	Pu	Cui	Vanderbilt	BiomHed	x-glove/j-glove	Flexo-glove	PRoGS
signal	controller	human authority	assistive	??	n	y	y	n	??	??	y	y	y	y	y
			resistive	??	n	n	n	n	??	??	n	n	n	n	n
			active	??	n	n	n	n	??	??	n	y	n	n	n
			passive (teleoperated)	??	y	n	n	n	??	??	n	n	n	n	n
			passive-mirrored	??	n	n	n	n	??	??	n	n	n	n	n
		shared authority	active-assist/resist	??	n	n	n	y	??	??	n	n	n	n	n
			passive (self-triggered)	??	n	y	n	n	??	??	y	n	n	n	n
			corrective	??	n	n	n	n	??	??	n	n	n	n	n
			path guidance	??	n	n	n	n	??	??	n	n	n	n	n
		machine	passive (automated)	??	n	n	n	n	??	??	n	n	n	n	n
	command signal	series	brain activity	??	n	n	??	n	??	??	n	n	n	n	n
			nerve activity	??	n	n	??	n	??	??	n	n	n	n	n
			muscle activation	??	n	n	??	n	??	??	n	n	n	y	y
			muscle contraction	??	n	n	??	n	??	??	n	n	n	n	n
			plant movement	??	n	n	??	n	??	??	n	n	n	n	n
			plant force/pressure	??	n	y	??	y	??	??	y	n	n	n	n
		parallel	eyes	??	n	n	??	n	??	??	n	n	n	n	n
			head	??	n	n	??	n	??	??	n	n	n	n	n
			mouth	??	n	n	??	n	??	??	n	n	n	n	n
			other limb	??	n	n	??	n	??	??	n	n	y	n	n
		external	other person	??	n	n	??	n	??	??	n	n	y	y	n
	user feedback	augmented feedback	visual	n	y	y	??	y	n	??	y	n	y	y	y
			auditory	n	n	n	??	n	n	??	n	n	n	n	n
			haptic	n	n	n	??	n	n	??	n	n	n	n	n
			multimodal	n	n	n	??	n	n	??	n	n	n	n	n
		attenuated feedback	visual	n	n	n	??	n	n	??	n	n	n	n	n
			auditory	n	n	n	??	n	n	??	n	n	n	n	n
			haptic	n	y	n	??	y	n	??	n	y	n	n	y
			multimodal	n	n	n	??	n	n	??	n	n	n	n	n
energy	storage	chemical	liquid fuel	n	n	n	n	n	n	n	n	n	n	n	n
			metabolic	n	n	n	n	n	n	n	n	n	n	n	n
		electric/magnetic	battery	n	n	y	y	n	n	y	y	n	y	y	y
			capacitor	n	n	n	n	n	n	n	n	n	n	n	n
			magnetic field	n	n	n	n	n	n	n	n	n	n	n	n
		mechanical	elastic energy	n	n	n	y	y	n	n	n	n	n	n	n
			hydraulic pressure	n	n	n	n	n	n	n	n	n	n	n	n
			pneumatic pressure	n	n	n	n	n	n	n	n	n	n	n	n
			kinetic energy	n	n	n	n	n	n	n	n	n	n	n	n
	actuation	chemical	human muscle	n	n	n	n	n	n	n	n	n	n	n	??
			combustion engine	n	n	n	n	n	n	n	n	n	n	n	??
		electric/magnetic	electromagnetic	y	y	y	y	y	y	y	y	y	y	y	??
			ceramic piezoelectric	n	n	n	n	n	n	n	n	n	n	n	??
			polymeric piezoelectric	n	n	n	n	n	n	n	n	n	n	n	??
		mechanical	smart fluid	n	n	n	n	n	n	n	n	n	n	n	??
			hydraulic	n	n	n	n	n	n	n	n	n	n	n	??
			pneumatic	n	n	n	n	n	n	n	n	n	n	n	??
		thermal	bimetallic	n	n	n	n	n	n	n	n	n	n	n	??
			TCP SMA	n	n	n	n	n	n	n	n	n	n	n	??
mechanical	transmission	cable-conduits	Bowden cable	n	y	y	y	y	n	n	y	n	n	n	n
			push-pull cable	n	n	n	n	n	n	n	n	n	y	y	n
			flexible shaft	n	n	n	n	n	n	n	n	n	n	n	n
		fluidic transmission	hydraulic	n	n	n	n	n	n	n	n	n	n	n	n
			pneumatic	n	n	n	n	n	n	n	n	n	n	n	n
		direct linkage	direct bar linkage	n	n	n	n	n	y	y	y	n	n	n	n
			compliant mechanism	n	n	n	n	n	n	n	n	n	n	n	n
			gears	n	y	n	n	y	n	n	n	n	n	y	n
			cam-followers	n	n	n	y	n	n	n	n	n	n	n	n
		pulley system	cable	y	y	y	y	y	y	n	y	y	y	y	y
			belt	n	n	n	n	n	n	n	n	n	n	n	n
			chain	n	n	n	n	n	n	n	n	n	n	n	n
	structure		portable	y	y	y	y	y	y	y	y	y	y	y	y
			fixed base	n	n	n	n	n	n	n	n	n	n	n	n
	mechanism	joint articulation	monocentric	n	y	n	n	n	y	n	n	n	n	n	n
			polycentric	n	y	y	n	y	n	y	y	n	n	n	n
			jointless	y	n	n	y	n	n	n	n	y	y	y	y
			external	n	n	n	n	n	n	n	n	n	n	n	n
		underactuation	across joints	y	y	y	y	n	y	n	y	y	n	n	y
			across fingers	n	n	n	n	n	n	n	n	y	n	n	n
			across limbs	n	n	n	n	n	n	n	n	n	n	n	n
		constraints	across joints	n	n	n	n	n	y	y	n	n	y	y	n
			across fingers	y	n	n	n	n	n	n	n	n	n	n	n
			across limbs	n	n	n	n	n	n	n	n	n	n	n	n

Table A.1 (continued, columns 13–24)

number				13	14	15	16	17	18	19	20	21	22	23	24
Name				Exotendon glove	Exo-glove	Delp II	M.ReS	ASR-glove	FEX	iGrab	Yang	soft robotic exo-sheath	Ong	Cheng	Pu II
signal	controller	human authority	assistive	n	y	y	y	y	y	y	y	y	y	y	y
			resistive	n	n	n	y	n	n	n	n	n	n	n	n
			active	n	n	n	n	n	n	n	n	n	n	n	n
			passive (teleoperated)	n	n	n	n	n	n	n	n	n	n	n	n
			passive-mirrored	n	n	n	n	n	n	n	n	n	n	n	n
			active-assist/resist	n	n	n	n	n	n	n	n	n	n	n	n
		shared authority	passive (self-triggered)	y	n	n	n	y	n	n	n	n	n	n	n
			corrective	n	n	n	n	n	n	n	n	n	n	n	n
		machine	path guidance	n	n	n	n	n	n	n	n	n	n	n	n
			passive (automated)	n	n	n	n	n	n	n	n	n	n	n	n
	command signal	series	brain activity	n	n	??	??	??	??	??	??	n	??	??	n
			nerve activity	n	n	??	??	??	??	??	??	n	??	??	n
			muscle activation	n	n	??	??	??	??	??	??	n	??	??	n
			muscle contraction	y	n	??	??	??	??	??	??	y	??	??	n
			plant movement	n	y	??	??	??	??	??	??	n	??	??	n
		parallel	plant force/pressure	n	n	??	??	??	??	??	??	n	??	??	n
			eyes	n	n	??	??	??	??	??	??	n	??	??	n
			head	n	n	??	??	??	??	??	??	n	??	??	n
			mouth	y	n	??	??	??	??	??	??	n	??	??	n
			other limb	n	n	??	??	??	??	??	??	n	??	??	n
		external	other person	n	n	??	??	??	??	??	??	n	??	??	n
	user feedback	augmented feedback	visual	y	n	??	y	??	??	??	??	y	??	??	n
			auditory	n	n	??	n	??	??	??	??	n	??	??	n
			haptic	n	n	??	n	??	??	??	??	n	??	??	n
			multimodal	n	n	??	n	??	??	??	??	n	??	??	n
		attenuated feedback	visual	n	n	??	n	??	??	??	??	n	??	??	n
			auditory	n	n	??	n	??	??	??	??	n	??	??	n
			haptic	n	y	??	y	??	??	??	??	n	??	??	n
			multimodal	n	n	??	n	??	??	??	??	n	??	??	n
energy	storage	chemical	liquid fuel	n	n	n	n	n	n	n	n	n	??	n	n
			metabolic	n	n	n	n	n	n	n	n	n	??	n	n
		electric/magnetic	battery	n	y	y	n	y	y	y	y	y	??	y	y
			capacitor	n	n	n	n	n	n	n	n	n	??	n	n
			magnetic field	n	n	n	n	n	n	n	n	n	??	n	n
		mechanical	elastic energy	y	y	y	n	n	y	n	n	y	??	y	n
			hydraulic pressure	n	n	n	n	n	n	n	n	n	??	n	n
			pneumatic pressure	n	n	n	n	n	n	n	n	n	??	n	n
			kinetic energy	n	n	n	n	n	n	n	n	n	??	n	n
	actuation	chemical	human muscle	n	n	n	n	n	n	n	n	n	??	n	n
			combustion engine	n	n	n	n	n	n	n	n	n	??	n	n
		electric/magnetic	electromagnetic	y	y	y	y	n	y	n	y	y	??	y	y
			ceramic piezoelectric	n	n	n	n	n	n	n	n	n	??	n	n
			polymeric piezoelectric	n	n	n	n	n	n	n	n	n	??	n	n
		mechanical	smart fluid	n	n	n	n	n	n	n	n	n	??	n	n
			hydraulic	n	n	n	n	n	n	n	n	n	??	n	n
			pneumatic	n	n	n	n	n	n	n	n	n	??	n	n
		thermal	bimetallic	n	n	n	n	n	n	n	n	n	??	n	n
			TCP			n	n	n	n	y	n	n	n	n	n
			SMA	n	n	n	n	y	n	n	n	n	??	n	n
mechanical	transmission	cable-conduits	Bowden cable	y	y	y	n	n	n	n	n	y	n	y	n
			push-pull cable	n	n	n	n	n	y	y	y	n	y	n	y
			flexible shaft	n	n	n	n	y	n	n	n	n	n	n	n
		fluidic transmission	hydraulic	n	n	n	n	n	n	n	n	n	n	n	n
			pneumatic	n	n	n	n	n	n	n	n	n	n	n	n
		direct linkage	direct	n	n	n	n	n	n	y	n	n	n	n	n
			bar linkage	n	n	n	n	n	n	n	n	y	n	n	y
			compliant mechanism	n	n	n	n	n	n	n	n	n	n	n	n
			gears	y	n	n	y	n	y	n	n	y	n	n	n
			cam-followers	n	n	y	n	y	n	n	n	n	n	n	n
		pulley system	cable	n	y	y	y	y	y	y	y	y	y	y	y
			belt	n	n	n	n	n	n	n	n	n	n	n	n
			chain	n	n	n	n	n	y	y	n	n	n	n	n
	structure		portable	y	y	y	y	y	y	y	y	y	y	y	y
			fixed base	n	n	n	n	n	n	n	n	n	n	n	n
	mechanism	joint articulation	monocentric	n	n	n	y	n	y	n	n	y	n	n	y
			polycentric	n	n	n	y	n	n	n	n	n	n	n	n
			jointless	y	y	y	n	y	n	y	y	n	y	y	n
			external	n	n	n	n	n	n	n	n	n	n	n	n
		underactuation	across joints	y	y	y	y	n	n	y	n	y	n	y	n
			across fingers	n	y	n	n	n	n	n	n	n	n	n	n
			across limbs	n	n	n	n	n	n	n	n	n	n	n	n
		constraints	across joints	n	n	n	n	n	n	n	n	y	n	y	n
			across fingers	y	n	n	n	y	y	n	n	n	n	n	n
			across limbs	n	y	n	n	n	n	n	n	n	n	n	n

Table A.1 (continued, columns 25–36)

number				25	26	27	28	29	30	31	32	33	34	35	36
Name				MRC-glove	Jiralerspong	PneuGlove	Hasegawa	UoA hand exoskeleton	Cappello	Shiota	Refour	Al-Fahaam	MR glove	Rehab glove	Biggar
signal	controller	human authority	assistive	n	y	n	y	y	y	y	y	y	n	y	y
			resistive	n	n	n	n	n	n	n	n	n	n	n	n
			active	n	n	n	n	n	n	n	n	n	n	n	n
			passive (teleoperated)	n	n	n	n	n	n	n	n	n	n	n	n
			passive-mirrored	n	n	n	n	n	n	n	n	n	n	n	n
		shared authority	active-assist/resist	n	n	y	n	n	n	n	n	n	y	n	n
			passive (self-triggered)	y	n	n	n	n	n	n	n	n	y	n	n
			corrective	n	n	n	n	n	n	n	n	n	n	n	n
			path guidance	n	n	n	n	n	n	n	n	n	n	n	n
		machine	passive (automated)	y	n	n	n	n	n	n	n	n	n	n	n
	command signal	series	brain activity	??	??	n	n	n	n	n	n	n	y	n	n
			nerve activity	??	??	n	n	n	n	n	n	n	n	n	n
			muscle activation	??	??	n	y	n	n	n	n	n	n	n	n
			muscle contraction	??	??	n	n	n	n	n	n	y	n	n	n
			plant movement	??	??	y	n	n	n	n	n	n	n	n	n
			plant force/pressure	??	??	n	n	y	n	n	n	n	n	n	y
		parallel	eyes	??	??	n	n	n	n	n	n	n	n	n	n
			head	??	??	n	n	n	n	n	n	n	n	n	n
			mouth	??	??	n	n	n	n	n	n	n	n	n	n
			other limb	??	??	n	n	n	y	n	y	n	n	y	n
		external	other person	??	??	n	n	n	y	n	n	n	n	y	n
	user feedback	augmented feedback	visual	n	??	n	n	n	n	n	n	n	n	n	n
			auditory	n	??	n	n	n	n	n	n	n	n	n	n
			haptic	n	??	n	y	n	n	n	n	n	n	n	n
			multimodal	n	??	y	n	n	n	n	n	n	n	y	n
		attenuated feedback	visual	n	??	n	n	n	n	n	y	n	n	n	n
			auditory	n	??	n	n	n	n	n	n	n	n	n	n
			haptic	n	??	n	n	y	n	n	y	n	n	n	n
			multimodal	n	??	n	n	n	n	n	n	n	n	n	n
energy	storage	chemical	liquid fuel	n	n	n	n	n	n	n	n	n	n	n	n
			metabolic	n	n	n	n	n	n	n	n	n	n	n	n
		electric/magnetic	battery	n	n	n	y	n	y	n	y	n	y	n	??
			capacitor	n	n	n	n	n	n	n	n	n	n	n	n
			magnetic field	n	n	n	n	n	n	n	n	n	n	n	n
		mechanical	elastic energy	n	n	n	n	y	n	n	n	n	y	y	n
			hydraulic pressure	n	n	n	n	n	n	n	n	n	n	n	n
			pneumatic pressure	y	y	y	n	y	y	y	y	y	y	y	n
			kinetic energy	n	n	n	n	n	n	n	n	n	n	n	n
	actuation	chemical	human muscle	n	n	n	n	n	n	n	n	n	n	n	n
			combustion engine	n	n	n	n	n	n	n	n	n	n	n	n
		electric/magnetic	electromagnetic	n	n	n	y	n	n	n	y	n	y	n	y
			ceramic piezoelectric	n	n	n	n	n	n	n	n	n	n	n	n
			polymeric piezoelectric	n	n	n	n	n	n	n	n	n	n	n	n
		mechanical	smart fluid	n	n	n	n	n	n	n	n	n	n	n	n
			hydraulic	n	n	n	n	n	n	n	n	n	n	n	n
			pneumatic	y	y	y	n	y	y	y	y	y	y	y	n
		thermal	bimetallic	n	n	n	n	n	n	n	n	n	n	n	n
			TCP	n	n	n	n	n	n	n	n	n	n	n	n
			SMA	n	n	n	n	n	n	n	n	n	n	n	n
mechanical	transmission	cable-conduits	Bowden cable	n	n	n	n	n	n	n	n	n	n	n	n
			push-pull cable	n	n	n	n	n	n	n	n	n	n	n	y
			flexible shaft	n	y	n	n	n	y	y	y	y	y	y	n
		fluidic transmission	hydraulic	n		n	n	n	n	n	n	n	n	n	n
			pneumatic	n	y	n	n	n	y	y	y	y	y	y	n
		direct linkage	direct	y	y	y	n	n	n	n	n	n	n	y	n
			bar linkage	n	n	n	n	n	n	n	n	n	n	n	n
			compliant mechanism	n	n	n	n	n	n	n	n	n	n	n	n
			gears	n	n	n	y	n	n	n	n	n	n	n	n
			cam-followers	n	n	n	n	n	n	n	n	n	n	n	y
		pulley system	cable	n	n	n	y	y	y	??	n	n	n	n	y
			belt	n	n	n	n	n	n	??	n	n	n	n	n
			chain	n	n	n	n	n	n	??	n	n	n	n	n
	structure		portable	y	y	y	y	y	y	y	y	y	y	y	y
			fixed base	n	n	n	n	n	n	n	n	n	n	n	n
	joint articulation		monocentric	n	n	n	y	y	y	n	y	n	n	n	n
			polycentric	n	n	n	n	n	n	y	n	n	n	n	n
			jointless	y	y	y	n	n	n	n	n	y	y	y	y
			external	n	n	n	n	n	n	n	n	n	n	n	n
	mechanism	underactuation	across joints	y	n	y	n	y	??	??	n	??	n	n	y
			across fingers	y	n	n	n	n	??	??	n	n	n	y	n
			across limbs	n	n	n	n	n	??	??	n	n	n	n	n
		constraints	across joints	n	n	n	n	n	??	??	y	??	n	n	n
			across fingers	n	n	n	y	n	??	??	n	??	n	n	n
			across limbs	n	n	n	n	n	??	??	n	??	n	n	n

Table A.1 (continued, columns 37–48)

			number	37	38	39	40	41	42	43	44	45	46	47	48
Name				Jiang	AirExglove	Lin	Gobee	Lobster inspired	Saeboflex	Tape spring orthosis	HandSome	RELab TenoExo	Niestanak	Liang	Gripit glove
signal	controller	human authority	assistive	y	y	n	y	n	y	y	y	y	n	n	y
			resistive	n	n	n	n	n	y	n	n	n	n	n	n
			active	n	n	n	n	n	n	n	n	n	n	n	n
			passive (teleoperated)	n	n	n	n	n	n	n	n	n	n	n	n
			passive-mirrored	n	n	n	n	n	n	n	n	n	n	n	n
		shared authority	active-assist/resist	n	n	y	n	y	n	n	n	n	y	y	n
			passive (self-triggered)	n	n	n	y	n	n	n	n	n	y	n	n
			corrective	n	n	n	n	n	n	n	n	n	n	n	n
			path guidance	n	n	n	n	n	n	n	n	n	n	n	n
		machine	passive (automated)	n	n	n	n	n	n	n	n	n	n	n	n
	command signal	series	brain activity	??	??	n	n	n	n	??	n	n	??	??	n
			nerve activity	??	??	n	n	n	n	??	n	n	??	??	n
			muscle activation	??	??	n	y	y	n	??	n	y	??	??	n
			muscle contraction	??	??	n	n	n	n	??	n	n	??	??	n
			plant movement	??	??	y	n	n	n	??	n	n	??	??	n
			plant force/pressure	??	??	n	n	n	n	??	n	y	??	??	n
		parallel	eyes	??	??	n	n	n	n	??	n	n	??	??	n
			head	??	??	n	n	n	n	??	n	n	??	??	n
			mouth	??	??	n	n	n	n	??	n	n	??	??	n
			other limb	??	??	y	n	n	n	??	n	n	??	??	y
		external	other person	??	??	y	n	n	n	??	n	n	??	??	n
	user feedback	augmented feedback	visual	??	??	??	y	n	n	??	n	y	??	??	n
			auditory	??	??	??	n	n	n	??	n	n	??	??	n
			haptic	??	??	??	n	n	n	??	n	y	??	??	n
			multimodal	??	??	??	n	n	n	??	n	n	??	??	n
		attenuated feedback	visual	??	??	??	n	n	n	??	n	n	??	??	y
			auditory	??	??	??	n	n	n	??	n	n	??	??	n
			haptic	??	??	??	n	n	y	??	y	n	??	??	y
			multimodal	??	??	??	n	n	n	??	n	n	??	??	n
energy	storage	chemical	liquid fuel	n	n	n	n	n	n	n	n	n	n	n	n
			metabolic	n	n	n	n	n	n	n	n	n	n	n	n
		electric/magnetic	battery	n	y	y	y	n	n	n	n	y	n	n	n
			capacitor	n	n	n	n	n	n	n	n	n	n	n	n
			magnetic field	n	n	n	n	n	n	n	n	n	n	y	n
		mechanical	elastic energy	n	n	y	y	n	y	y	y	y	y	n	n
			hydraulic pressure	n	n	n	n	n	n	n	n	n	n	n	n
			pneumatic pressure	y	y	y	y	y	n	n	n	n	n	n	n
			kinetic energy	n	n	n	n	n	n	n	n	n	n	n	n
	actuation	chemical	human muscle	n	n	n	n	n	y	n	y	n	n	n	y
			combustion engine	n	n	n	n	n	n	n	n	n	n	n	n
		electric/magnetic	electromagnetic	n	y	y	n	n	n	n	n	y	y	y	n
			ceramic piezoelectric	n	n	n	n	n	n	n	n	n	n	n	n
			polymeric piezoelectric	n	n	n	n	n	n	n	n	n	n	n	n
		mechanical	smart fluid	n	n	n	n	n	n	n	n	n	n	n	n
			hydraulic	n	n	n	n	n	n	n	n	n	n	n	n
			pneumatic	y	y	y	y	y	n	n	n	n	n	n	n
		thermal	bimetallic	n	n	n	n	n	n	n	n	n	n	n	n
			TCP	n	n	n	n	n	n	n	n	n	n	n	n
			SMA	n	n	n	n	n	n	n	n	n	n	n	n
mechanical	transmission	cable-conduits	Bowden cable	n	y	y	n	n	n	y	n	y	n	n	n
			push-pull cable	n	n	n	n	n	n	n	n	n	y	n	y
		fluidic transmission	flexible shaft	y	n	n	y	y	n	n	n	n	n	n	n
			hydraulic	n	n	n	n	n	n	n	n	n	n	n	n
			pneumatic	y	y	y	y	y	n	n	n	n	n	n	n
		direct linkage	direct	y	n	n	n	y	n	y	n	y	y	n	y
			bar linkage	n	n	n	n	n	n	n	y	n	n	n	n
			compliant mechanism	n	y	y	y	n	n	n	n	n	n	n	n
			gears	n	n	n	n	n	n	n	n	n	n	n	n
		pulley system	cam-followers	n	n	n	n	n	n	n	n	n	n	n	n
			cable	n	y	y	y	n	y	y	y	y	y	n	y
			belt	n	y	n	n	n	n	n	n	n	n	n	n
			chain	n	n	n	n	y	n	n	n	n	n	y	n
	structure		portable	y	y	y	y	y	y	y	y	y	y	y	y
			fixed base	n	n	n	n	n	n	n	n	n	n	n	n
	mechanism	joint articulation	monocentric	n	n	n	n	n	n	y	y	y	y	n	n
			polycentric	n	n	n	n	n	n	n	n	n	n	y	n
			jointless	y	y	y	y	y	y	n	n	n	n	n	y
			external	n	n	n	n	n	n	n	n	n	n	n	n
		underactuation	across joints	y	y	y	y	y	y	y	y	y	y	n	n
			across fingers	y	y	n	n	n	y	y	y	y	y	n	n
			across limbs	n	n	n	n	n	n	n	n	n	n	n	n
		constraints	across joints	n	n	y	n	n	n	n	n	n	n	n	n
			across fingers	n	n	n	n	y	n	n	n	n	n	n	y
			across limbs	n	n	n	n	n	n	n	n	n	n	n	n

III

Final report appendices

B

Human hand anatomy

This appendix will show the human anatomy which is first analyzed before the different concepts were made. Section B.1 describes the function of the skin. Section B.2 describes the bones and joints in the human hand. Finally Section B.3 gives an overview of the muscles in the human hand.

B.1 Skin

The human hand is a complicated mechanism consisting of different part. First the skin, the skin protects the hand and is responsible for the tactile senses. The tactile senses register light touch, pressure touch and they register heat, cold and pain (Jones and Lederman, 2006). Extensibility and innervation of the skin influence the optimal functioning of the hand. Furthermore, proprioception is important in hand functioning. The proprioception gives feedback about the inner body status. It provides information if the body is moving or not (Ribot-Ciscar et al., 2004).

B.2 Bones and joints

The human hand consists of bones and joints. The total number of bones in the hand is twenty-seven. These are subdivided into eight carpal bones, five metacarpal bones and fourteen phalanges. These bones are connected with the help of joints and ligaments. An overview is given in Figure B.1. The carpal bones are more or less fixed in place with the help of ligaments. The lower part of the wrist joint shown in red mark in Figure B.1, consists of the scaphoid bone, lunate bone and the radius. The metacarpal bones are located in the middle of the hand. Each finger and the thumb has one of these bones. The saddle-shaped carpometacarpal joint forms the joint of the thumb which made that the thumb can rotate more than the other fingers. The phalanges are the finger bones. The human hand has four fingers and one thumb. Each fingers consists of three bones, while the thumb consists of two. Each finger consists of the metacarpophalangeal (MCP), proximal interphalangeal (PIP), and distal interphalangeal (DIP) joint. These joints have one degree of freedom (DOF) each, for flexion and extension, while the MCP joint also has one DOF for adduction and abduction. These movements are shown in Figure B.2. This made a total DOF of four for the fingers (InformedHealth, 2018).

B.3 Muscles

The hand consists of more than thirty muscles, all working together and some are shown in Figure B.3. The muscles are located in the forearm, while the tendons are located directly in the hand and fingers. Therefore, these muscles are called the extrinsic muscles. The extensor tendons, needed to extend the finger, are located on the dorsal side of the hand and fingers. The two long flexor tendons, the flexor digitorum superficialis tendon and the flexor digitorum profundus tendon, are located on the palmar side of the hand and fingers. The superficial flexor attaches to the middle phalanx, and the digitorum flexor connects to the distal phalanx. The interosseous muscles are responsible for the abduction and adduction movements of the fingers. The lumbrical muscles flex the MCP joint and extend the interphangeal joints. The ligaments control the movement and stability of the fingers.

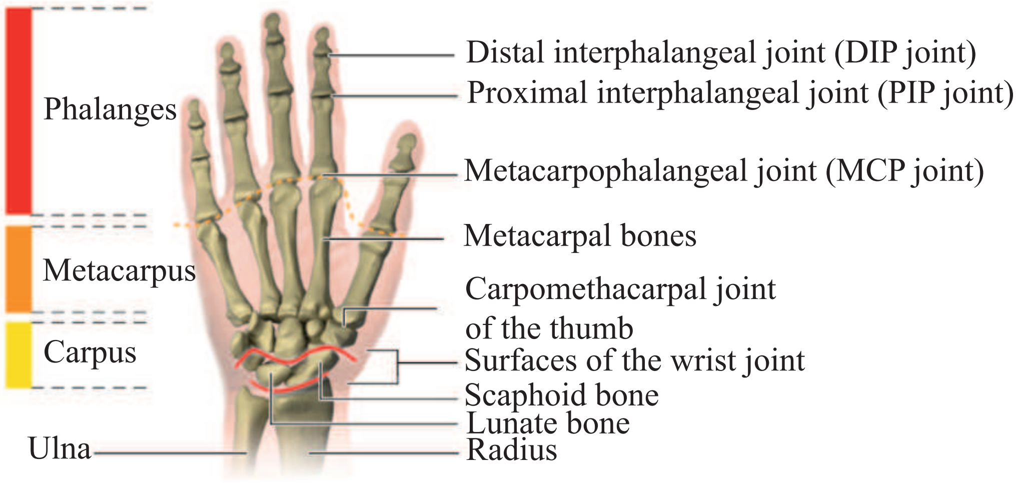

Figure B.1 Bones and joints in the human hand.

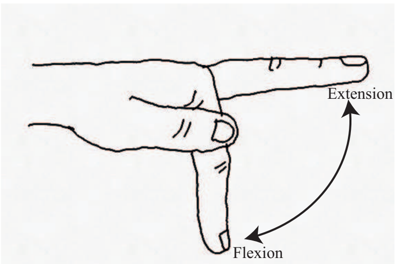

(a) Flexion and extension movement of the finger.

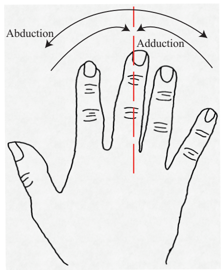

(b) Abduction and adduction movement of the finger.

Figure B.2 Overview of the human hand movements with flexion and extension and abduction and adduction.

The hand is able to use the power grip or precision grip. It depends on the size, shape and weight of the object which of these two ways is used. Where the power grips is the best to use for large, heavy objects, precision grip prefers the small, lightweight objects. The power grip works in the following way, the object is placed in the palm of the hand. The long flexor tendons pull the four fingers and the thumb. The thumb is in this case positioned in opposite direction of the fingers. In the precision grip work the fingers like tweezers, the thumb is opposite of one fingertip. This makes it possible to grip very small objects in a controlled way (Feix et al., 2015).

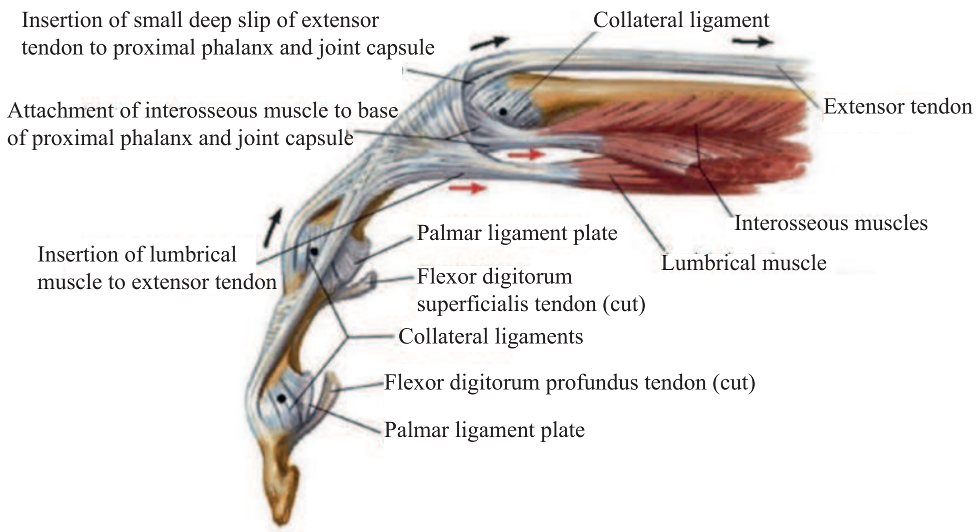

Figure B.3 Muscles of the human hand (Schreuders et al., 2019).

C

Conceptual design

This appendix gives an overview of the different steps that are taken to end up with the final design. Section C.1 shows the design criteria for the complete hand orthosis, including the wishes. Furthermore, an overview of the tasks which consist of the ADL tasks is given. Section C.2 gives an overview of the different concepts. The Harris profile that is used to choose the final concept is explained in Section C.3. Section C.4 gives an explanation of the negative score of the Harris profile. The final concept selection is shown in Section C.5 and the explanation of the selection of the final concept is described in Section C.6.

C.1 Design criteria

1. The device should not be bigger than cross-sectional area 20 mm $\times$ 18 mm. This is the size of the finger of an adult man (Molenbroek, 2004).
2. The device should not weight more than 300 g (Boser et al., 2018). The mass for each finger is 50 g.
3. The actuator will be placed externally on the wheelchair.
4. The device should be used for ADL. List of ADL tasks can be found below.
5. While wearing the device the tactile and proprioceptive senses can still be used (Jones and Lederman, 2006).
6. The maximum output force of the device is 10.5 N. This is the force on top of the finger, pointing towards an object (Smaby et al., 2004).
7. The device should be able to make a palmar grasp and pinch grasp (Feix et al., 2015).
8. The flexion angle range of the fingers is 20°–80° (Bain et al., 2015). The MCP, PIP and DIP joints have functional angles of 61°, 60°, and 39°, respectively (Boser et al., 2018).
9. The device should be safe and not physically harm the user.
10. The device should be used independently, donning and doffing should be possible without help (Case et al., 2018).
11. All the fingers of the device can be controlled at once.
12. The DOF of the fingers is 2. The fDOF is 1 (Bos et al., 2017).
13. The device should have a coupled motion between the MCP, PIP, and DIP joint (Nimbarte et al., 2008).
14. The shear force between the device and the skin should be as low as possible (Bos et al., 2017).
15. The actuator response should be within 2 s (Boser et al., 2018). This is after sending the signal, the time it takes before moving.
16. The actuator should have a cycle frequency of 2 Hz. This is the time it takes to move the fingers (Nizamis et al., 2017).
17. The device should not produce a sound louder than 70 dB. From 70 dB sound becomes annoying (Fink, 2019).
18. The material of the device should not irritate the skin.
19. The device can be controlled with series control. The control of the hand is with muscle activation, plant movement or plant force (Bos et al., 2016).

20. The device should work on a battery for a whole day without charging.
21. If pneumatic: gas tank should be big enough for at least one day.
22. If electromagnetic: motor power that can reach 10.5 N.
23. The device can be cleaned in the dishwasher.

Wishes:

1. The time to learn to use the device is limited to 1 day.
2. The total costs of the device should not be more than 150 euro.
3. The orthosis should look attractive (Plettenburg, 1998).
4. The size of the device should be adaptable to increase wear comfort. The device is custom-made, but sometimes fingers are thicker, and would it be nice if small adaptations are possible.
5. The device needs maintenance once a year. When it is 2 times a year it is fine, not every week.

The ADL taskas are tasks that most people can perform on daily basis without any help. The different categories are the same as mentioned by Edemekong and Levy (2019). These categories are:

1. Dressing: being able to dress and undress and being able to manage buttons, zippers and other fasteners.
2. Eating: the ability to feed oneself, cooking excluded.
3. Washing: being able to shower or taking a bath independent, including shaving, brushing teeth and doing hair.
4. Continence: being able to control bowels and bladder or to manage incontinence independently.
5. Toileting: the ability to use the toilet and being able to go to the toilet independently.
6. Transferring: being able to walk, get in and out of bed, and if person is not ambulatory, ability to transfer from bed to wheelchair on their own.
7. Using the phone independently.
8. Maintaining the home: housekeeping, laundry.
9. Shopping: being able to go to the shop for groceries independently.
10. Transport: the ability to drive or use public transportation for appointments or shopping.

C.2 Concepts

1. This concept is based on the same principle as described in Cool and Van Hooreweder (1971). This principle consists of three hard parts, connected with a hinge. This whole device is covered with a tube. The tubes are smaller than in Cool and Van Hooreweder (1971) and are placed sideways on both sides of the finger. The tube can bend because of the inner structure. The lower part has some extra support material and can flip open when air enters the tube. This means that the actuation system is pneumatic. When air enters the tube, the finger starts to bend. Important is that the air enters the tubes with the same amount and speed on both sides of the finger, to prevent unequally bending. This principle is shown in Figures C.1(a) and C.1(b).
2. This is the same principle as concept 1. However, in this case there is one tube placed on top of the own finger. A tube directly placed on the finger is not comfortable. Therefore, a bedding made of silicone is placed on top of the finger in which the tube will be placed. Straps or special glue will connect the tubes to the finger. To make flexion possible, there are some openings (flip parts) connected to the tube alternated with some harder parts. The flip part opens as soon as air enters to make flexion possible. This concept is pneumatic actuated. To make it possible to actuate all four fingers at once, the total volume of each finger is the same. This design is shown in Figures C.1(c) and C.1(d).
3. The origami design, in this design the finger consists of different flat parts of metal which are connected with tape. As soon as the proximal part of the design is pushed or pressed, the finger can flex. The flexion angle is dependent on the structure of the metal parts. The bigger the angle between the parts, the more it bends. This system can be pneumatically or hydraulic driven. This is shown in Figures C.1(e) and C.1(f).
4. This concept is a flat 3D printed structure. This makes it lightweight. This structure is placed on top of the own fingers with two 3D printed hinges. Inside the structure is a cable. This cable is fixed at the distal end of the finger. By pulling on the cable, the finger will flex. By adding an extension spring in the system the finger keeps bended until the cable will be loosened. At this point the finger will extend. This mechanism works with an electromotor. This is shown in Figures

C.1(g) and C.1(h).

5. This concept uses electromagnets. The magnets are placed on top of the finger near the DIP, PIP and MCP joints. When there is no current in the circuit the magnets are connected. This means that the finger is extended. When the electromotor is activated, the magnets will bounce off each other which will cause the finger to flex. This system uses an electromotor as actuator system. This is shown in Figures C.1(i) and C.1(j).
6. This concept is based on the same principle as hairclips work. In open position of the hairclips on top of the own finger, the finger is extended. After pushing against the clips, the clips will close which results in a bending motion. This causes the finger to flex. After pulling on the cable the clip will open again, which extends the finger. A cover is needed to prevent physical harm to the user. The actuator system is an electromotor. This is shown in Figures C.1(k) and C.1(l).
7. This concept uses PAM with a special inner structure. The central point is located more towards the top, instead of the middle. The PAM is placed on top of the own fingers. After entering air, the PAM will start bending because of the inner structure. This results in flexion of the finger. When there is no air added anymore, and the PAM will leave the air, the finger starts to extend. This system is therefore pneumatically driven. This is shown in Figures C.1(m) and C.1(n).
8. This concept makes use of a rigid body structure. It consists of a linkage finger mechanism as designed by Herath et al. (2018). However, in that design a complete finger as part of a prosthesis is shown. In this situation the frame will be placed on top of the own finger. As soon as the nylon string is activated the frame will start bending. This causes the own finger to flex. When there is no activation anymore the finger will extend. The actuation system is an electromotor. This is shown in Figures C.1(o) and C.1(p).
9. This concept is a tube place on top of the own fingers. Inside the tube is a cable, connected to the distal end. The tube has some openings around the PIP and MCP joints. When there will be pulled on the robe, the finger will flex. When releasing the robe, the fingers will extend. This system uses an electromotor. This is shown in Figures C.1(q) and C.1(r).
10. This concept makes use of hinges, a spring and a cable. The mechanism is located sideways of the finger. There is one cable to extend and one cable to flex. The finger at the end saves energy. The mechanism can be clicked around the finger, while the finger tip stays free to be used for tactile and proprioceptive senses. This mechanism uses an electromotor. This is shown in Figures C.1(s) and C.1(t).

A Harris profile in combination with weighted criteria is used to select the three most promising solutions. The Harris profile is shown in the next section.

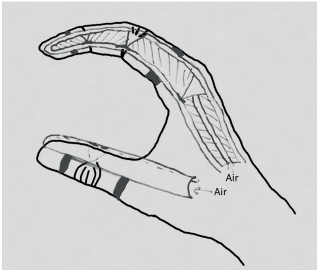

(a) Concept 1 side view.

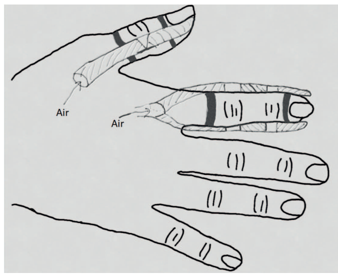

(b) Concept 1 top view.

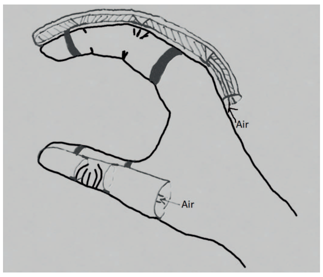

(c) Concept 2 side view.

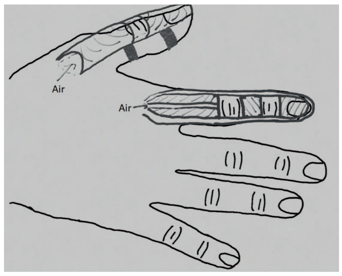

(d) Concept 2 top view.

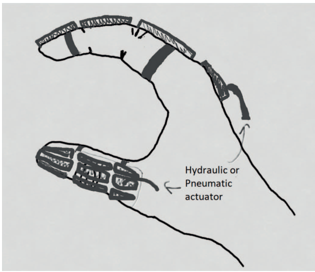

(e) Concept 3 side view.

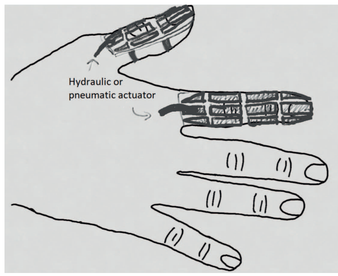

(f) Concept 3 top view.

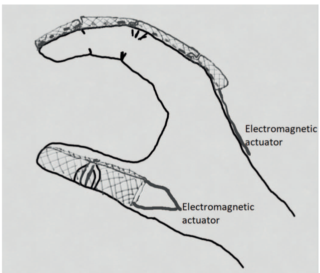

(g) Concept 4 side view.

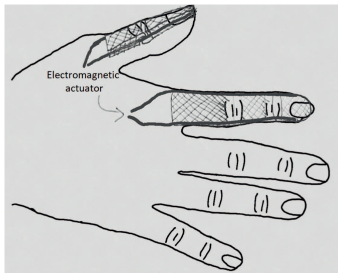

(h) Concept 4 top view.

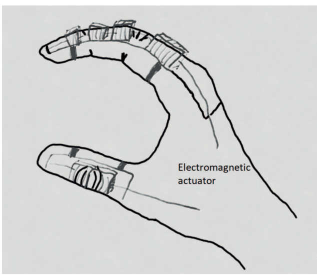

(i) Concept 5 side view.

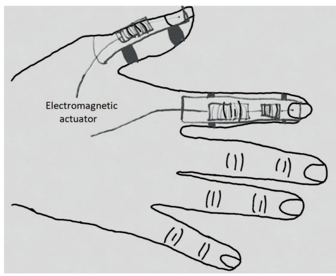

(j) Concept 5 top view.

Figure C.1 Overview different concepts from the side and the top.

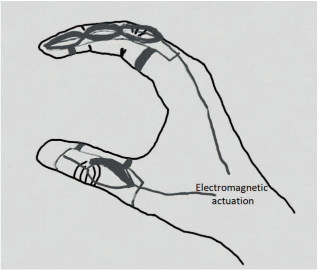

(k) Concept 6 side view.

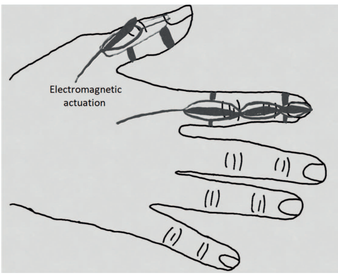

(l) Concept 6 top view.

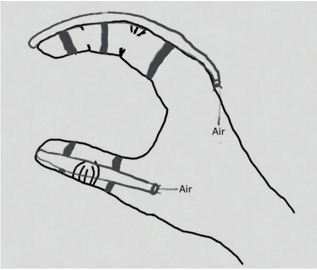

(m) Concept 7 side view.

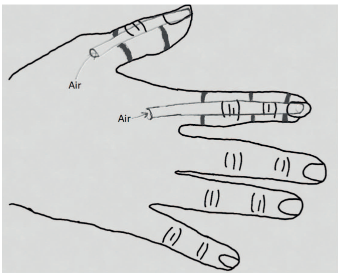

(n) Concept 7 top view.

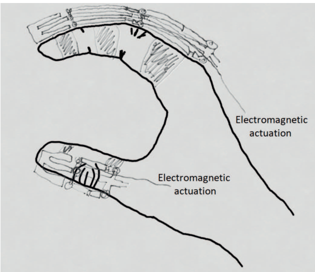

(o) Concept 8 side view.

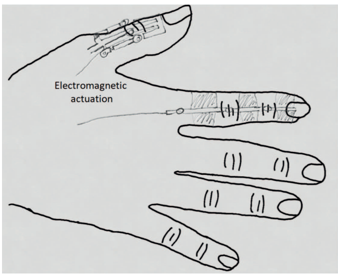

(p) Concept 8 top view.

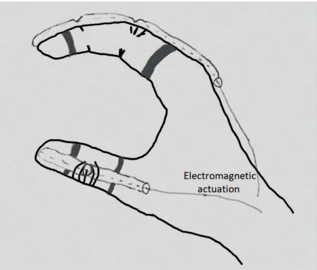

(q) Concept 9 side view.

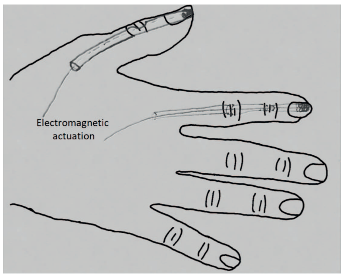

(r) Concept 9 top view.

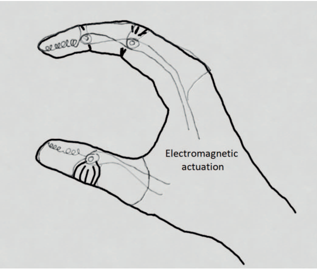

(s) Concept 10 side view.

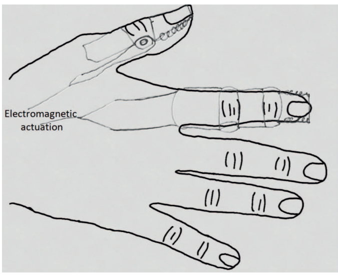

(t) Concept 10 top view.

Figure C.1 (continued)

C.3 Harris profile

Table C.1 shows the Harris profile in combination with weighted criteria. The given weights for the criteria are described. The negative scores received by a concept are explained as well. The selection of the final concept is shown subsequently. An explanation for the given weights for the criteria:

- Dimensions: as the main goal of this project was to design a flat hand orthosis, the dimensions are seen as most important. Therefore it receives 10 points.
- Weight: as weight is an important factor why people do not use their prosthesis or orthosis it is seen as important as well. Therefore, 8 points are given.
- Location actuator: when it is not possible to place the actuator externally on a wheelchair, the weight will increase. The location of the actuator does also have influence on the design. Therefore it receives 8 points as well.
- ADL use: as the goal is that the user becomes more independent, it should be possible to use the device during ADL. It receives 7 points because when some tasks from ADL can be fulfilled, this will also help the user.
- Senses: DMD patients can still use their own senses, that is something you do not want to reject. Therefore, it also receives 7 points.
- Output force: the output force has influence on the use of the device. When no force can be generated the device cannot be used for what it is designed for. As with a bit force some things can be done with it, is scored one point less than the senses with 6 points.
- Grasp: to make it possible to grasp something, the device should be possible to make a grasping movement. However, when you can grasp something but there is no force, you still can't do anything. Therefore 5 points are given to the grasp criteria.
- Flexion/extension: to use the device during ADL it would be nice if the hand can make a flexion/extension movement. As grasping and flexion/extension are more or less dependent from each other, 5 points were given..
- Safe: the device should be safe. It is seen as important but because it depends on the design it was not seen first priority, therefore 5 point were given.
- Donning/doffing: when the user cannot donning/doffing the device by himself, the user is still dependent of others. It was seen as even important as safety with 5 points.
- Finger control: receives 4 points because it is not a first priority but it is nice when this is possible. It makes the device less complex.
- DOF fingers: this depends on the movements, when it is possible to flex and extend the fingers, the dof is reached, therefore 4 points were given.
- Coupled motion: the coupled motion does not have first priority but it will be nice for the user when this is possible, therefore 4 points are given.
- Shear force: as DMD patients have a sensitive skin, shear force should be as low as possible. However, there is always some shear force and it depends more on the attachment mechanism than on the design. Therefore, 3 points are given to this criteria.
- Response time: for the ease of use a short response time is great. However, it is not the first priority for the design, this explains the 3 points.
- Cycle frequency: this is the same reason as the response time.
- Noise: it will harm the user when the noise is really loud, however there are tricks to solve this and is not really design dependent, therefore 3 points are given.
- Skin irritation: it is important that a material will be chosen that does not be noted for skin irritation. However, it is also person dependent which explains the 2 points.
- Control: how the device will be controlled depends on the actuation system and is not really dependent of the design, therefore, it receives 2 points.
- Battery: the same reason for the battery.
- Actuator: also for the actuator, this can be added later on and is not dependent of the design.
- Cleaning: it would be nice to clean the device in the dishwasher, however it is not necessary, therefore 2 points were given.

Table C.1 Overview of Harris profile for the different concepts (concepts 1–3).

Criteria	W	Concept 1 Total	Concept 2 Total	Concept 3 Total
Dimensions	10	-20	10	20
Weight	8	16	16	16
Location actuator	8	16	16	16
ADL use	7	14	14	14
Senses	7	14	14	14
Output force	6	-6	-6	-6
Grasp	5	10	10	5
Flexion/ Extension	5	10	10	5
Safe	5	10	10	10
Donning/ doffing	5	5	5	-5
Finger control	4	8	8	4
DOF fingers	4	4	4	4
Coupled motion	4	8	8	8
Shear force	3	-3	-3	-3
Response time	3	6	6	3
Cycle frequency	3	3	3	3
Noise	3	3	3	3
Skin irritation	2	2	2	2
Control	2	2	2	2
Battery	2	2	2	2
Actuator	2	2	2	2
Cleaning	2	4	4	-2
Total	**100**	**110**	**140**	**117**

Table C.1 (continued, concepts 4–6)

Criteria	W	Concept 4 Total	Concept 5 Total	Concept 6 Total
Dimensions	10	20	10	10
Weight	8	8	8	16
Location actuator	8	16	16	16
ADL use	7	14	14	14
Senses	7	14	14	14
Output force	6	-6	6	-6
Grasp	5	5	5	5
Flexion/ Extension	5	5	5	-10
Safe	5	-5	-5	-5
Donning/ doffing	5	5	5	5
Finger control	4	8	4	4
DOF fingers	4	4	4	4
Coupled motion	4	8	8	4
Shear force	3	-3	-3	-3
Response time	3	3	-3	3
Cycle frequency	3	3	3	-3
Noise	3	6	-3	-3
Skin irritation	2	2	2	2
Control	2	2	2	2
Battery	2	2	2	2
Actuator	2	2	2	2
Cleaning	2	-2	-2	2
Total	**100**	**111**	**94**	**75**

Table C.1 (continued, concepts 7–10)

Criteria	W	Concept 7 Total	Concept 8 Total	Concept 9 Total	Concept 10 Total
Dimensions	10	10	-10	20	-10
Weight	8	16	8	8	8
Location actuator	8	16	16	16	16
ADL use	7	14	14	14	14
Senses	7	7	14	7	14
Output force	6	6	-6	6	6
Grasp	5	10	10	5	5
Flexion/ Extension	5	5	5	5	10
Safe	5	10	-5	5	-5
Donning/ doffing	5	-10	5	-5	5
Finger control	4	4	4	4	8
DOF fingers	4	-4	4	4	4
Coupled motion	4	8	4	8	8
Shear force	3	-3	-6	-3	-3
Response time	3	3	3	3	3
Cycle frequency	3	3	-3	3	3
Noise	3	3	3	3	3
Skin irritation	2	2	2	2	-2
Control	2	2	2	2	2
Battery	2	2	2	2	2
Actuator	2	2	2	2	2
Cleaning	2	2	-4	-2	-2
Total	**100**	**108**	**64**	**109**	**91**

C.4 Explanation of the negative scores from the Harris profile

Concept 1:

- Dimensions: because the tubes on each side of the finger exceed the given dimensions. For one finger it could work but the next finger does not fit anymore.
- Output force: because two small tubes which makes it harder to reach the right output force.
- Shear force: the tubes on the side of the finger will move over the skin during bending, this causes shear force.

Concept 2:

- Output force: smaller tube than the original design makes it unsure to reach the right output force.
- Shear force: direct contact on skin which causes shear force.

Concept 3:

- Output force: unknown if the system can reach the output force.
- Donning and doffing: flexible structure that makes it harder to donning and doffing independently.
- Shear force: material flat on skin causes shear force.
- Cleaning: Hard to clean with all the edges.

Concept 4:

- Output force: not sure if output force will be reached as there will be a lot of friction in the hinge.
- Safety: the 3D printed hinge with a cable might be not so safe.
- Shear force: device is flat on skin which causes shear force.

Concept 5:

- Safety: electromagnets on the finger is not safe.
- Shear force: device is flat on the hand which causes shear force.
- Response time: will be slow before the magnets react.
- Noise: clicking of the magnets causes noise.
- Cleaning: electromagnets cannot be placed on the dishwasher.

Concept 6:

- Output force: hard to be reached.
- Flexion and extension: it is hard to generate a smooth flexion and extension movement.
- Safety: it is not safe, because something can come between the clip.
- Shear force: place on top of the finger so shear force.
- Response time:clicking will be slow.
- Noise: clicking causes noise.

Concept 7:

- Donning and doffing: flexible tubes are hard to donning and doffing.
- Dof: only 1 DOF.
- Shear force: directly on the skin which causes shear force.

Concept 8:

- Dimensions: structure is higher than the 20 mm.
- Output force: the output force of the prosthesis was not high enough and this design is smaller.
- Safe: there are some open parts where something can get stuck.
- Shear force: Device is on top of the fingers which causes shear force.
- Cycle frequency: the rigid mechanism is slow.
- Cleaning: the material cannot in the dishwasher and has a lot of small parts you cannot come in between.

Concept 9:

- Donning/doffing: flexible tubes make it hard to donning and doffing the device.
- Shear force: tubes are placed on top of the finger and causes shear force.
- Cleaning: cannot placed in the dishwasher because the cables are connected inside.

Concept 10:

- Dimensions: wider than 18 mm.
- Safety: some parts that could go wrong.
- Shear force: placed on the finger where the cable will move. This causes shear force.
- Skin irritation: material next to the finger could cause skin irritation.
- Cleaning: cannot placed in the dishwasher because cables are connected.

C.5 Selection final concept

In this section is an overview made to select the final concept from the best three designs.

Table C.2 Selection final concept in relation to the design criteria.

Design criteria	Concept 2	Concept 3	Concept 4	Best
Dimensions	+	++	+	3
Weight	++	+	+	2
Actuator	+	+	+	all
ADL	+	+	+	all
Output force	+	?	+	2 and 4
Grasp	++	++	++	all
Flexion	+	+	+	all
Tactile	+	+	+	all
Safe	++	++	+	2 and 3
Donning	+	+	++	4
Control	+	+	+	all
DOF	+	+	+	all
Decoupled	+	+	+	all
Shear force	?	?	?	all
Reaction time	?	?	?	all
Cycle freq	+	+	+	all
Noise	+	+	+	all
Skin irritation	+	+	-	2 and 3
Series control	+	+	+	all
Battery	+	+	+	all
Tank size	+	+	+	all
Motor power	+	+	+	all
Cleaning	++	++	+	2 and 3

Table C.3 Selection final concept in relation to the wishes.

Wishes	Concept 2	Concept 3	Concept 4	Best
Learning time	+	+	+	all
Costs	+	+	+	all
Attractive	-	+	+	3 and 4
Adaptable	-	-	+	4
Maintenance	+	+	+	all

This means that concepts 2 and 3 have the same amount of points. Therefore, with both designs a feasibility test will be carried out.

C.6 Explanation of concept choice

Concept 2:

1. The device should not be bigger than cross-sectional area 20 mm $\times$ 18 mm. This is the size of an adult man. The tubes on top of the finger are not bigger than 20 mm $\times$ 18 mm and are a bit longer than the finger length.
2. The device should not weight more than 300 g. Weight of complete hand prosthesis was 180 g. This design is smaller, which means that it is lighter.
3. The actuator will be placed externally on the wheelchair. The pneumatic actuator will be placed external on the wheelchair.
4. The device should be used for ADL. List of ADL tasks can be found below. The flexion and extension is possible for the fingers, the thumb is static but makes it possible to grasp something.
5. The maximum output force of the device is 10.5 N. This is the force on top of the finger. This is most probably possible, as this design is used as a prosthesis.
6. The device should be able to make a palmar grasp and pinch grasp. Finger flexion and extension is possible, this makes palmar grasp possible. Pinch grasp is possible with no complete flexion of the PIP joint.
7. The flexion angle range of the fingers is 20°–80°. This is possible.
8. While wearing the device the tactile and proprioceptive senses can still be used. This is possible

because the tube is place on top of the finger and is connected with three small straps or special glue. This keeps the finger tops free.

9. The device should be safe and not physically harm the user. The tubes do not have any sharp edges. Furthermore, the actuation system is pneumatic, the air tube is placed at the wheelchair, and air cannot harm the user.
10. The device should be used independently, donning and doffing should be possible without help. The tubes are stable which makes it easier to place on top of the fingers. The fingers are separated from each other which makes it easier for the donning and doffing. The straps could be hard to attach when only one disfunctioning hand can be used.
11. All the fingers of the device can be controlled at once. The four finger tubes come together into one tube which is connected to the actuation system. Not all the fingers have the same length, therefore some tubes are wider to give all the four fingers the same volume. This makes it possible to bend all the four fingers at once.
12. The DOF of the fingers is 2. The DOF of the fingers is 2, flexion and extension for the MCP and PIP joint.
13. The device should have a coupled motion between the MCP and PIP joint. The device does have a coupled motion between the MCP and PIP joint.
14. The shear force between the device and the skin should be as low as possible. There is silicone between the tube and the finger to reduce the shear force. Or the shape of the tube on top of the fingers is half round that it nicely fits the finger. But there will always be some shear force on the finger.
15. The actuator response should be within 2 s. This is after sending the signal the time it takes before moving. Not possible to measure before. It depends on the used actuator.
16. The actuator should have a cycle frequency of 2 Hz. This is the time it takes to move the fingers. This should be possible. The design of Cool took 0.3s a cycle frequency of 2 Hz is 0.5 s. The fingers for the orthosis design are smaller but their volume is also smaller. This is more or less the same time.
17. The device should not produce a sound louder than 70 dB. From 70 dB sound becomes annoying. With the help of a damper the noise is below 70 dB.
18. The material of the device should not irritate the skin. Silicone does not cause skin irritation. This is the part that touches the skin. Therefore, there is no problem.
19. The device can be controlled with series control. This means that the control of the hand is with muscle activation, plant movement or plant force/pressure. This should be possible.
20. The device should work on a battery for a whole day without charging. A battery is needed to guide the Arduino. This battery works the whole day.
21. If pneumatic: gas tank of at least enough for one full day. The tank is big enough because it can be place somewhere on the wheelchair.
22. If electromagnetic: motor power should be high enough to generate output forces of 10.5 N
23. The device can be cleaned in the dishwasher. The tubes can be cleaned in the dishwasher. This is because the fingers can be decoupled from the pneumatic system. The finger parts can be placed in the dishwasher.

Wishes

1. The time to learn to use the device is limited to 1 day. Easy to control
2. The total costs of the device should not be more than 150 euro. Cheap design
3. The orthosis should look attractive. No
4. The size of the device should be adaptable to increase wear comfort. The device is custom-made, but sometimes fingers are thicker, and would it be nice if small adaptations are possible. Not possible
5. The device needs maintenance once a year. When it is 2 times a year it is fine, not every week. I think this is fine.

Concept 3:

1. The device should not be bigger than cross-sectional area 20 $\times$ 18 mm. This is the size of an adult man. The origami structure has a height below 20 mm. the width is at a maximum of 18 mm.
2. The device should not weight more than 300 g. The origami design will be made of metal and foil. This is lightweight and will stay below 300 g.
3. The actuator will be placed externally on the wheelchair. The hydraulic or pneumatic actuator will be placed external on the wheelchair.
4. The device should be used for ADL. List of ADL tasks can be found below. The flexion and extension are possible for the fingers, the thumb is static but makes it possible to grasp something.
5. The maximum output force of the device is 10.5 N. This is the force on top of the finger. Not sure if this is possible.
6. The device should be able to make a palmar grasp and pinch grasp. Finger flexion and extension is possible, this makes palmar grasp possible. Pinch grasp is possible with no complete flexion of the PIP joint.
7. The flexion angle range of the fingers is 20°–80°. This is possible.
8. While wearing the device the tactile and proprioceptive senses can still be used. This is possible because the origami structure is placed on top of the finger and is connected with two small straps. This keeps the finger tops free.
9. The device should be safe and not physically harm the user. The origami structure is made of metal plates and foil. This does not have any sharp edges. The actuation system is hydraulic or pneumatic and is tested before connected.
10. The device should be used independently, donning and doffing should be possible without help. Because the device is deformable this will be a bit harder. However, when there will be chosen for a small metal plate this is not a problem. The fingers can be placed independently which is necessary for DMD patients.
11. All the fingers of the device can be controlled at once. The four finger actuators come together into one tube which is connected to the actuation system. All the four fingers need the same force. The input force is the output force independent of the size.
12. The DOF of the fingers is 2. This is the case, for the MCP and the PIP joint a flexion and extension movement.
13. The device should have a coupled motion between the MCP and PIP joint. The device does have a coupled motion between the MCP and PIP joint.
14. The shear force between the device and the skin should be as low as possible There is silicone between the device and the finger to reduce the shear force. Because it is a compliant mechanism the shear force is lower as well. But shear force is still present.
15. The actuator response should be within 2s. This is after sending the signal the time it takes before moving. Not possible to measure before. It depends on the used actuator.
16. The actuator should have a cycle frequency of 2 Hz. This is the time it takes to move the fingers. The bending time is fast, not sure if this will be possible.
17. The device should not produce a sound louder than 70 dB. From 70 dB sound becomes annoying. With the help of a damper the noise is below 70 dB.
18. The material of the device should not irritate the skin. Silicone does not cause skin irritation. This is the part that touches the skin. Therefore, there is no problem.
19. The device can be controlled with series control. This means that the control of the hand is with muscle activation, plant movement or plant force/pressure. This should be possible.
20. The device should work on a battery for a whole day without charging. A battery is needed to guide the Arduino. This battery works the whole day.
21. If pneumatic: gas tank of at least enough for one full day. The tank is big enough because it can be place somewhere on the wheelchair.
22. If electromagnetic: motor power high enough to generate output forces of 10.5 N
23. The device can be cleaned in the dishwasher. The device cannot be placed in the dishwasher.

Wishes

1. The time to learn to use the device is limited to 1 day. Easy to control, hard to understand the mechanism.
2. The total costs of the device should not be more than 150 euro. Cheap design

3. The orthosis should look attractive. Can choose own color etc. and it is flat which makes it more attractive.
4. The size of the device should be adaptable to increase wear comfort. The device is custom-made, but sometimes fingers are thicker, and would it be nice if small adaptations are possible. Not possible
5. The device needs maintenance once a year. When it is 2 times a year it is fine, not every week. I think this is fine.

D
Prototyping

This appendix gives an explanation of the different prototypes made during my thesis. First the origami based design in Section D.1. Followed by Section D.2, where the Cool based concept will be discussed. The new variations on the Cool based design are described in Section D.3. Finally the final design is explained in Section D.4.

D.1 Origami

The first concept was the origami design as shown in Figure D.1(a). This design consisted of metal plates which were connected to each other with foil. The angle between the plates determines the output angle. By pushing sideways of the mid-plane, a flexion movement will be generated. This was done with the white block on the left as shown in Figure D.1(b) during the tests. Some weight was added to the rope and a force sensor was place on the white push block. As the device will always move back to its origianl state, it was possible to make an extension movement as well. Unfortunately, it was not possible to generate movements when the device was moved more than five times. Next to that, the forces were too low. The output forces were below 1 N. To find a solution to increase the durability and the force of the device, another connection between the plates was made. The aim was to generate more stable compliant mechanism based on the principle as shown in Machekposhti et al. (2015) where they call it an xr-joint as shown in Figure D.1(c). The red line is one part aluminum foil and the green line is one aluminum foil which connects two of the metal parts. Again, the outer part was covered with foil. With this principle it was not possible anymore to generate the bending movement as the connection between the plates was too stiff. Furthermore, it would be hard to activate the device in the same way is done in this setup, when connected to the finger. To sum up, because of the low output forces, the problems with the durability and the problem how to activate the device when connected to the hand, there has been chosen to go for concept number 2, the design inspired by Cool.

D.2 Cool based design

This concept is based on the same principle as described in Cool and Van Hooreweder (1971). This is a pneumatic actuation system. Four stiff tubes are connected behind each other with a hinge. These tubes are covered with a flexible silicone tube and a nylon rope. The four stiff tubes with the hinges are shown in Figure D.2. As soon as air enters the stiff tube, a bending movement takes place. To prevent radial expansion, the flexible tube is surrounded with a nylon rope. The stiff tubes are made of polylactic acid (PLA), the soft hinges from thermoplastic polyurethane (TPU). They are 3D printed at once with the Ultimaker 3. The silicone tube is glued to the PLA parts. Unfortunately it was not possible to generate a movement. This is most probably because the silicone tube was not flexible enough. Therefore, a re-design was made. In this case, the silicone tube was replaced by the hinge. The hinge consisted of different layers like as in the air chambers of an accordion, to generate space as soon as air enters the tube. By using the ultimaker 3 to print 2 materials at once this design could be made as shown in figures Figure D.3(a) and Figure D.3(b). Two different mechanisms were tested to see which connection method would work the best. This did not generate the movement it should make. The reason for this was that the TPU is flexible but does not have the property to expand.

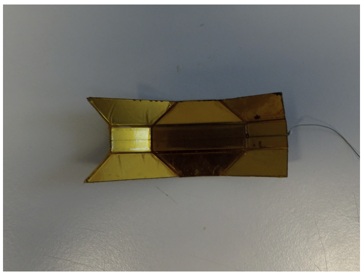

(a) Overview of the origami design prototype. This device consists of metal plates and foil.

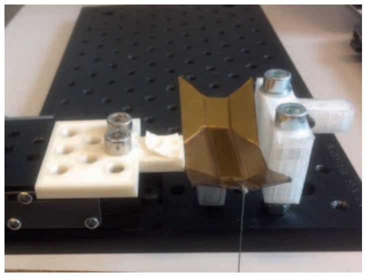

(b) Overview test setup origami design. The push movement of the white block on the left results in bending of the finger.

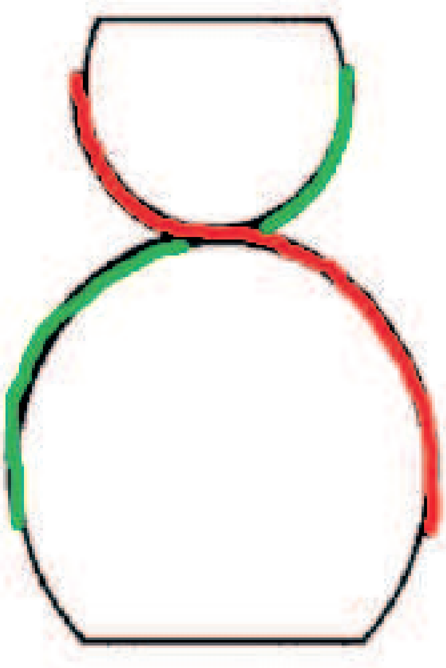

(c) Schematic overview of the XR-joint. Red resembles one connection and green resembles on conenction.

Figure D.1 Overview origami design and the prototype during the test setup.

Therefore, it was not possible to make a bending movement. After this conclusion, new concept were designed which will be described in the next section.

D.3 Variation on cool

Four new concepts were designed to solve the problems with the Cool based design. These problems were that the device did not generate a bending movement and no expansion took place within the hinges. The following concepts were designed as shown in Table D.1.

Concept number 4 has been chosen as final design. The expected problems were the easiest to solve, and the manufacturing is feasible. This concept will be further explained in the next section and the paper in Part I.

D.4 Final design

This section shows the final design which consists of a silicone outer part with an inner structure of PLA. There is a combination of flexible and inflexible elements. The flexible elements consists of PLA fins, which will generate air chambers. The finger has nine different air chambers, which will expand as soon as air enters the fin. The expansion of the first fin will touch the next fin which in the end results in a bending movement. The first prototype is made with the maximum size that was mentioned in

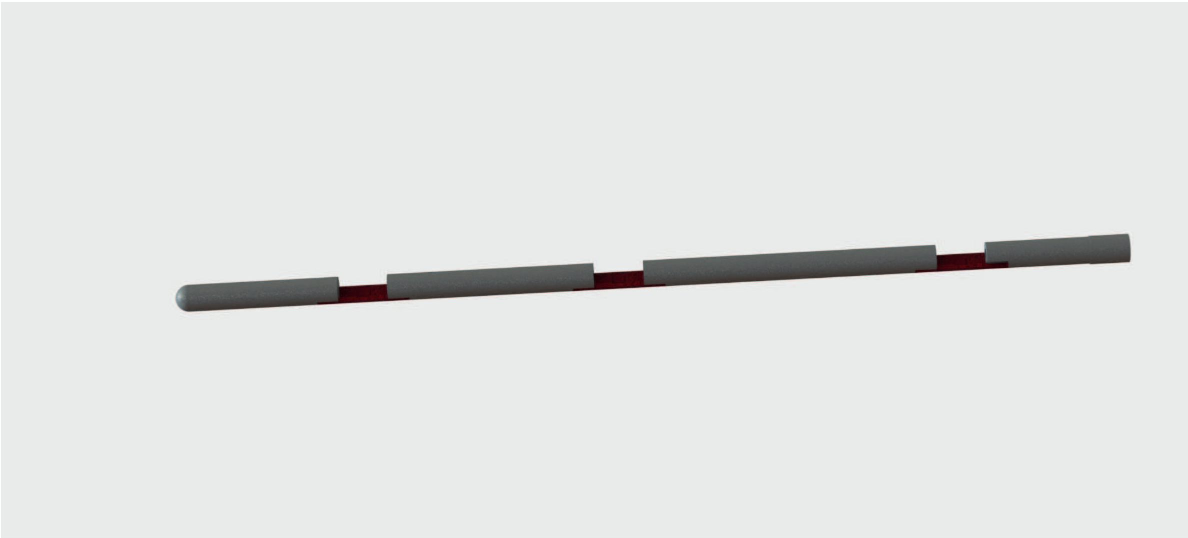

Figure D.2 Overview design based by Cool. The white parts are the PLA tubes, the red parts are the TPU hinges.

(a) Overview of the first design option for the hinge.

(b) Overview of the second design option for the hinge.

Figure D.3 Overview of two attachment systems for the hinge as an alternative on the design inspired by Cool.

the design criteria. This made it easier to fabricate and to analyze. The biggest problem was how to connect the air tube without any leakages. The silicone does not attach to anything else than silicone. Therefore, the attachment system was a weak point. First a small aluminum plate with a threat was placed at the entrance. The push-in fitting for the air tube could be ensured to this place. However, as the silicone did not bind to this plate and the aluminum plate started to move, this was not a good solution. Finally, silpoxy glue was found, which is a glue that attaches to silicone and any other material. This made it possible to place the air tube in the entrance of the silicone finger and add some silpoxy glue to make it air tight. A cable tie was added as well to keep it on its place. After this discovery, the small design was manufactured, as the main goal was to keep it as small as possible. First some tests were carried out with the bigger size. Then the tests were only done with the small design. There was started with the tests with the different fin structures, second the maximal output forces in horizontal position were analyzed. After that the difference in output force between the A20 and A30 silicone was measured, and finally the differences in bending angle with a different amount of fins were analyzed.

Table D.1 Overview new designed concepts.

Number	Principle	Expected problems
1	Add a spherical plastic plate instead of silicone tube.This plate is connected to the bottom plate. Connected to bottom are hard stiff parts and lower flexible parts	How to connect plastic plate to the bottom? Is the plate flexible enough to generate a movement?
2	Print the same design as the redesign from Cool with printer from Shape-ways	Chance to get the same problem as before.
3	Hard and stiff parts with flexible hinge. Pour this with half round tube of silicone.	How to connect silicone part to the PLA?
4	Pour half round circles from silicone. Inside silicone PLA parts to make air chambers.	How strong is silicone?

An overview of all the fingers made is shown in Figure D.4.

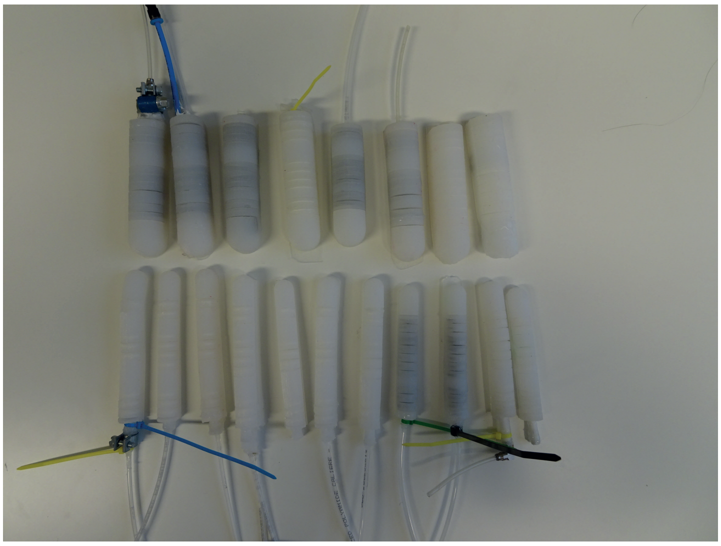

Figure D.4 Overview of all manufactured fingers.

E

Additional information paper

This appendix shows the additional information for the paper. Section E.1 describes the different steps taken for the design as shown in Part I. Section E.2 shows the results from the big finger design. The additional results from the small finger design are shown in Section E.3. Section E.4 explains the FBD to analyze the functioning of the final design of the finger.

E.1 Design approach

First, the principles used for other soft pneumatic actuators were analyzed. It was noted that the output forces could be increased. One way to increase the forces was to change the shape of the air chamber. This was done with the help of PLA fins. As silicone does not bind to anything else than silicone, air chambers could be generated. By leaving the PLA fins on the inside of the finger, the molding process could be done within one step, this will reduce the chance on leakages. With this principle in mind, a first prototype was manufactured. This finger consisted of a width of 22 mm and a height of 25 mm. The larger size made it easier to analyze and check if the principle should work. From here, the design was optimized with the help of finite element methods (FEM) analysis and measurements.

The final design had a width of 13.5 mm and a height of 13.2 mm. The optimal shape of the outer silicone structure that was found, has been used for the final size. Within this final size, different shapes of the inner fins were made. The shapes were analyzed with a FEM analysis. After that, the output forces of the different shapes were measured. The measurements were seen as leading. Two different prototypes with a different number of fins were manufactured and tested to analyze the differences in bending angles. By combining all these results, the final design was chosen.

E.2 Big finger

The first design was made with bigger dimensions to make it easier to manufacture and to analyze the movements. Some tests were carried out in horizontal position to get an indication about the forces. These results are shown in Figure E.1. The three tests are quite similar. The big finger is able to generate an output force of 4.5 N by a pressure of 0.6 bar.

E.3 Small finger

The final design is made in the small size. The results of the A30 silicone are shown in Part I, the paper. The results of the A20 silicone are shown in Figure E.2. As can be seen in the graph, this finger does not move consistently in comparison to the A30 silicone. Although, the output forces are higher compared to the A30 silicone, with a maximum output force of 5.4 N at 1.3 bar, there has been chosen to use the A30 silicone for the other tests. The finger Version 2 was also tested in horizontal position as shown in Figure E.3. Here a maximum output force of 1.4 N at 1.6 bar was reached. However, during the first test the inflation of the air chamber of the DIP joint was so extreme that the fin inside turned upside down. This happened because there was a leakage which was repaired with the A20 silicone as the cure time of that silicone was 4 hours in stead of the 16 hours of the A30. This silicone is more flexible which resulted in a lot of space in the air chamber.

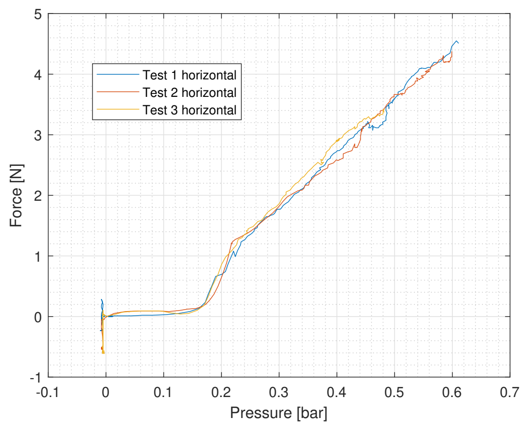

Figure E.1 Results of three tests of the big finger in horizontal position. The output force in relation to the pressure is shown.

This resulted in lower output forces compared to Version 1. These results were not shown in the paper because this was an unusual circumstance and therefore not possible to compare with Version 1. Based on theory, it was not expected to measure differences between Version 1 and Version 2 in horizontal position. Therefore, no new prototype was made to test this.

The resulted output forces were too low to use the device during ADL. To increase the output forces, a cover could be a solution. A quick test has been carried out by covering the last flexible element with nylon thread. The vertical tests were carried out three times. The results are shown in Figure E.4. The maximum output force was 0.8 N at 1.9 bar. This shows that a cover could work as a solution to increase the output forces.

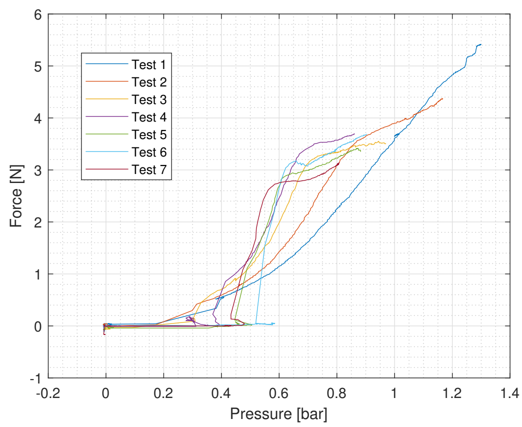

Figure E.2 Results of the tests for the small finger in horizontal position for A20 silicone. The output force in relation to the pressure is shown for seven tests.

E.4 Free body diagram

After the measurements a simplified free body diamgram (FBD) has been made. This was done for the horizontal direction for the last air chamber in the DIP joint and the tip of the finger. The tip of the finger had a bending angle of 18° in this situation. There was assumed that in horizontal position for the last fin in the DIP joint, the contact surface with the distal phalanx was 80%. This will be at 0°, while at 90° there is no contact surface. By generating a cosines with these values, there was found that at a bending angle of 18°, the contact surface can be set at 76%. This is shown in Figure E.5. The air chamber had a radius of 6.5×10^{-3} m. The contact area of the circle is calculated as shown in Eq. (E.1). With A_{Contact} as area, and r as radius. This resulted in a value of 4.9×10^{-5} m^2. The moment arm was dependent on the height of the contact area. This was calculated with Eq. (E.2).

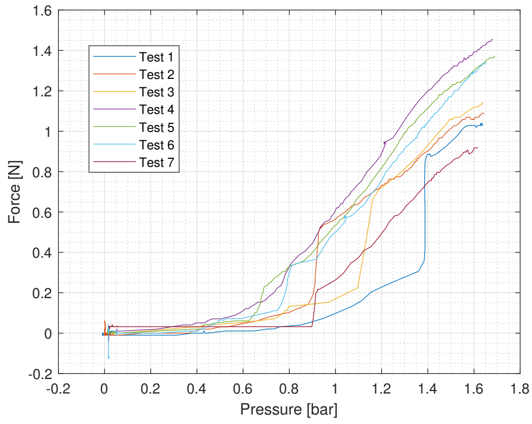

Figure E.3 Results of seven tests of the finger in horizontal position with finger Version 2. The output force in relation to the pressure is shown.

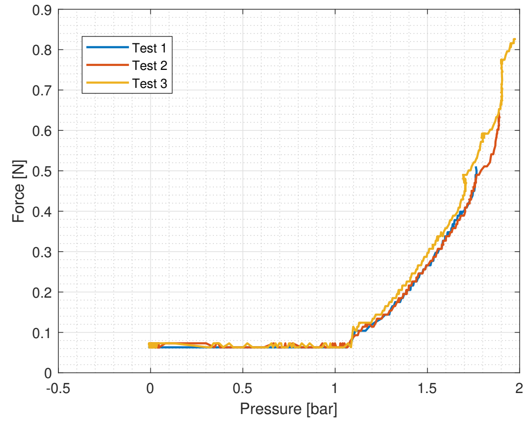

Figure E.4 Results of three tests of the finger in vertical position with finger Version 1 with cover. The output force in relation to the pressure is shown.

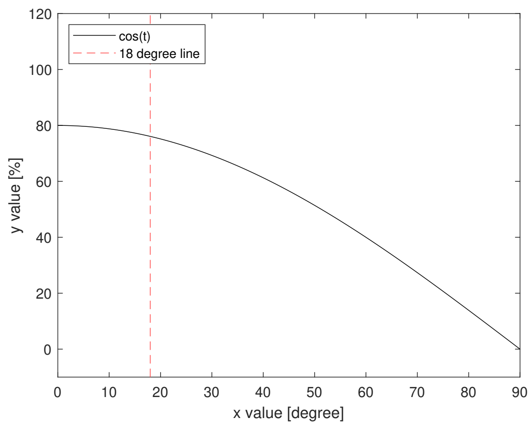

Figure E.5 Cosine with the 18 degree line.

$$A_{\text{Contact}} = \frac{1}{2}\pi r^2 \tag{E.1}$$

$$H = \frac{4r}{3\pi} \tag{E.2}$$

$$F_{\text{out}} \cdot r_{\text{out}} = p \cdot A_{\text{Contact}} \cdot r_{\text{in}} \tag{E.3}$$

This resulted in a height H of 4.9×10^{-5} m. The sum of the moments was used to calculate the needed pressure p as shown in Eq. (E.3). From the results from the measurements an output force F_{out} of 1.4 N was chosen. The moment arm r_{out} had a value of 10.5×10^{-3} m as this was the middle part of the phalanx which touches the force sensor. This resulted in a pressure of 0.74 bar. This result is lower than the measured value of 1.15 bar. The FBD of this situation is shown in Figure E.6. The reason for this is that the contact surface was an assumption. Apparently the true contact surface is smaller. Furthermore, there will be some pressure losses in the material as in this situation only the final air chamber was calculated. As these values are already lower than the measure values, no calculation was made for the bending situation. Theoretically, in horizontal position, the input/output relation of the force should be equal as otherwise movement would take place. This situation is shown in Figure E.7. When the air chamber makes an angle in relation to the other air chamber, the lever arm will be reduced. This results in a lower output force. The difference is shown in Figure E.8. This means that the more fins on a short area, the less losses will take place, and the higher the output forces. Therefore are the output forces of finger Version 1 higher than for finger Version 2.

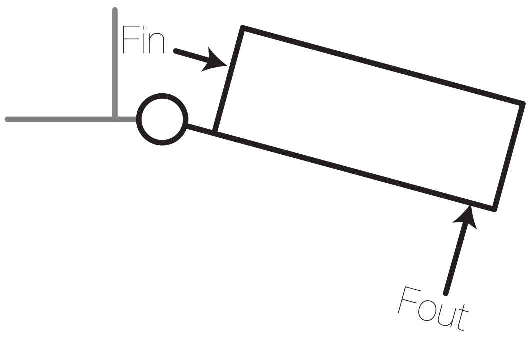

Figure E.6 FBD of the DIP joint in horizontal position.

Figure E.7 FBD of two air chambers in neutral position.

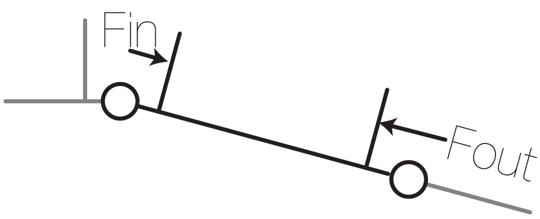

Figure E.8 FBD of two air chambers when bended.